LATERAL LOADS ON REENTRANT CORNER STRUCTURES

By

BETHANY MARIE BROWN

A thesis submitted in partial fulfillment of
the requirements for degree of

MASTER OF SCIENCE IN CIVIL ENGINEERING

WASHINGTON STATE UNIVERSITY
Department of Civil and Environmental Engineering

MAY 2014

To the Faculty of Washington State University:

The members of the Committee appointed to examine the thesis of BETHANY MARIE BROWN find it satisfactory and recommend that it be accepted.

_____
Daniel J. Dolan, Ph.D., Chair.

_____
William Cofer, Ph.D.

_____
Don Bender, Ph.D.

_____
Steve Pryor, P.E., S.E.

ACKNOWLEDGEMENTS

The author would like to extend her warmest thanks to Dr. Daniel Dolan for his guidance and support. A special thanks also goes to Dr. William Cofer, Dr. Donald Bender, and Steve Pryor for serving as a committee members.

The author would also like to thank her loving and supportive mother and family for their dedication and patience through this process.

LATERAL LOADS ON REENTRANT CORNER STRUCTURES

Abstract

by Bethany Marie Brown, M.S.
Washington State University
May 2014

Chair: Daniel J. Dolan

For this study, the effect of lateral loads on the forces in the reentrant corner of structures was examined so as to better understand why damage occurs in this location after major wind or seismic events. Thirty models were analyzed using finite element analysis in SAP2000 with varying dimensions and wall locations. Theses changing parameters were used to see how the axial forces in the reentrant corner also changed accordingly. The models were configured so as to mimic light-framed timber construction. In each case the models were subjected to the same load conditions with the only variation between the models being either the dimensions or locations of walls. The study found that the axial force for the interior and exterior struts acted linearly, as the length of the diaphragm increased so did the axial force. The results for the interior and exterior chord showed that the analog for the diaphragm transition is from a propped cantilever to a simply supported beam as the length of the diaphragm increased. Finally it was also found that the addition of walls, both exterior shear walls and interior shear walls, greatly decreases the axial forces for both the interior and exterior strut and interior and exterior chords in the reentrant corner.

TABLE OF CONTENTS

TABLE OF FIGURES

TABLE OF TABLES

CHAPTER 1: INTRODUCTION

1.1 INTRODUCTION

In recent years there has been a change in the complexity of residential and commercial structures from that of a few decades ago. It used to be that residential and commercial structures were primarily rectangular in shape and thus followed traditional lateral load paths. With advances in technology, these structures are now more complex in shape and contain multiple irregularities. Such irregularities include, but are not limited to, nonparallel systems, diaphragm discontinuities, torsional effects and reentrant corners (ASCE 2010) which make following the traditional lateral load paths more difficult. These complex diaphragms require more in-depth analysis to determine the complete lateral load path. In the case of this study, only the issue of reentrant corners will be examined.

According to ASCE 7-10 a "reentrant corner irregularity is defined to exist where both plan projections of the structure beyond a reentrant corner are greater than 15% of the plan dimension of the structure in the given direction." A reentrant corner can also be referred to as a notched diaphragm. A notched diaphragm occurs when a disruption in the diaphragm chord or strut is caused by the main wall line being offset by a portion of the exterior wall line (Malone, 2012.) When a discontinuity, like a reentrant corner, occurs, the code requires that the force must be transferred across the discontinuity via an alternative load path. The difficulty with reentrant corners is in determining the actual magnitude of the force that is being transferred.

There are a couple of reasons why it is difficult to determine the magnitude of forces in reentrant corners. The first is the difference in the rigidity due to the general

layout of the structure. The second major difficulty is that the torsional forces imposed on the structure cause deflection amplifications at various locations on the entire structure. Both of these issues occur simultaneously which compounds the difficulty.

The variance in rigidity is caused by the general layout of the structure. At one point in time, one part of the structure is bending about its strong axis while another part is bending about its weak axis. This concept is illustrated in Figure 1.1. In this rendition, the ground motion is occurring in the east-west direction. The structure to the left of the image is oriented in the east-west direction (strong axis) so is naturally going to respond more rigidly than the other structure which is oriented in the north-south direction (weak axis). The way the structure is deflecting affects the differential motion of the structure as well. The differences in motion and rigidity in the different parts of the structure result in a concentration of local stress at the "notch" of the reentrant corner (Naeim, 1989.)

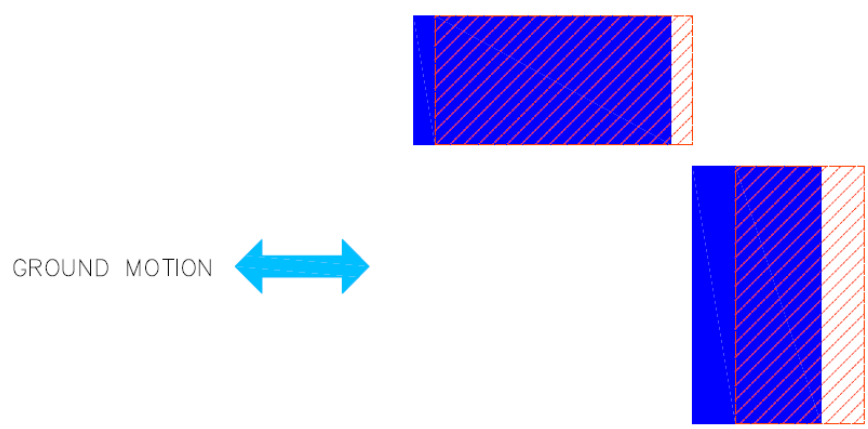

Figure 1.1 Rigidity of Separate Buildings

The concentrated local stresses at the reentrant corner are illustrated in Figure 1.2. In this illustration the two wings are connected. When the ground motion is applied, the two wings want to move differently from each other because of their orientation. This difference between strong axis bending verses weak axis bending essentially creates a push-pull effect on the structure. This push-pull effect on the structure creates a local stress concentration at the reentrant corner.

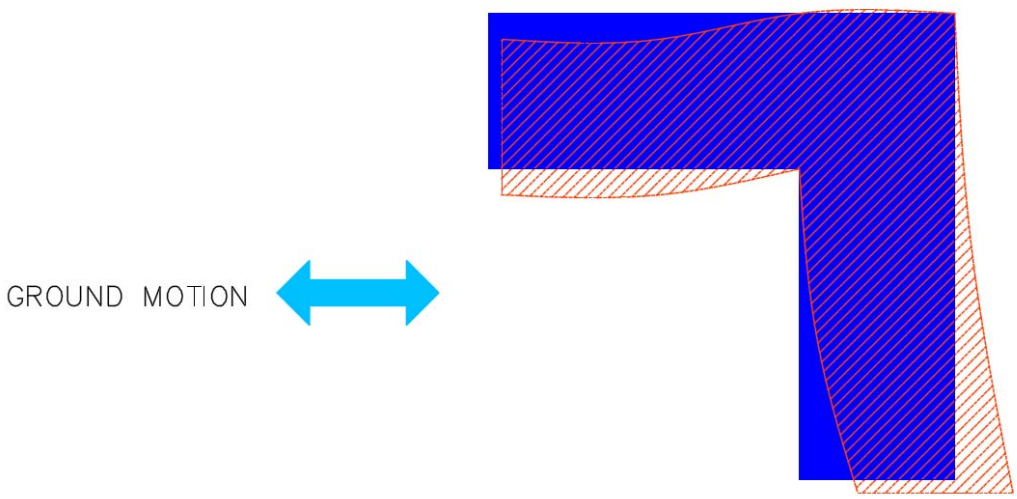

Figure 1.2 Stress concentration in L-Shape Building

The second problem with structures that include reentrant corners is the torsional effect. Torsion is introduced to the structure because the center of mass and the center of rigidity do not necessarily occur in the same location. The center of mass and the center of rigidity also can change locations depending on the magnitude and direction of the lateral load imposed and the general shape of the structure (Naeim, 1989.) The difference in locations of the center of mass and the center of rigidity can be seen in Figure 1.3. Since the center of mass and the center of rigidity are not located in the same location,

torsion is introduced into the structure. This torsion also creates a local concentrated stress at the reentrant corner. Since deformation of the structure is based on the magnitude and direction of the lateral loading, it is difficult to analyze how the structure is going to respond, since the lateral load can vary from event to event. The structure is undergoing torsion in conjunction with the push-pulling that is going on from strong axis/ weak axis bending, thus making these two mechanisms interrelated. Since these issues are superimposed on each other, it makes it difficult to accurately calculate what the local stress concentration is at the reentrant corner. There are other mechanics that also contribute to the magnitude of the stress concentration; they include the mass of the building, the structural system, the length of the wings and their aspect ratios, and the height of the wings and their height/depth ratios (Naeim 1989). Another mechanic that contributes to the magnitude of the stress concentration is whether or not a shear wall is located under the reentrant corner.

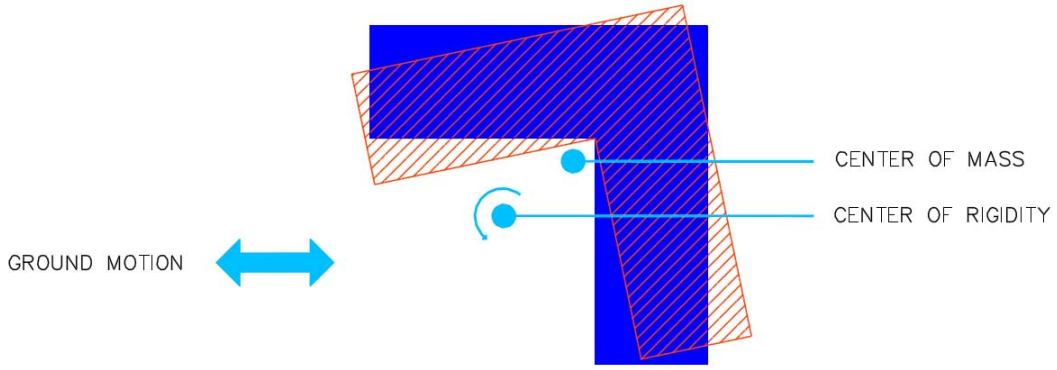

Figure 1.3 Center of Mass verses Center of Rigidity

1.2 OBJECTIVES AND SCOPE OF RESEARCH

The objective of this study is to evaluate lateral loads on a reentrant corner structure, specifically an L-shaped structure via finite element analysis, to develop a better estimation of the local stress concentration in the reentrant corner and a better concept of the load path in the reentrant corner area of the structure. Determining the stress concentration would give a better understanding as to what is occurring in the structure in a lateral loading event. The capability to better estimate the local stress concentration would allow for structures to be more appropriately designed and thus enhance the safety of the structure as well.

Historically, since before the turn of the twentieth century and even in modern structures, significant damage has been observed in structures with reentrant corners after a lateral loading events, such as an earthquake. Damage in the reentrant corners of structures was significantly noted after the 1923 Kanto earthquake, the 1925 Santa Barbara earthquake, the 1964 Alaska earthquakes, and the 1985 Mexico City earthquake (Naeim, 1989.) In some of these significant events, it was noted that damage to the structure occurred in the reentrant corner first, and then traveled to other parts of the structure. Damage observed in the roof diaphragm and upper floors radiating out from the reentrant corner of the Ministry of Telecommunication building in Mexico City after the 1985 earthquake can be seen in Figure 1.4.

Figure 1.4 Damage to Reentrant corner and Upper stories of the Ministry of Telecommunications Building in Mexico City after the 1985 earthquake.
Source: USGS U.S. Geological Survey Photographic Library

Currently, a several different approaches are used in the design of structures with reentrant corners. One approach is to treat the different wings of the structure as separate and individual, performing a structural analysis for each part. In treating the wings as separate and individual, it simplifies the overall structure making analysis more manageable. In this case as well, each wing needs to be able to individually support the vertical and lateral loads imposed on it. As part of this analysis, in regards to the reentrant corner, the maximum lateral drift for each wing needs to be calculated. The sum of these values equals the amount of space needed between the wings to allow for, at worse case scenario, the different wings to deflect without banging into each other. An expansion joint is used in these cases to connect the wings together. In addressing each wing as individual structures, the reentrant corner is essentially ignored. While the vertical and lateral loads are taken into account for the individual wings, the resultant

force in the reentrant corner is not addressed, but the differential displacements in the corner are difficult to accommodate without special seals and expansion joints being incorporated into the design.

Another design approach that is currently used to address the forces in the reentrant corner is to use a splay instead of the traditional 90° angle of a reentrant corner. In changing the degree of the angle in the reentrant corner the resultant force is decreased. The splays "tie the building together strongly at lines of stress concentrations and locate resistant elements to reduce torsion" (Naiem 1989.) While this approach more directly addresses the reentrant corner than the other approach stated above, neither approach fully takes into account the total resultant forces. That is because current design approaches do not determine the total resultant forces in reentrant corners that develop under lateral loads. These design approaches and simplifications to the structure are allowed by current building codes because they aid in the development of a reasonable or rational design.

In this study, several light-framed L-shape structures are subjected to a lateral load using finite element analysis to which the results are analyzed afterwards. The overall objective of the finite element modeling is to develop a method that better estimates what the local stress concentration at the reentrant corner of a given structure under a lateral load really is and determine what the plausible load paths in the corner might be.

This specific task is accomplished by a series of finite element models that is succeeded by a careful analysis of the resulting data. The finite element modeling and

procedure is discussed in detail in Chapter 2. Data collected from the finite element modeling is evaluated in Chapter 3 for numerical trends.

1.3 LITERATURE REVIEW

While damage in the reentrant corner after a lateral loading event has been noted for over a hundred years now, it is only in the last twenty years that research has been done to try to better understand and determine the magnitude of forces in the reentrant corner. Since it is difficult to determine analytically the magnitudes of the forces, as explained previously, models have been developed and tested either in wind tunnels or on shake tables to investigate the forces in reentrant corner structures.

In an article published by the Journal of Structural Engineering, (Songlai, Chengmou, & Jinglong, 2010) a team investigated the behavior of engineered light-frame wood construction under lateral loads. Part of the investigation was to examine diaphragm action with reentrant corners. A uniformly distributed load was applied to the model through the use of gasbags set along the exterior floor edges. As a part of their investigation, a series of tests were executed, one of which was an ultimate load test. After the ultimate load test was performed, the reentrant corner of the model was examined. It was found that no visible damage had been done. They concluded that lateral loads could be successfully resisted without continuous end chord if the reentrant corner of the diaphragm was less than 1.0 meter (Songlai, Chengmou, & Jinglong, 2010.) Their decision to have a reentrant corner in their model less than 1.0 meter was based on a finite element analysis study on openings and offsets in buildings (Prion, 2000.) Their results confirmed some of the data presented in that study.

Swaminathan Kishnan from the Seismological Laboratory of the California Institute of Technology did a case study of damage to 19-story irregular steel moment-frame buildings under near-source ground motion (Krishnan, 2007.) The purpose of his study was to compare the performance of buildings that do not adhere to wind drift limits to those that do, by comparing 3 19-story irregular steel moment-frame buildings. Two of the buildings had reentrant corner irregularities, while the third had a plan torsional irregularity. Kishnan used the UBC97 and assumed that each structure was located in a Seismic Zone 4 with soil Type S_b. Kishnan also selected three different sets of three-component ground motion records so as to compare results. He concluded that none of the buildings, whether they adhered to wind drift limits or not, would satisfy the life-safety performance level for existing buildings as given by FEMA-356 (Kishnan, 2007.) Kishnan also concluded that the results from his investigation were similar to results found in structures after the 1994 Northridge earthquake. While the stress concentration in reentrant corners was not a part of his primary investigation, he did comment on it. Kishnan concluded that the specific stress concentrations were averaged out over a large area near the reentrant corners. The results were also inconclusive in regards to an increase in stress concentration in the reentrant corners since a stress concentration increase in the reentrant corners was only noticed in one of the two models containing reentrant corners. A more rigorous and detailed analysis is required to conclusively rule out the incidence of stress concentration at the reentrant corners (Kishnan 2007.)

J.A. Amin and A.K. Ahuja, of the Department of Civil Engineering, Sardar Vallbhbhai Patel Institute of Technology, Vasad, India, investigated the effects of wind induced pressures on buildings of various geometries (Amin and Ahuja, 2011.) The

purpose of their investigation was to determine the efficiency of irregular building plan shapes in which the wind pressure distribution changed, depending on the wind direction. A secondary purpose was to provide information on wind pressure distributions, as well as mean and peak pressure coefficients over an extended range of incidence wind directions (Amin & Ahuja, 2011.) Their study consisted of two L-shaped and two T-shaped models of varying heights and dimensions. Pressure tape was then placed strategically on the different models so that on all sides of the models a good pressure distribution could be obtained (Amin & Ahuja, 2011.) The models were tested using a wind tunnel so as to simulate actual conditions that a structure might encounter if it was located in an area of open country terrain. In their results they noted that, unlike structures that are purely rectangular in shape where symmetry is observed over the vertical centerline for the wind pressure coefficient distribution, this was not the case with the irregular shaped models. Instead they noted that as one neared the reentrant corners of the structures the pressures increased due to the blockage of wind flow and subsequent stagnation of the flow (Amin & Ahuja, 2011.) This was observed and noted across all of their models. They also concluded that the amount of pressure and the size of the stagnation zone were based on the dimensions of the structure and the angle at which the wind was coming from.

Results from these experiments conclude that size of the reentrant corner, based on the dimensions of the building, has an impact on the forces seen in the reentrant corner region. From Songlai, Chengmou, and Jinglong's study (Songlai, Chengmou, & Jinglong, 2010), if the reentrant corner is less than a certain dimension, based off of other criteria, it can adequately withstand lateral loads without visible damage being observed.

Again, their results confirmed a pervious finite element study by Prion (Prion and Lam, 2000), which gave parameters to a maximum size reentrant corner that a structure could have without visible damage being observed in the reentrant corner under lateral loading. In Amin and Ahuja's study (Amin & Ahuja, 2011), they found that they dimensions of the structure and the direction that the wind was coming had a direct correlation to the size of the stagnation zone and the magnitude of the pressure in the reentrant corner. As the height of the structure or the length of the projection increased, so did the stagnation zone and the pressure. While both of these studies comment more globally about the impacts of lateral loads on reentrant corners, they do not look actually look at the forces in the structure at the reentrant corner. Kishnan (Kishnan, 2007) addressed this issue more in his study but concluded that his results were inconclusive and that a detailed finite element approach needed to be taken in order understand stress concentrations that develop in the reentrant corner region.

CHAPTER 2: ANALYSIS PROCEDURE

2.1 Scope of Testing

A parametric study was performed to understand lateral loads' effect on reentrant corners using finite element analysis and SAP2000 (Computers and Structures, 2011). Specifically, the purpose of the study was to examine the resulting force concentration in the reentrant corner caused by a lateral loading event so as to improve understanding that would eventually help lead to designing and constructing more robust structures.

The study consisted of light-frame, timber models that were developed in SAP2000. The building configuration used to investigate the forces in the reentrant corner consisted of an L-shaped building; one leg was kept at a fixed dimension and the other leg was given variable dimensions. All of the models were based on the planar dimensions of the constant leg, which were 48 x 24 ft. In this study, each model was loaded under the same uniformly distributed load. The response parameters that were investigated to quantify the effects of lateral loads on reentrant corners were: 1) the change in chord and strut forces with respect to the length of the variable leg of the building, and 2) the change in chord and strut forces when interior walls were added along the length of the variable leg of the building.

2.2 Parameters of Parametric Study

There were two main parts of the parametric study of lateral loads on reentrant corner structures. The first part of the study examined how the length of the leg of the building wing perpendicular to the loading affected the diaphragm chord and strut force concentrations observed at the reentrant corner. The second part of the study examined how the addition of interior shear walls in the leg perpendicular to the loading affected

the diaphragm chord and strut forces in the reentrant corner. These parametric studies were designed in such a way so as to bring new understanding to potential damage problems seen in reentrant corner structures after major lateral loading events.

The first part of the parametric study examines how relative size affects forces in the reentrant corner. The dimensions of one of the legs of the structure (main axis parallel to the loading) was held constant while the dimensions for the other leg (main axis perpendicular to the loading) were varied. The dimensions of the varied length were based off of the dimensions of the constant leg. For this particular study, the constant leg's plan dimensions were 48 x 24 ft. The dimensions for the variable leg were then set as a percentage of the constant leg's length.

The dimensions for the variable leg were defined as a percentage of the length of the constant leg because of how ASCE 7-10 defines a reentrant corner. In its definition, so as to make it applicable to any structure, ASCE 7-10 uses percentages of lengths to define dimensions of a structure. This same concept of using percentages of length to define the dimensions of the building was used in this study so as to make the results applicable beyond the scope of the models used to analyze the building. For this study, the minimum length of the variable length leg was 15% of the long dimension of the constant leg. This dimension was less than the minimum requirement for a reentrant corner as defined in ASCE 7-10. From the minimum defined length, the dimensions of the variable leg increased to 25% of the long dimension of the constant leg. After this point the dimensions of the variable leg were increased at intervals of 25%, ending at 300% of the long dimension of the constant leg. All of the models in the study were

loaded under the same distributed load, from the same direction, so that the only variable in this part of the study was the dimensions of the variable leg.

In the second part of the parametric study, interior shear walls were added to examine how the forces in the reentrant corner are affected by the additional paths for extraction of the diaphragm loads. For this part of the study, the variable length leg of the diaphragm was held at 300% of the fixed length leg. Its selection was based on it being the largest model used in the first part of the study, and it allowed for the addition of more interior shear walls than the other models. Interior shear walls were added one at a time, at equal intervals, up to eight interior shear walls. For instance, when one shear wall was added, it was located approximately at the one-half point of the longer leg of the diaphragm. When two shear walls were included, they were located approximately at the one-third points of the longer diaphragm leg. When three shear walls were used, they were located approximately at the one-quarter points of the longer diaphragm leg, and so on for the remainder of the study. Again, like the first part of the parametric study, each of the models was loaded under the same distributed load, from the same direction so that the only variable parameter was the number of interior shear walls. Again, the purpose of adding the interior shear walls was to examine how the addition of alternate load paths, in the form of shear walls, affects the forces in the reentrant corner.

2.3 DEVELOPMENT OF MODELS

SAP2000 was the modeling software chosen for this study. It was chosen based on its availability and the fact that it is a commonly used program for structural modeling and finite element analysis. The main difficulty with using SAP2000 is that it comes preprogrammed with concrete and steel cross sections and materials, but not timber.

Since the focus of this study was light-frame timber structures, each of the cross sections of members and material properties had to be manually programmed into SAP2000. A detailed description of how material cross sections and material properties were programmed into the software can be found in the following sections. A description of how these parts were then combined to develop the models for the parametric study also follows.

2.3.1 Development of Material Properties

In order to define a member's cross sectional parameters, its material property must be defined first. In SAP2000, material properties are defined through the *Define Materials* command located in the *Define* menu. For this particular study, the material properties for Number 2 grade Douglas-Fir Larch, and manufactured I-joists are defined. Douglas-Fir Larch was chosen as a material for the wall studs based on it use and availability as a building material on the West Coast. I-joists are used as roof joists because of their ability to span long distances.

Material property values for the Douglas-Fir Larch came from Table 4A of the NDS and material properties for the I-joist came from the manufacturer's specifications, which can be found in Appendix A.

2.3.2 Development of Material Cross Sections

The cross-sections for new materials were developed in a similar manner to how the new material properties were set up in SAP2000. For the purpose of this study, the cross section properties for a 2 x 4 and an I-Joist were programmed into the software. Section property values for the 2 x 4 were taken from Table 1B of the NDS, and the

section properties for the I-Joist were taken from manufacturer's specifications which can be found in Appendix A.

2.3.3 Development of Non-linear Links

Instead of using areas to simulate sheathing for the models, it was proposed to use non-linear links or springs. This was proposed based on modeling work previously done for the NEESWood Capstone Building. (Pryor, van de Lindt, & Pei, 2010) The development of links in SAP2000 is similar to that of developing material cross sections. To generate links, the *Link/Support Properties* command, found under *Define, Section Properties,* is used. For this study, a Multi-Linear Plastic Link type was chosen. By choosing Multi-Linear Link type it allows links to simulate the nonlinear response of each sheathing panel in a shear wall or diaphragm under lateral loads. The values for the force and displacement are based on height and width of wall or roof segments, nailing schedule, stiffness, inter-story drift, and angle of inclination for the link.

For this study, two different links were developed: one for the wall panels and one for the roof panels. The links for the walls were based on wall segments that were 12 x 4 ft. Four feet was chosen as the width of the wall segment based on the nominal width of a sheet of wood structural panel (WSP) sheathing. Twelve feet was chosen as the height based on the height of the structure and could be constructed using oversized OSB wall sheathing in reality, or the segment could represent 1.5 sheets of sheathing and after being blocked and nailed properly. Since it was the main part of the diaphragm, it was decided to keep the links in the roofs as similar to standard WSP sheathing dimensions as possible. For that reason the roof links represented 4 x 8 ft panels. Two links were used

to simulate each sheet of sheathing so as to take into account both the tensile and compressive capacities of the sheathing.

As previously stated, the development of the links was based off of work done for computer modeling of the NEESWood Capstone Building. As part of the shear wall calculations, Pang, et al, (2010) determined the shear wall backbone curves (force versus displacement). The modified Stewart hysteretic model, which is a five-parameter equation, was used to define the shear wall backbone curve. From here they were able to develop a displacement-based shear wall design table per unit wall length. These forces compared the backbone forces to different drift levels to the type of sheathing, edge nail spacing and height of the wall. With this table defined, other correlating parameters such as secant stiffness (K_s) and apparent shear stiffness (G_a) can be derived. By knowing K_s and G_a, as well as the nailing schedule and dimensions of wall segments, the Multi-Linear Force-Deformation definition for the links can be developed. The same procedure as used for the NEESWood Capstone Building was used in this study, but modified to fit the parameters of this study. The data for the Multi-Linear Force-Deformation definition was obtained from tests conducted by Steve Pryor (2009) can be found in Appendix D.

2.3.4 Development of Models

As previously stated in the description of the parametric study, this study focused on the effects of lateral loads on the reentrant corner of L-Shaped structures. To maintain uniformity and consistency between the models, one leg of the L-Shape structures remained constant. The dimensions of the variable leg were based on this constant leg's dimensions. The dimensions for the constant leg were 48 x 24 x 12 ft. The plan dimensions of 48 x 24 ft. were chosen based on the standard size of sheathing of 4 x 8 ft.

Since 48 and 24 are both divisible by 4 and 8, “whole” sheets of sheathing can be used on the diaphragm, thus simplifying the model. The models’ wall heights of 12 ft. were based on engineering judgment that the appropriate height for a single story structure is 12 ft.

The purpose of leaving one leg constant was so the dimensions of the other variable leg could be changed without changing the fixity experienced at the reentrant corner. As previously stated, the dimensions of the variable leg were percentage lengths of the plan projection of the constant leg’s length so that the results of the study should be applicable beyond the results for the particular building used for this study. A length of 15% of the long dimension of the constant leg was chosen as the minimum length for the variable leg. For this particular case, the plan dimensions of the variable leg were 7.2 x 24 ft. The next interval length for the variable leg was 25% of the plan length of the constant leg. From this point, the length of the variable leg increased at intervals of 25% up to 300% of the plan length of the constant leg. At a length of 300% of the plan length of the constant leg, the dimensions of the variable leg were 144 x 24 ft. Again, the lengths of the variable leg were based on percentages of the length of the constant leg so that the results would be applicable beyond the scope of the study.

The walls supporting the legs of the diaphragm were modeled as being 2 x 4’s, 2 ft. on center. Each stud in the model was constrained as if it was pinned at both ends in both horizontal directions to simulate the lack of fixity for end-grain nailed connections. The bottom and top plates were also modeled as 2 x 4’s. In the model, the plates were only 2 ft. long, each going from stud to stud. However, the end constraints for the plates were assigned to be continuous along the length of the wall. So while they consisted of

2- ft. segments, all together they acted like one unit. For the roof joists, I-joists were selected since they would have the ability to span a 24 ft. distance without any intermediate support. As described in the last section, non-linear links or springs were used to simulate the sheathing in the models.

Between the constant leg and the variable leg, there existed a 24 x 24 ft. box that connected the two legs together. This box was not considered in the length or dimensions of either of the legs. However, for the purpose of the roof diaphragm, the roof was sheathed as a continuation of the variable leg. The two interior wall faces of the block were set up so that their lateral mechanical properties were essentially zero. Assigning these wall segments to have essentially zero lateral stiffness and strength properties forces the roof diaphragm to act either as a strut or a chord, depending on direction, under loading at the reentrant corner. This configuration, therefore, allows one to study the effects of lateral loads in the diaphragm at the reentrant corner. The mechanical properties of the interior wall sharing its face with the variable leg were later set to match the mechanical properties of the exterior walls when the effects of how the addition of interior shear walls affects the forces in the reentrant corner was examined.

Unlike an actual structure that one would build, no openings exist in any of the models to avoid the added complication that the openings would cause in affecting the load path of the diaphragm or shear walls. Again, the purpose of this particular study is to examine how lateral loads affect forces in reentrant corners and to gain base level knowledge on the matter. Once this has been achieved, additional parameters can be added or modified to widen that knowledge. This is the same reason why a flat roof was chosen instead of the common pitched roof associated with gable roofs.

2.4 DEVELOPMENT AND APPLICATION OF LATERAL LOADS

Since the focus of this study is to quantify how lateral loads affect reentrant corner structures, an appropriate lateral load needed to be developed. For the purpose of keeping the computer models as realistic as possible, it was decided to apply a wind load to the structure instead of applying just an arbitrary load for testing. Based on wind load requirements from Chapter 26 of ASCE 7-10 (ASCE, 2010), the models were designated as Risk Category II thus making the basic wind speed on the west coast 100 mph. The models were also designated to be in Exposure Category B. With this information and using the procedures for the Main Wind Force Resisting System from Chapter 28 of ASCE 7-10 (ASCE, 2010) a pressure of 19.2 psf was calculated. To determine the distributed load, half of the height of the structure was taken and multiplied against the wind pressure. This gave a distributed load of 115.2 plf. A full calculation of the distributed load can be found in Appendix C.

It was found in the development of the models that the distributed load needed to be applied at nodes where the springs intersected with the exterior of the structure in order to be transferred throughout the structure correctly. Tributary area was used to determine the appropriate point load to be applied at each of the nodes. Figure 2.1 shows the value and location of the point loads. Calculations for these point loads can be found in Appendix C.

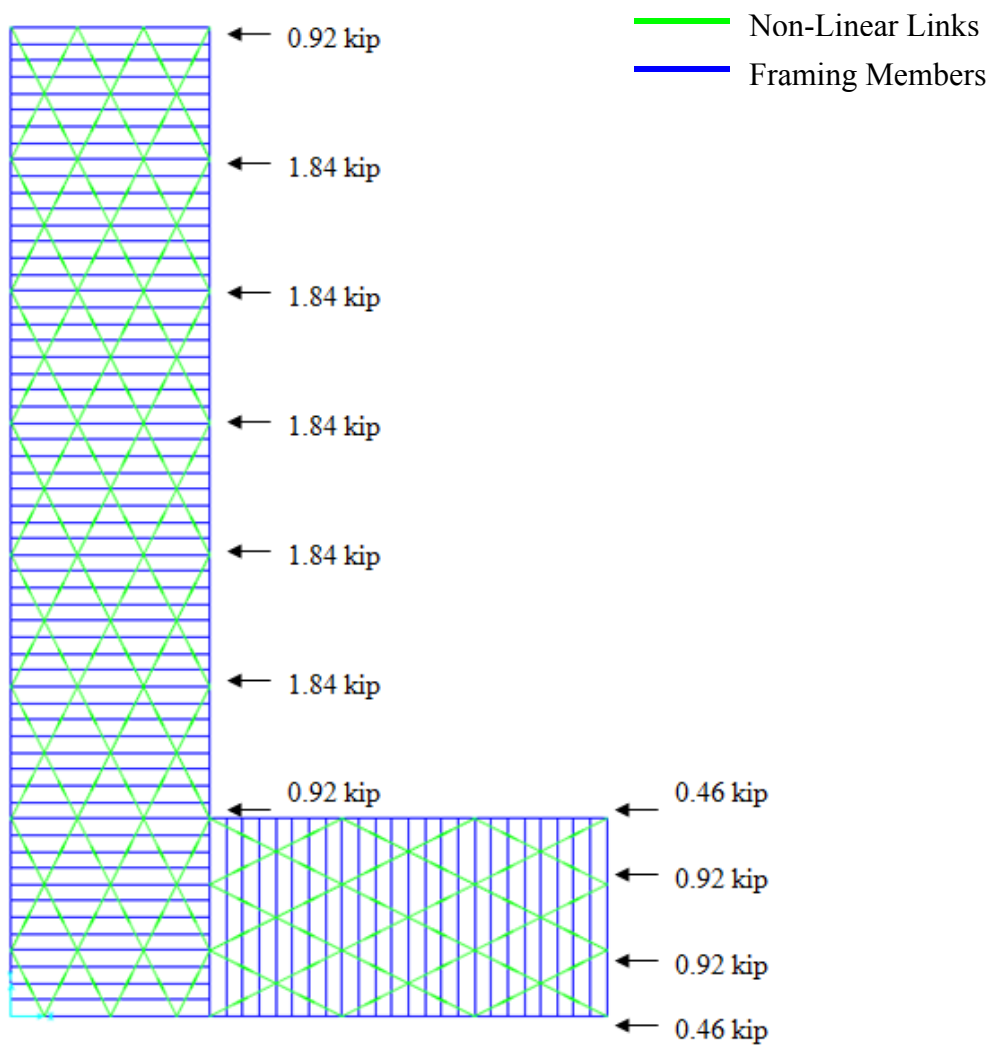

Figure 2.1 Magnitude and Location of Point Loads on Models

2.5 VERIFICATION OF MODELS

To verify the models and to determine if the models behaved similarly to actual structures, the defection of the diaphragm as predicted by SAP2000 was compared to the deflection calculated using the Special Design Provisions for Wind and Seismic (SDPWS) (2005). The model with the variable leg at 300% of the constant leg was chosen to compare values, since it had the greatest deflection of any of the models due to

its size. To determine the deflection in SAP2000 in comparison with the calculated deflection from SDPWS, all of the walls were removed, except the shear wall at the end of the variable leg, leaving only the roof diaphragm. The end of the diaphragm containing the constant leg was restrained as fixed. This essentially made the variable leg portion of the diaphragm a simply supported beam. This configuration can be seen in Figure 2.2. A distributed load was applied to the diaphragm, as described in the previous section, which resulted in a maximum deflection in SAP2000 of 1.39 inches at the mid-span of the variable leg. The deflection results from SAP2000 and the full analytical results are presented in Appendix B.

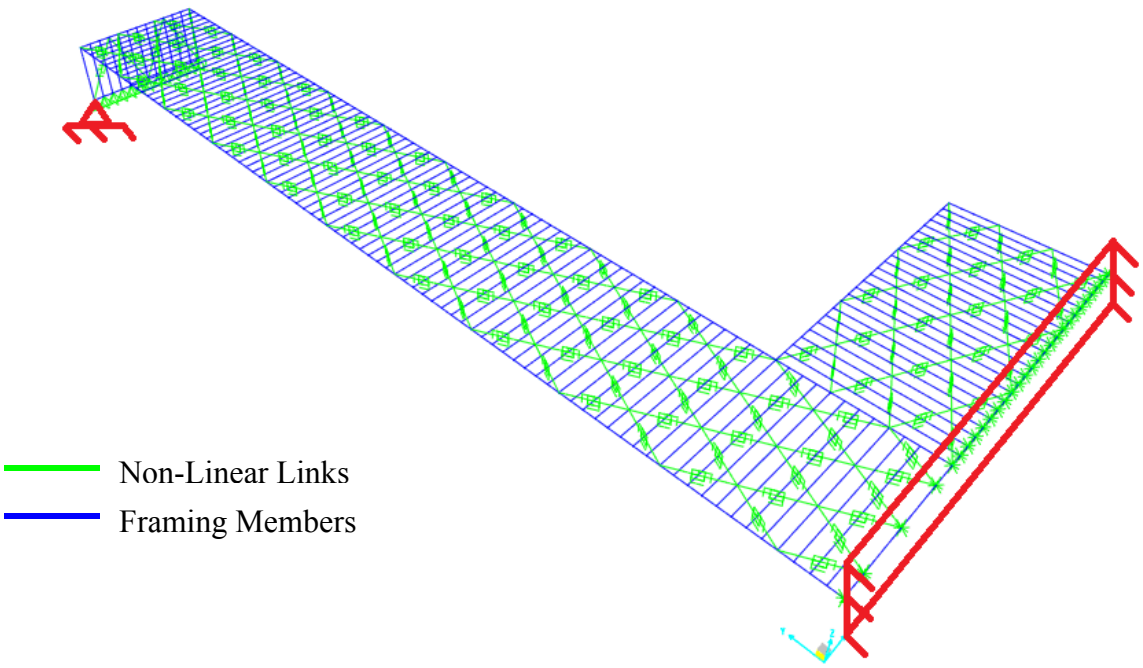

Figure 2.2 Model Configuration for Diaphragm Deflection Check

Equation 4.2.2-2 from SDPWS was used to manually calculate the deflection of the diaphragm. It was assumed that no chord connection slip would occur, thus making that part of the equation zero. Values for the rest of the variables came from either the model itself or from manufacture's specifications. The diaphragm deflection was calculated to be 1.37 inches. A full calculation of the diaphragm deflection can be found in Appendix B. Since there is only a 0.02 inch or 1.5% difference between the diaphragm deflection given by SAP2000 and the calculated diaphragm deflection from SDPWS it was presumed that the models were acting reasonably.

In another check the model was configured like a shear wall and the deflection computed in SAP2000 was compared to the deflection calculated from Equation 4.3-1 of the SDPWS. In this configuration all the walls were removed and the end of the diaphragm containing the consistent leg was restrained as fixed. This configuration can be seen in Figure 2.3. A point load of 2000lb was applied to the end of the variable leg which resulted in a maximum deflection in SAP2000 of 1.49 inches at the end of the variable leg. The deflection results from SAP2000 and the full analytical results are presented in Appendix B.

Equation 4.3-1 from SDPWS was used to manually calculate the deflection of the model configured as a shear wall. It was assumed that no chord connection slip would occur, thus making that part of the equation zero. Values for the rest of the variables came from either the model itself or from manufacture's specifications. The diaphragm deflection was calculated as 1.09 inches. Between the diaphragm deflection calculated in SAP2000 and from Equation 4.3-1 there is a 36% difference. This difference could be contributed to the orientation of the joist to the load. In a standard shear wall, studs are

oriented perpendicular to the applied load. In this case, because of how the model was set up, the joist are oriented parallel to the applied load. With the joist oriented parallel to the applied load instead of perpendicular when the model is analyzed as a shear wall it is going to be more flexible and thus deform more. Equation 4.3-1 assumes

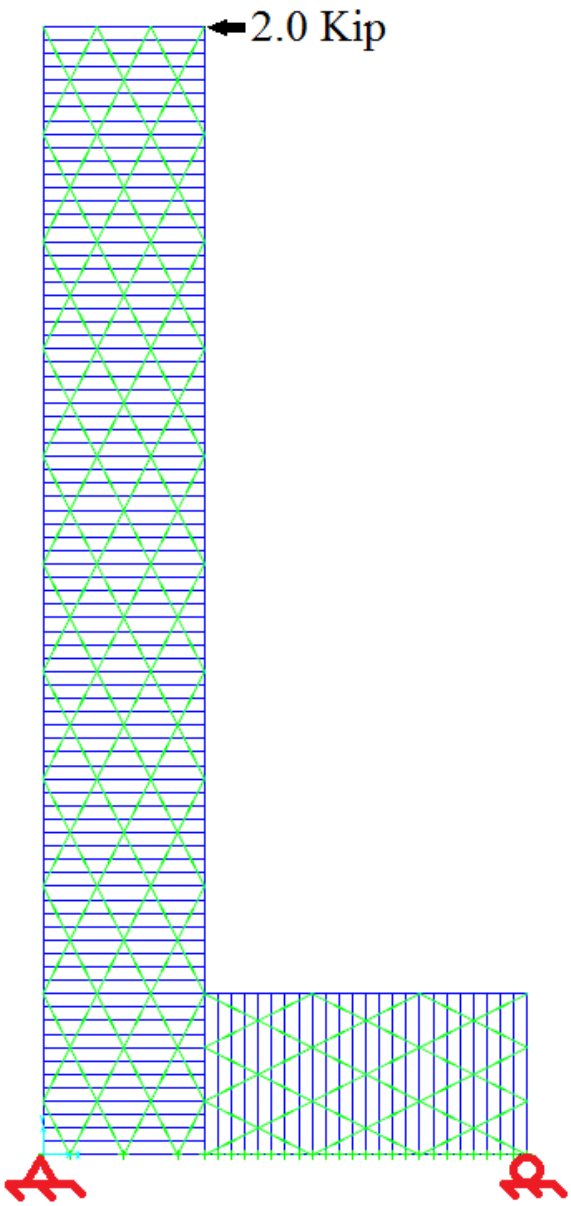

Figure2.3 300% Model Configured as a Shear Wall

that the joist or studs are configured perpendicular to the applied load. This explains why the deflection in SAP2000 is greater than the deflection calculated from Equation 4.3-1. Having shown that the models acted similarly to real structures, the parametric study was initiated.

Another way the model was verified was by comparing the deflected shapes and forces in the model to what you would expect from beam analysis. The model with the variable leg being 300% of the constant leg was again used in this comparison. In the model's original condition, without any modifications, it was assumed that under loading, the model would behave like a simply supported beam with one support being the end wall at the end of the variable leg and the other support being at the reentrant corner where the variable leg comes into the constant leg. This configuration can be seen in Figure 2.4.

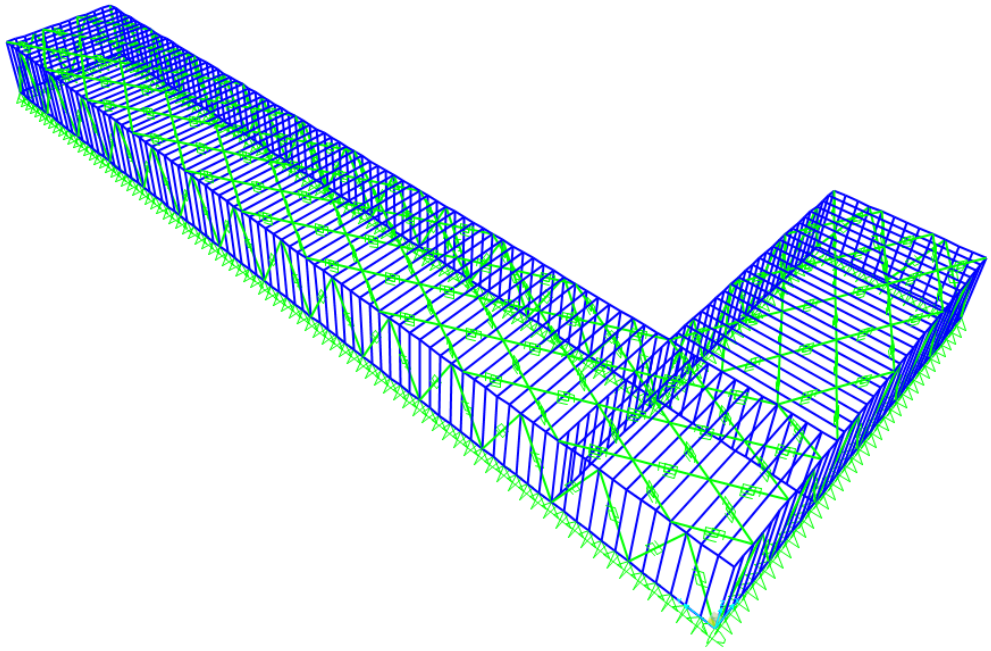

Figure 2.4 300% Model without any modifications

In a simply supported beam, the maximum deflection and moment occurs at the mid-span of the beam and are zero at either end of the beam. The model loaded with a 115 plf uniform load going right to left. In this configuration, the model deformed similarly to how a simply supported beam deforms. The undeformed shape verses the deformed shape can be seen in Figure 2.5.

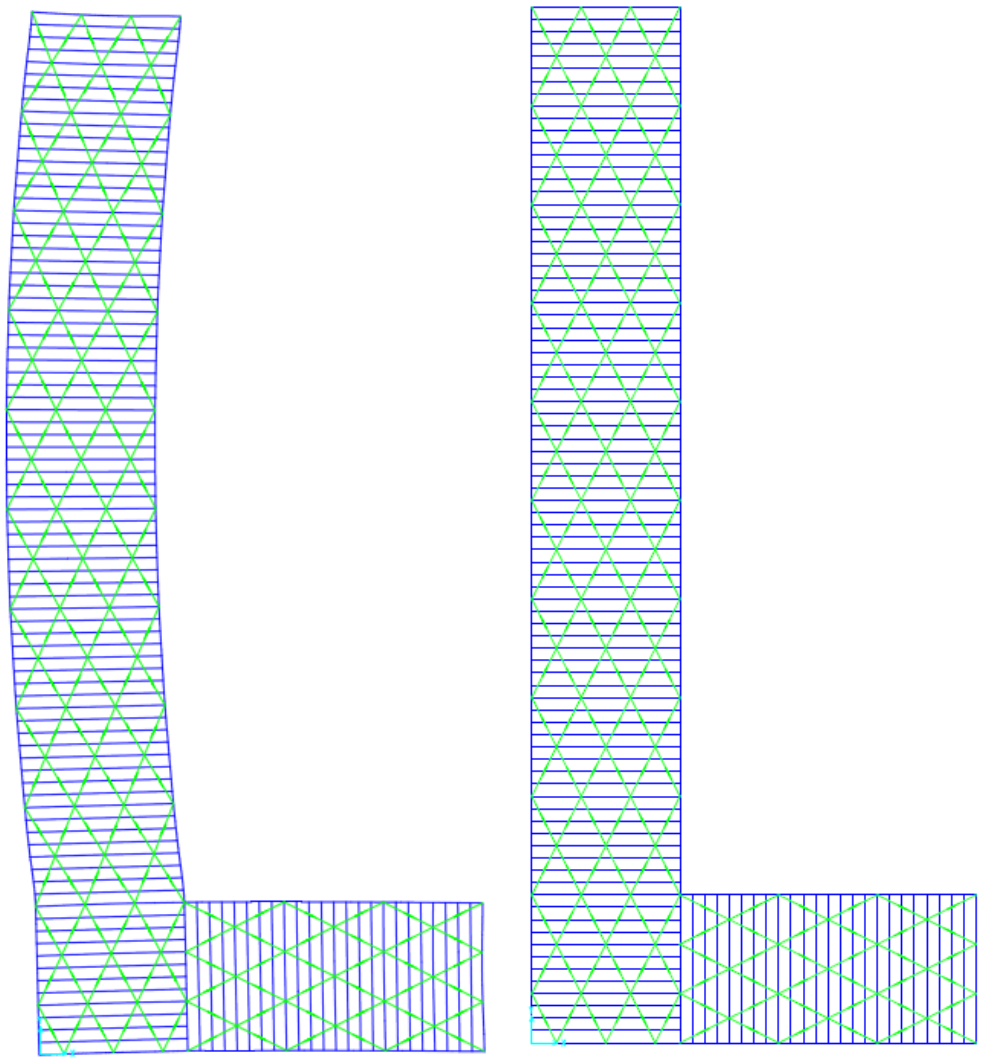

Figure 2.5 Deformed shape verses undeformed shape of 300% model

The maximum axial forces in the chords of the diaphragm in the model at the mid-span, the end of the variable leg, and at the reentrant corner were compared to determine where the maximum forces were occurring. As with a simply supported beam, where the maximum moment is at the mid-span, the maximum axial forces in the model chords were found at the mid-span and decreased in value as you moved to the supports. The comparison of the axial forces can be seen in Figure 2.6 and Table 2.1.

Maximum Axial Load	
Member	P (kip)
1	5.854
4	0.829
305	-2.386
337	-7.295
338	-7.152
339	-7.152
340	-7.152
341	-7.151
342	-7.152
343	-7.152
344	-7.244
551	7.409
803	-2.443
871	-2.443
872	-2.443
873	-2.443
875	-2.445
876	-3.484
877	-3.484
878	-3.484

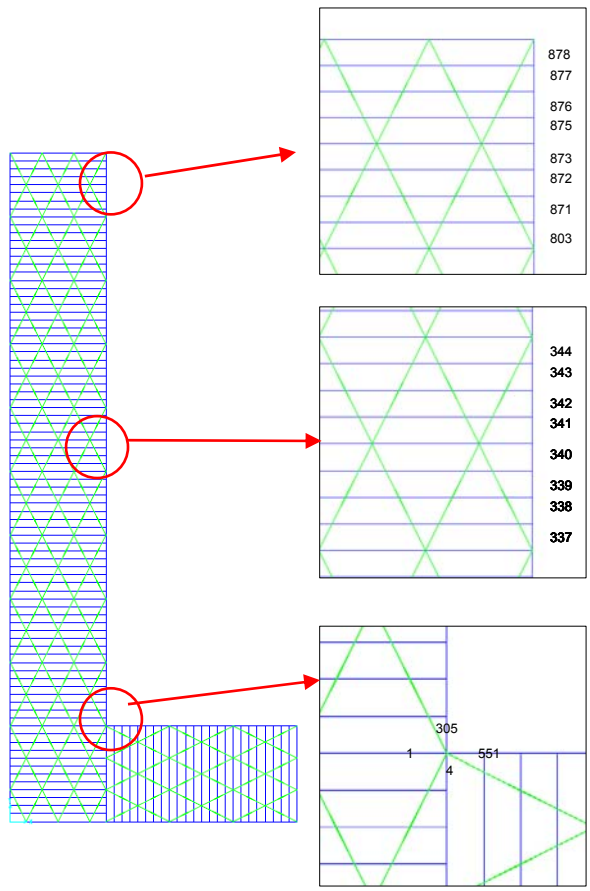

Figure 2.6 Labeled Axial Members at reentrant corner, mid-span, and end of 300% Model
Table 2.1 Axial forces at reentrant corner, mid-span, and end of 300% Model

It was also noted that the axial forces at the end of the variable leg, and at the reentrant corner were not zero as you would expect with a simply supported beam. This was found

to be from the non-linear links and the residual force left in them. With the addition of more links in the roof diaphragm to reduce the residual effect, the forces at the end of the variable leg and at the reentrant corner did decrease and were more inline with the simply supported beam theory. This test was rerun with the uniform load going from left to right instead. The results were again consistent with the simple beam theory. The model deformed similarly to a simply supported beam with the maximum axial force noted at the mid-span. The results from this test can be found in Figure 2.7 and Table 2.2.

Maximum Axial Load	
Member	P (kip)
1	-8.648
4	-1.862
305	-0.878
337	7.281
338	7.105
339	7.105
340	7.104
341	7.105
342	7.105
343	7.104
344	7.163
551	-9.067
803	0.445
871	0.445
872	0.445
873	0.445
875	0.457
876	1.237
877	1.237
878	1.237

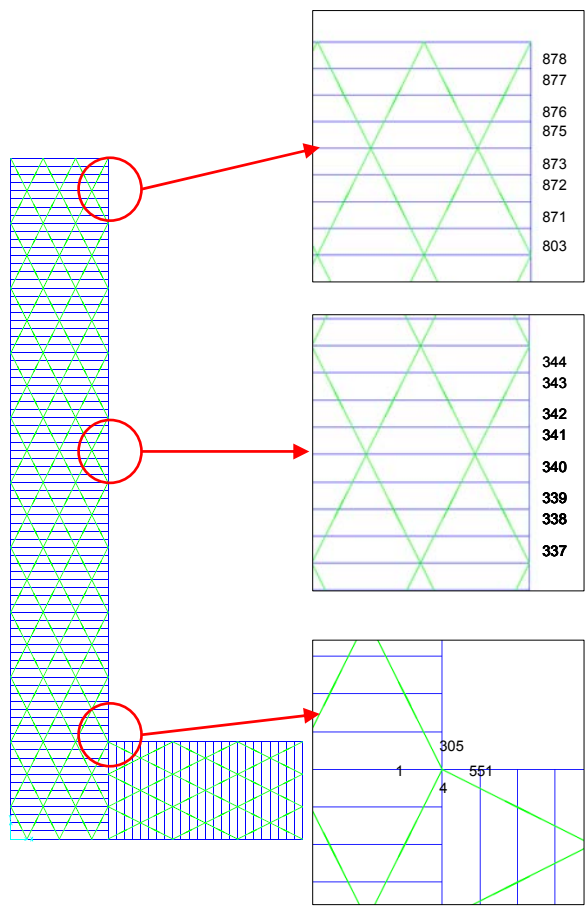

Figure 2.7 300% Model and deformed shape with Uniform load going from left to right
Table 2.2 Axial forces in the 300% Model with uniform load going from Left to Right

Beyond comparing the model to a simply supported beam, it was also compared to a cantilever beam. In order that the model might behave like a cantilever beam, the end wall at the end of the variable leg was removed. The other end of the variable leg that butts up to the consistent leg was assumed for comparison purposes to be the fixed end. In this configuration it was assumed that the maximum deflection would be at the end of the variable leg and the maximum axial forces would occur at the reentrant corner. This would be consistent with cantilever beam theory where the maximum deflection occurs at the free end and the maximum moment occurs at the fixed end. The model was then loaded again from right to left with an 115plf uniform distributed load. As expected the maximum deflection occurred at the end of the variable leg and the maximum axial force was found to be in the reentrant corner. These results can be found in Figure 2.8 and Table 2.3.

Maximum Axial Load	
Member	P (kip)
1	13.811
4	4.461
305	-0.26
337	-9.362
338	-6.199
339	-6.188
340	-6.178
341	-6.169
342	-6.16
343	-6.15
344	-3.189
551	16.014
803	-2.106
871	-2.106
872	-2.016
873	-2.016
875	-2.108
876	0.093
877	0.093
878	0.093

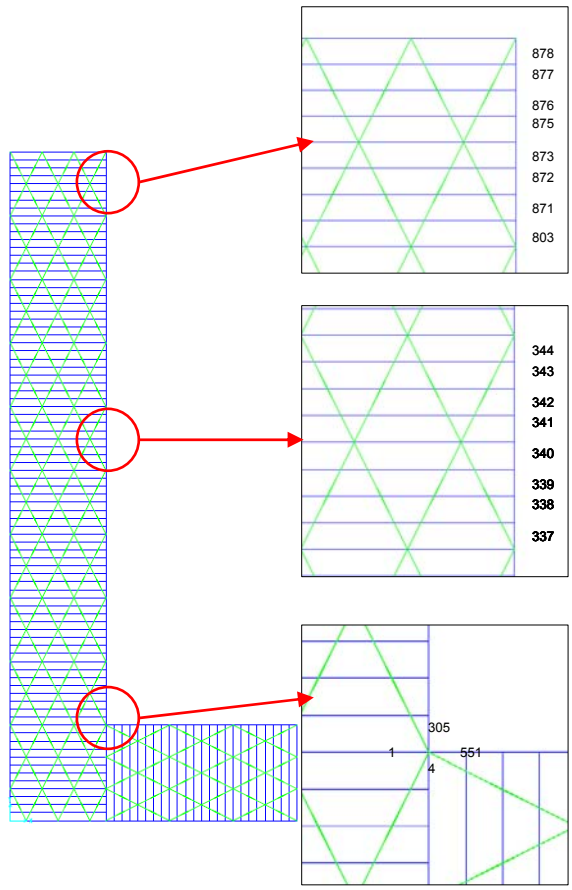

Figure 2.8 300% Model with end wall removed
Table 2.3 Axial forces in the 300% Model without end wall

One of the last verifications used was to compare the axial forces in the reentrant corner under three different configurations. The first configuration was the 300% model that has previously been used, without any modifications. This configuration can be seen in Figure 2.4. The second configuration consists of the 300% model without the non-linear links in the side walls. The links were left in the end wall at the end of the variable leg so as to act as a support for the variable leg. This second configuration can be seen in Figure 2.9. This configuration was used to investigate whether the shear walls oriented perpendicular to loading significantly affected the response of the diaphragm. The concern is whether the individual studs begin to resist the diaphragm loading by developing axial loads due to the rotation of the studs as the diaphragm deflects.

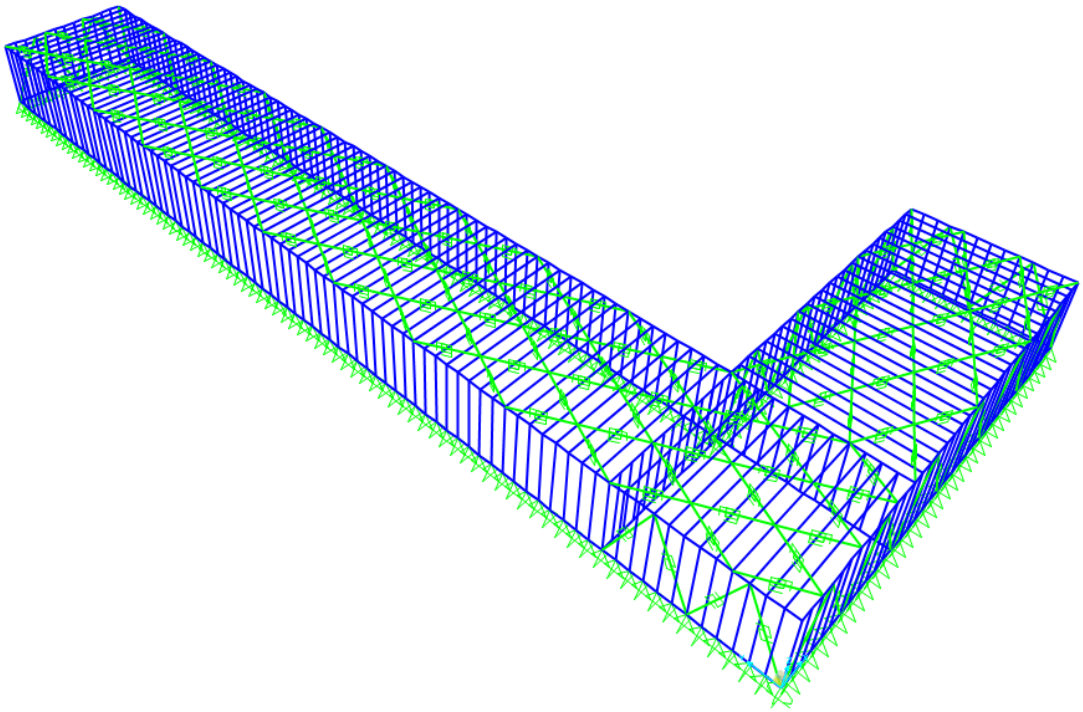

Figure 2.9 300% Model without non-linear Links removed in side walls

The third and final configuration consisted of the roof diaphragm only. The end wall at the end of the variable leg was left to provide a support for the diaphragm. Restraints were also added to the constant length leg, making it fixed, and therefore adding support to the other end of the variable leg. This configuration can be seen in Figure 2.10.

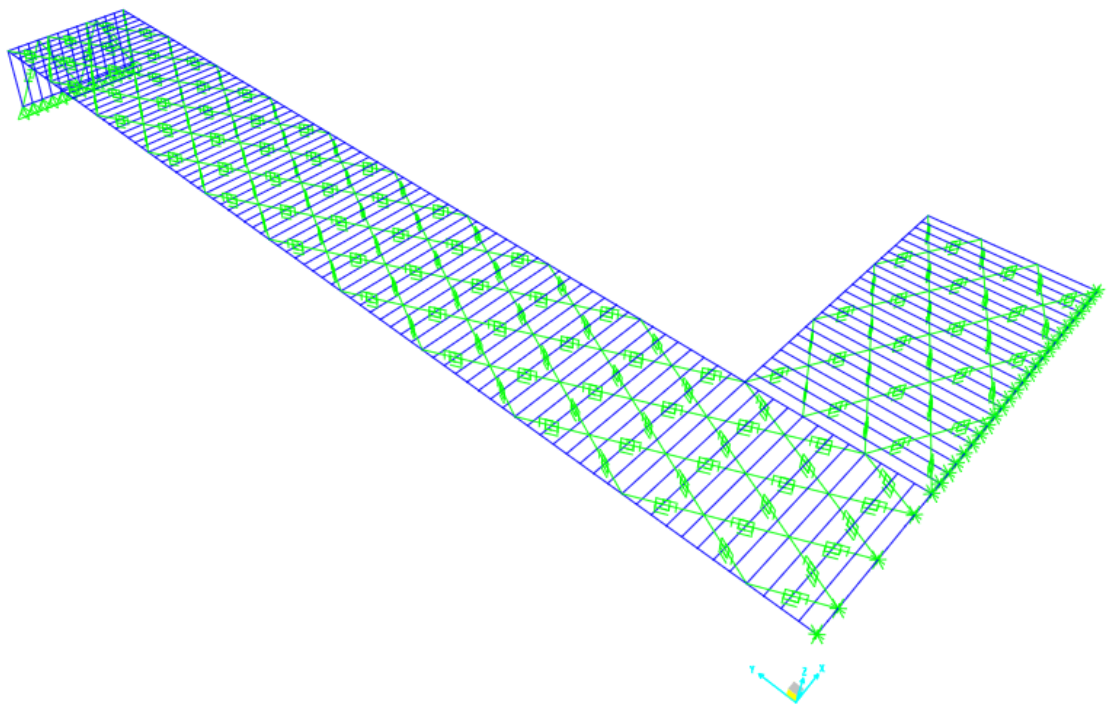

Figure 2.10 300% Model with roof diaphragm only

Each of these configurations were loaded from right to left with the same 115plf uniform distributed load. The axial forces in each of theses configurations were then compared. These results can be seen in Table 2.4.

Table 2.4 **Compared Axial Forces between Models**

Frame Member Forces			
	Diaphragm Only	w/o Links in Walls	300% Model
Member	P (Kip)	P (Kip)	P (Kip)
1 (Interior Strut)	6.682	6.381	5.854
4 (Interior Chord)	11.228	1.354	0.829
305 (Exterior Chord)	3.325	-1.719	-2.386
337	-17.561	-10.308	-7.295
338	-17.561	-10.309	-7.152
339	-17.561	-10.309	-7.152
340	-17.561	-10.309	-7.152
341	-17.56	-10.309	-7.151
342	-17.56	-10.31	-7.152
343	-17.56	-10.31	-7.152
344	-17.56	-10.312	-7.244
551 (Exterior Strut)	7.531	7.893	7.409
803	-6.195	-3.384	-2.443
871	-6.195	-3.384	-2.443
872	-6.195	-3.384	-2.443
873	-6.195	-3.384	-2.443
875	-6.202	-3.388	-2.445
876	-6.202	-3.388	-3.484
877	-6.202	-3.388	-3.484
878	-6.202	-3.388	-3.484

Members in 300 range are in middle of long leg
Members in 800 range are at end of long leg

From the results, the configuration that consists of only the roof diaphragm has the largest axial forces in the reentrant corner and the 300% model has the smallest axial forces in the reentrant corner. This difference in axial force was noted primarily for the

interior and exterior chord as there was no significant difference between the axial forces in the interior and exterior strut between these different configurations. Based on the results, the addition of stud-walls and sheathing (as represented by the non-linear links) removes load from the top chord and transfers it to the foundation rather than transferring the load through the diaphragm to the constant leg of the diaphragm. While in reality you cannot have a “floating diaphragm” as configured in the diaphragm only model, the results for the configuration without links in the walls, and for the 300% model are consistent with what would be found in real structures. The addition of sheathing on a stud wall in a real building stiffens the wall thus decreasing the deflection in the wall under loading.

CHAPTER 3: RESULTS AND DISCUSSION

3.1 Introduction

The objective of this parametric study was to examine the force concentration resulting in the reentrant corner under a lateral loading event, so as to improve understanding on the issue. Combined, 30 different models were analyzed in this study. Because of the high volume of data obtained from this study, a side-by-side analysis of each of the models will not be preformed. A thorough explanation of how the data was organized and arranged in general terms will be made. The remaining part of this chapter focuses on the trends found in the data. Individual model results can be found in Appendix E.

3.2 Parametric Study Results

For this analysis, the interior and exterior chords, and the interior and exterior struts adjacent to the reentrant corner were primarily examined. These members are labeled in Figure 3.1. Each of these members, under a finite element analysis was divided into 5 elements. The maximum axial force (either in tension or compression) was then selected and compared against results for the other members and the other models. This was done for each of the interior and exterior chords and struts in each of the models. The results were then tabulated and arranged in a chart so that trends could be identified.

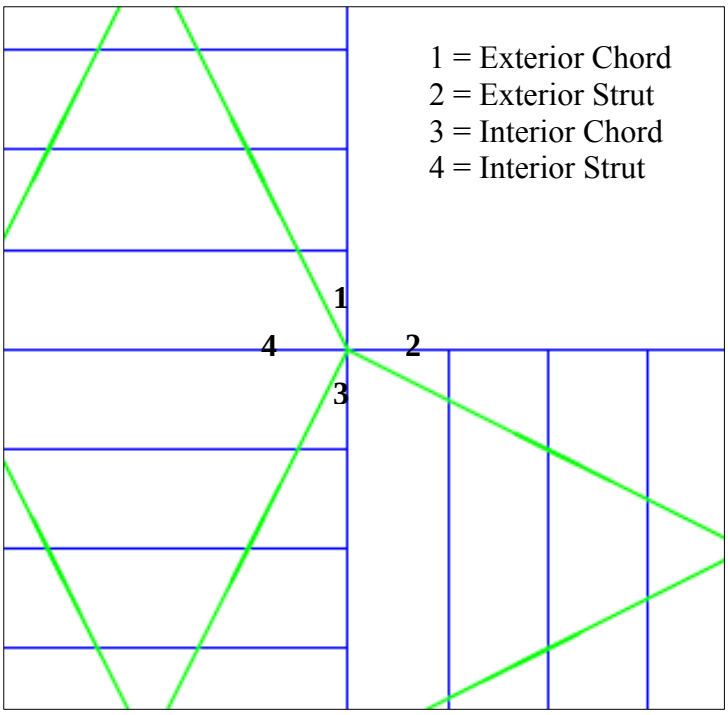

Figure 3.1 Labeled interior and exterior chords and struts

3.2.1 Exterior and Interior Strut Results

The exterior and interior struts exhibited similar results in the parametric study. As expected, the results for force magnitude for both the interior and exterior strut were linear, increasing as the length of the variable leg increased, with the axial force in the exterior strut being slightly more than the axial force in the interior strut. This linear increase was expected since the force for the reaction of a diaphragm idealized as a simple beam would increase linearly as the beam length increased. Results for the exterior and interior struts can be found in Table 3.1 and Figure 3.2.

Table 3.1 Maximum Axial forces for the Exterior and Interior Struts.

Maximum Axial Force		
Model	**Exterior Strut**	**Interior Strut**
15	0.008034	-0.324
25	0.321	-0.032
50	0.741	0.444
75	1.351	1.118
100	1.768	1.581
125	2.436	2.316
150	2.925	2.856
175	3.657	3.661
200	4.234	4.295
225	5.007	5.147
250	5.621	5.825
275	6.427	6.716
300	7.319	7.699

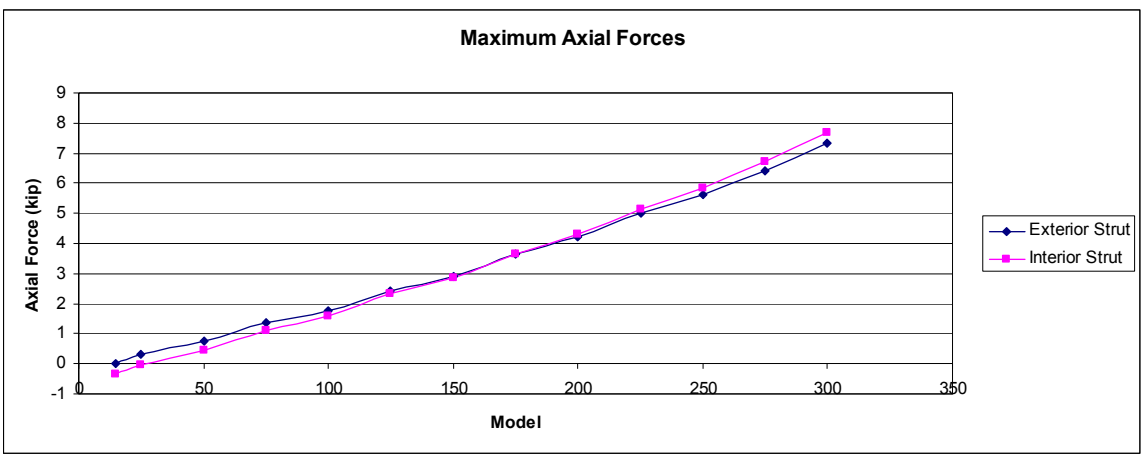

Figure 3.2 Maximum Axial forces verse length of variable leg

3.2.2 Exterior and Interior Chord Results

Like the exterior and interior struts, the results for the exterior and interior chords exhibited similar patterns. However, unlike the exterior and interior struts, the results for the exterior and interior chords were not linear. Instead, they were more parabolic; the

axial forces in the interior chord were greater than the axial forces in the exterior chord. Part of the reason why the exterior chord has slightly lower axial forces could be that the exterior chord has a more direct load path than the interior chord. That is because the exterior chord sits on top of an exterior wall, which also acts as a shear wall. The interior chord, however, is not sitting over a shear wall. The interior chord is acting as a drag strut, or collector, dragging the shear along its length until it reaches a point where the load can be transferred down to the foundation; which, in this case, is at the reentrant corner. Since the interior chord is dragging some of the shear from the diaphragm, the resulting axial forces in it are going to be greater than those in the exterior chord. The trends in the axial forces for both the exterior chord and interior chord can be seen in Figure 3.3 and Table 3.2. It was initially assumed that the trend in the axial forces for the interior and exterior chord would be linear, like the trend in the axial forces in the interior and exterior struts. Since this was not the case, other aspects of beam theory were examined. in order to understand the results for the interior and exterior chords.

Table 3.2 Maximum Axial forces for the Exterior and Interior Chords

Maximum Axial Force		
Model	**Exterior Chord**	**Interior Chord**
15	-0.067	-0.107
25	-0.152	-0.121
50	-0.375	-0.243
75	-0.511	-0.247
100	-0.705	-0.325
125	-0.727	-0.218
150	-0.808	-0.19
175	-0.7	0.035
200	-0.653	0.184
225	-0.441	0.497
250	-0.292	0.725
275	-0.009607	1.092
300	0.298	1.489

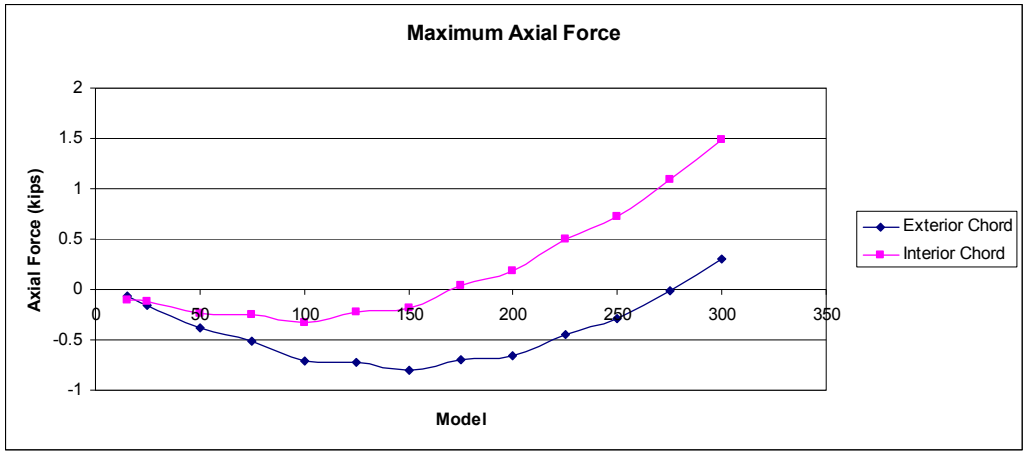

Figure 3.3 Maximum Axial force verses length of variable leg in Interior and exterior chords

One of these other aspects was the deformed shape and deflection of the models. To examine this aspect further, an examination of the displacement of nodes was preformed. For this comparison, the displacement of the node at the reentrant corner and the displacement of the node at the end of the variable leg were examined. The locations of these nodes can be seen in Figure 3.4.

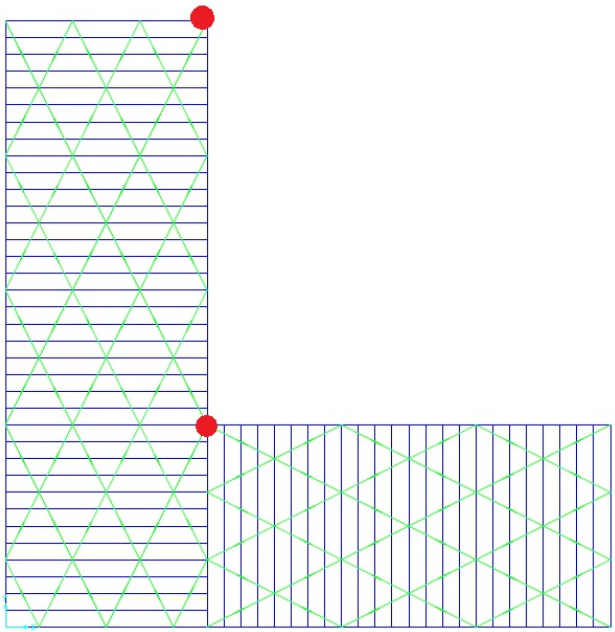

Figure 3.4 Location of nodes used to compare relative displacement

The nodes locations were compared from their original, undeformed starting location to their displaced location after loading. Knowing the initial distance between the nodes and their displacement from their original location, it was possible to determine how the length of the variable leg either elongated or shrank under loading. The results for the difference in length between the undeformed length and deformed length were then tabulated. It was determined from these results that this change in length had the same trend as the axial forces in the exterior and interior chords. This similarity in the trends of the data can be seen in Figure 3.5. Since the change in length and axial forces had the same trend, it can be concluded that a correlation exists between the deformation of the variable leg and the magnitude of the axial forces in the reentrant corner.

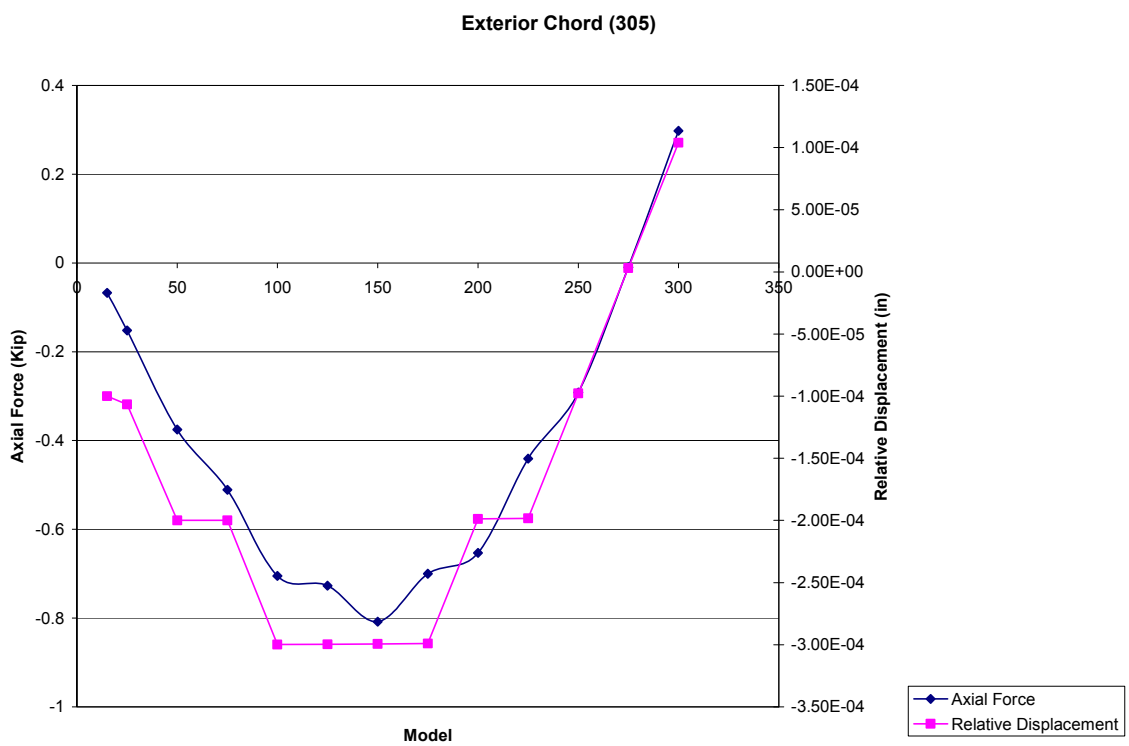

Figure 3.5 Comparison of Maximum axial forces in models and relative displacement in the models

Since the trend in the data between the axial forces in the interior and exterior chords and the change in distance between the node at the reentrant corner and the end of the variable leg were so similar, led to examining how chord forces are determined for a diaphragm. Chord forces for the diaphragm are determined by dividing the bending moment of the diaphragm by the depth of the diaphragm. In the 15% model, the smallest model in this study, the bending moment near the reentrant corner is relatively minimal compared to the depth of the diaphragm. In this case the diaphragm is quite stiff and doesn't deform as much. This results in low chord forces. Since the bending moment is a function of the length of the diaphragm, as the length of the diaphragm changes so does the bending moment. For the smaller models, such as the 15% model through 75% model, the diaphragm acts more like a propped cantilever. In these cases the diaphragm in the variable leg is quite stiff so almost acts in one unit with the constant leg under loading. As the length of the variable leg increases it starts to become more flexible thus starts to behave more like a simply supported beam than a propped cantilever. As it transitions from a propped cantilever to a simply supported beam, the diaphragm in the variable leg becomes more flexible and starts to act and deform separately from the constant leg. It is this transition between the diaphragm acting like a propped cantilever and a simply supported beam that causes the trend in the axial forces interior and exterior chords to be more parabolic. In the 15% model through the 75% model the diaphragm act more like a propped cantilever system leading to the negative trend in the data. Between the 75% model and the 225% model the diaphragm is transitioning from a propped cantilever system to a simply supported beam system. This is the area in the data where the direction is changing from a negative slope to a positive slope. Finally,

from the 225% model to the 300% model the diaphragm acts like a simply supported beam system. This causes the positive trend for the axial forces in the interior and exterior chord.

3.2.3 Interior Wall Results

The second part of this study examined how the addition of interior shear walls, to the variable leg of the building, affected the forces in the reentrant corner. As assumed, the addition of interior walls decreased the axial forces in the reentrant corner, with the most significant decrease in forces seen in the addition of just one interior shear wall. After the addition of 4 interior shear walls, the change in the magnitude of the axial forces in the members becomes insignificant. The decrease in axial forces in the interior and exterior chord and interior and exterior strut can be attributed to the aspect ratio of the diaphragm of the variable leg. In examining the 300% model, the aspect ratio of the variable leg was 6:1. This aspect ratio can be seen in Figure 3.6.

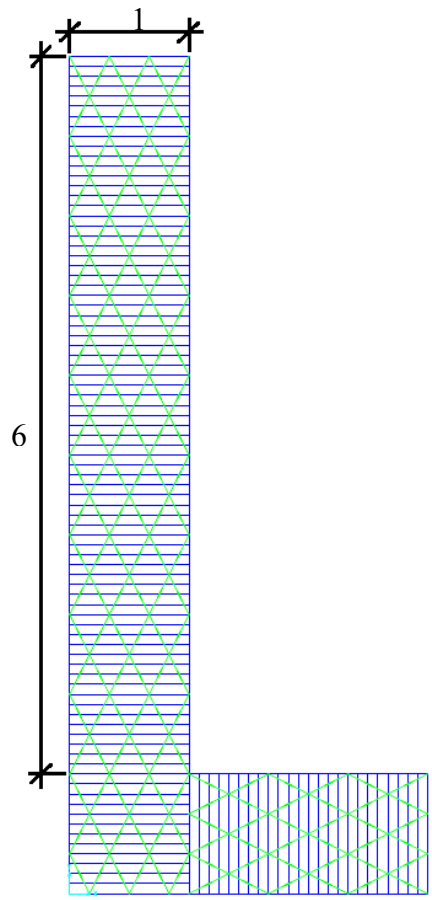

Figure 3.6 1:6 Aspect Ratio in Variable leg

In this situation, the variable leg can be compared to a long, slender, simply- supported beam. By using a slender beam verses a deeper beam, the deflection and bending stresses in the slender beam are going to be greater than those in the deeper beam under the same loading. In the case of the beams, the deeper beam, which has a larger cross sectional area resulting in a larger section modulus and moment of inertia, has more capacity for shear and bending than the slender beam. Since the deeper beam has more capacity because of its section properties, under the same loading as the slender beam, the deeper beam will have lower stresses and lower deflection than the slender beam. This is equivalent to aspect ratios in diaphragms. The 300% model with a 6:1 aspect ratio is equivalent to the slender beam. The addition of one interior wall, at the mid-span of the

variable leg, changes the aspect ratio of the variable leg to 3:1. This change in the aspect ratio can be seen in Figure 3.7.

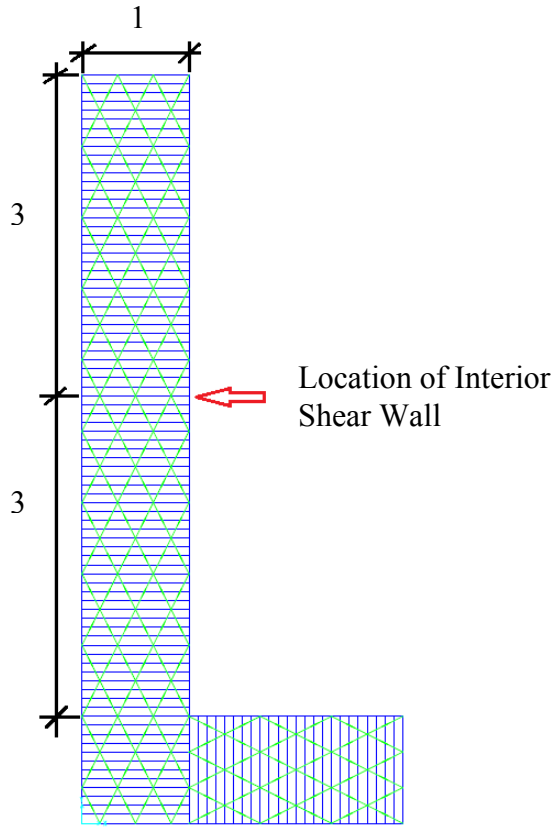

Figure 3.7 1:3 Aspect Ratio in Variable leg with the addition of one interior wall at the mid-span

This change in the aspect ratio essentially "deepens" the diaphragm, giving it greater shear capacity and thus reducing the deflection and axial forces. By adding more interior walls, the aspect ratio of the diaphragm continues to decrease, therefore increasing the capacity of the diaphragm. That results in lower forces. In the case of this study, it was found that after the addition of 4 interior walls, or a diaphragm aspect ratio of 1.2:1, no significant changes occurred in the resulting axial forces for both the interior and exterior chord and interior and exterior strut, if the aspect ratio continued to decrease.

Another reason for the decrease in axial forces in the reentrant corner, with the addition of interior walls, is the load path. In the 300% model, the load has to be transferred through the sheathing (links) to the exterior walls before it can be transferred to the foundation. The distance that the load had to be transferred through can be seen in Figure 3.8.

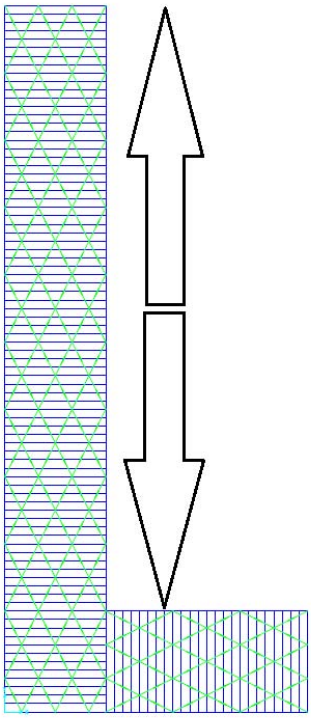

Figure 3.8 Load path of 300% model without any interior shear walls

The addition of the interior walls provided a more localized load path to the foundation, thus decreasing the distance through which the load has to travel to be transferred to the foundation. This shortening of the length reduces the forces and deflection. The load path with the addition of one interior shear wall can be seen in Figure 3.9.

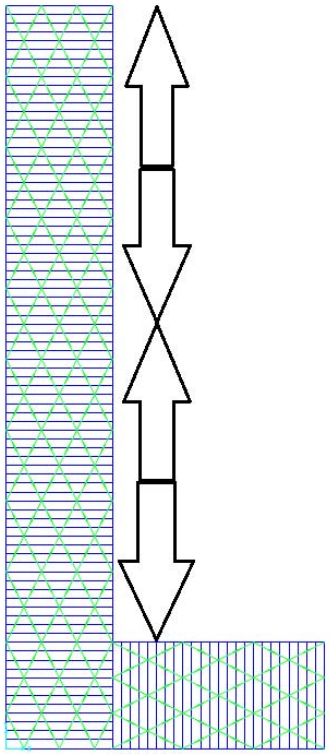

Figure 3.9 Load Path with the addition of 1 interior shear wall

Each of the four members being examined exhibited a similar trend in the data. The decrease in the forces in the reentrant corner was due to the additional shear walls taking a portion of the load, and thereby reducing both the shear and bending forces at the reentrant corner. Results for the axial forces verses the number on interior shear walls are shown in Table 3.3 and Figure 3.10.

Table 3.3 Maximum Axial Force in reentrant corner with the addition of Interior Shear Walls

TABLE: Element Forces				
# of Interior walls	**Axial Force (Kip)**			
	Interior Strut Member 1	Interior Chord Member 4	Exterior Chord Member 305	Exterior Strut Member 551
0	7.699	1.489	0.298	7.319
1	2.919	0.066	-0.498	2.985
2	1.745	-0.11	-0.472	1.922
3	1.306	-0.186	-0.475	1.524
4	0.716	-0.108	-0.266	0.994
5	0.615	-0.164	-0.313	0.901
6	0.597	-0.191	-0.342	0.884
7	0.504	-0.217	-0.353	0.798
8	0.203	-0.152	-0.23	0.533

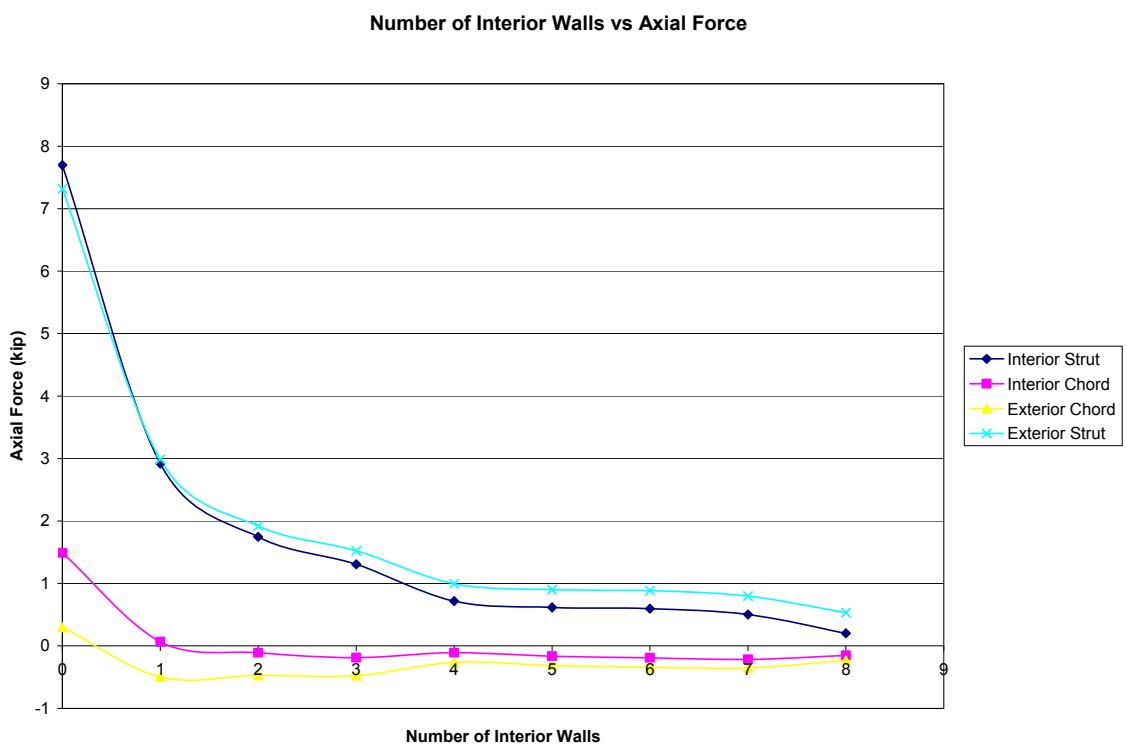

Figure 3.10 Axial Forces in Reentrant Corner verses number of interior Shear walls

This study was conducted a second time with the addition of a shear wall at the reentrant corner acting to supplement the interior strut. The results were almost identical to the models that did not have a shear wall at the reentrant corner. The only difference was that the axial forces were lower with the addition of the shear wall at the reentrant corner. The reason why the axial forces were lower with the addition of a shear wall at the reentrant corner was because the shear wall provided a more localized load path to the foundation. Without the shear wall, the load path, that the resulting shear in the reentrant corner would take, was through the diaphragm sheathing (or links, in this case) to the exterior walls, before it could be transferred down to the foundation. In the case of the shear wall at the reentrant corner, the shear forces could be transferred directly to the foundation through the shear wall, instead of having to be transferred through all the diaphragm sheathing first. The shorter load path results in lower axial forces in the reentrant corner. Again, the most significant change in magnitude of the forces was seen with the addition of just one interior shear wall in the variable leg. Also, the change in magnitude of the forces is due to the aspect ratio of the variable leg. Starting with the 300% model, the aspect ratio is 6:1, and has the longest length between lateral lines of support. By adding interior lines of shear, both the aspect ratio and length between lines of support are decreased. Since the forces resulting in the diaphragm are related to aspect ratio and length between supports, by decreasing the aspect ratio and length between supports the forces are also decreased. The same can be said of the deflection in the diaphragm, as well. After the addition of 4 interior shear walls, or an aspect ratio of 1.2:1, with the exception of the shear wall at the reentrant corner, the change in

magnitude in the axial forces became insignificant. Results for the axial forces verses the number on interior shear walls can be found in Table 3.4 and Figure 3.11.

Table 3.4 Maximum Axial Force in reentrant corner with the addition of Interior Shear, including shear wall at reentrant corner

TABLE: Element Forces (Wall at Reentrant Corner)*				
# of Interior walls	**Axial Force (Kip)**			
	Interior Strut Member 1	Interior Chord Member 4	Exterior Chord Member 305	Exterior Strut Member 551
0	5.322	1.933	0.574	4.515
1	1.837	0.421	-0.297	1.644
2	0.985	0.183	-0.311	0.96
3	0.664	0.079	-0.332	0.703
4	0.269	0.096	-0.168	0.389
5	0.186	0.04	-0.214	0.321
6	0.168	0.013	-0.243	0.305
7	0.094	-0.018	-0.257	0.245
8	-0.095	0.015	-0.148	0.09

Note: * Wall at Reentrant Corner is not counted as one of the Interior walls

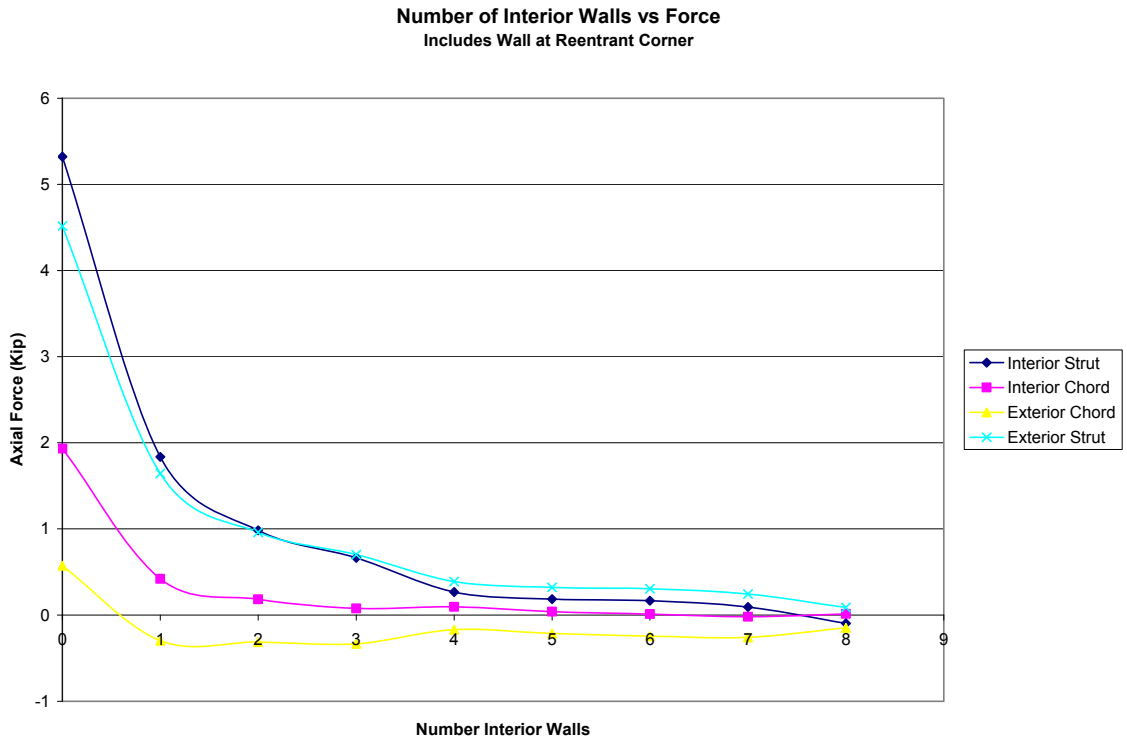

Figure 3.11 Maximum Axial Forces versus number of interior shear walls

3.2.4 Impact of Shear Walls on Axial Forces in Reentrant Corner

One result that was noticed in the verification of the models was how the addition of the side walls to the diaphragm significantly reduced the forces in the interior and exterior chords. In this verification three models were compared: the 300% model, the 300% model without the non-linear links, and a model that consisted only of the diaphragm. The configuration of these models can be seen again in Figure 3.12, Figure 3.13, and Figure 3.14 respectfully.

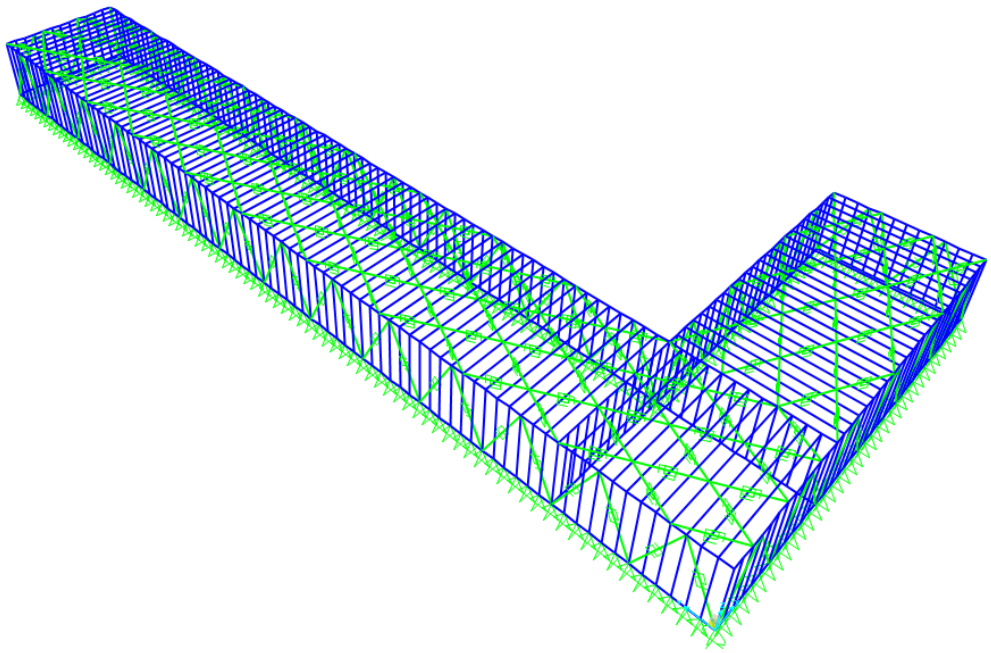

Figure 3.12 300% Model without any modifications

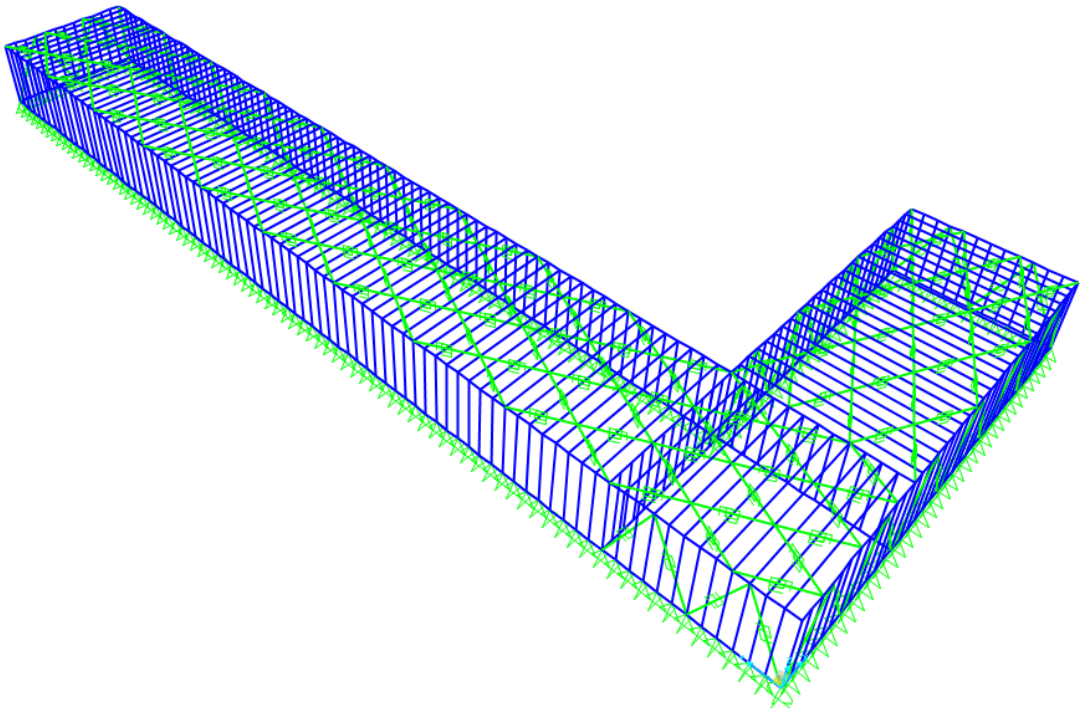

Figure 3.13 300% Model without non-linear Links removed in side walls

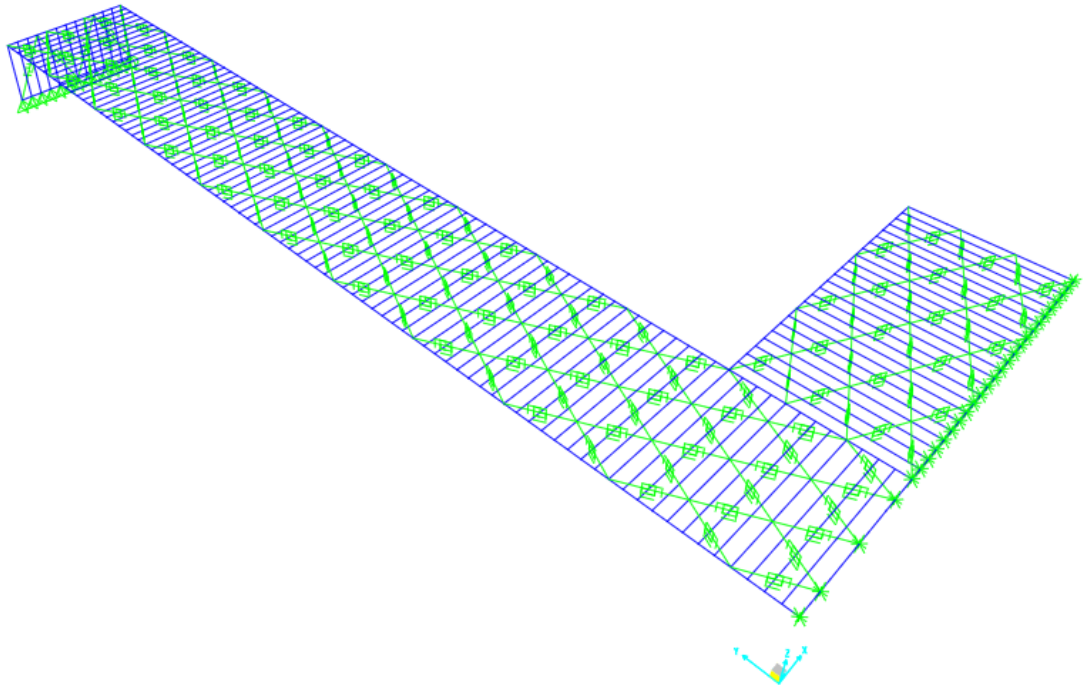

Figure 3.14 300% Model with roof diaphragm only

In comparing the axial forces for the interior chord between these three models it was found that the axial force for the interior chord in the diaphragm only model was 13.5 times greater than the axial force for the interior chord of the 300% model. It was also found that by adding sheathing to the stud wall that the axial force in the interior chord was decreased by about a third. These results as well as the results for other members can be found again in Table 3.5.

Table 3.5 Compared Axial Forces between Models

Frame Member Forces			
	Diaphragm Only	w/o Links	300% Model
Member	P (Kip)	P (Kip)	P (Kip)
1 (Interior Strut)	6.682	6.381	5.854
4 (Interior Chord)	11.228	1.354	0.829
305 (Exterior Chord)	3.325	-1.719	-2.386
337	-17.561	-10.308	-7.295
338	-17.561	-10.309	-7.152
339	-17.561	-10.309	-7.152
340	-17.561	-10.309	-7.152
341	-17.56	-10.309	-7.151
342	-17.56	-10.31	-7.152
343	-17.56	-10.31	-7.152
344	-17.56	-10.312	-7.244
551 (Exterior Strut)	7.531	7.893	7.409
803	-6.195	-3.384	-2.443
871	-6.195	-3.384	-2.443
872	-6.195	-3.384	-2.443
873	-6.195	-3.384	-2.443
875	-6.202	-3.388	-2.445
876	-6.202	-3.388	-3.484
877	-6.202	-3.388	-3.484
878	-6.202	-3.388	-3.484

Members in 300 range are in middle of long leg
Members in 800 range are at end of long leg

As was found in the previous section, the addition of interior shear walls dramatically reduces the axial forces in the interior and exterior chords and the interior and exterior struts in the reentrant corner. However the comparison between the diaphragm only model, the 300% model without the non-linear links, and the 300% model also shows how dramatically the addition of walls reduces the axial forces in the interior chord.

In following up with this, the deflections of these three models were also compared. For this the relative displacement between the node at the reentrant corner and the node at the end of the variable leg were compared to their original location. The location of these nodes can be seen in Figure 2.10.

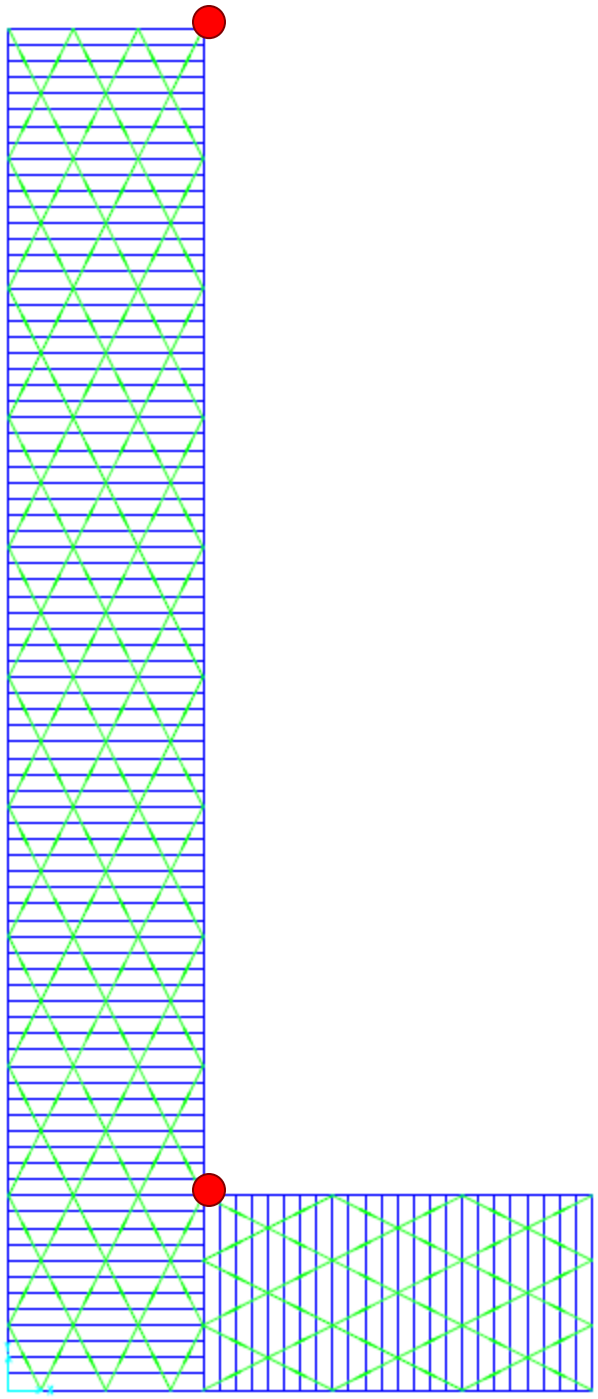

Figure 3.15 Location of Nodes for comparing relative displacement

In comparing the relative displacements between these configurations, the diaphragm only configuration was found to have the greatest relative displacement between the

nodes at 2.31 inches and the 300% model was found to have the smallest relative displacement between the nodes at 0.61 inches. The results for the relative displacements can be found in Table 3.6.

Table 3.6 Comparison of Relative Displacements between Models

Relative Displacement 300% Model			
Node at Reentrant Corner		Node at End of Leg	
Direction	Displacement (in)	Direction	Displacement (in)
X	-0.0951	X	-0.1674
Y	0.0478	Y	-0.051
Z	-0.00001287	Z	0.0004
Distance between Nodes (ft)×			143.949
Difference from Original Distance (in)*			0.6108
Relative Displacement W/out Springs in Walls			
Node at Reentrant Corner		Node at End of Leg	
Direction	Displacement (in)	Direction	Displacement (in)
X	-0.0989	X	-0.1649
Y	0.0568	Y	-0.0768
Z	-0.00001334	Z	0.0004
Distance between Nodes (ft)×			143.9231
Difference from Original Distance (in)*			0.9228
Relative Displacement Diaphragm Only			
Node at Reentrant Corner		Node at End of Leg	
Direction	Displacement (in)	Direction	Displacement (in)
X	-0.2738	X	-0.3063
Y	0.0072	Y	-0.1986
Z	-1.3068	Z	0.0007
Distance Between Nodes (ft)×			143.8073
Difference from Original Distance (in)*			2.312

Notes:
× Distances between Nodes comes from Data in AutoCad
* Original Distance between Nodes is 144ft

These results were consistent with the results for the axial forces. Based on the results, the addition of stud-walls and sheathing (as represented by the non-linear links) stiffens the diaphragm, reducing how much the diaphragm deflects, thus reducing the forces in the reentrant corner. While in reality you cannot have a “floating diaphragm” as

configured in the diaphragm only model, the results for the configuration without links in the walls, and for the 300% model are consistent with what would be found in real structures.

3.3 Discrepancies with Results

While the computer models behave similarly to how buildings behave in reality, there are a few discrepancies with the results. One of these discrepancies is with how the sheathing was modeled. Two non-linear links were used to model each piece of sheathing in the roof diaphragm. While each link has the capacity to take both compressive and tensile forces, it became evident in earlier versions of the models that when one link, instead of two, was used, the links either took only compressive forces or only tensile forces. This resulted in residual forces in the axial members. The representation of one link for the sheathing and the residual force can be seen in Figure 3.16.

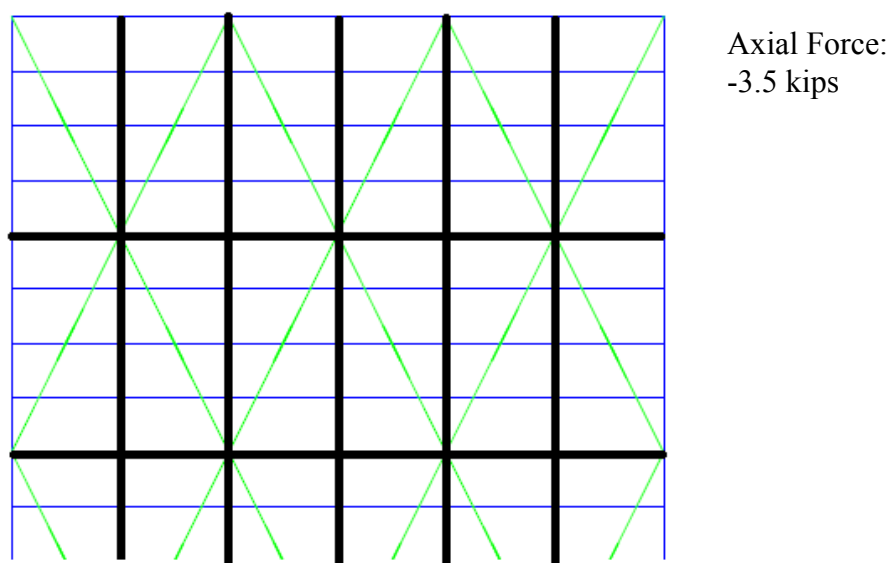

Figure 3.16 One Link used to represent one sheet of sheathing and the axial force of the top chord

Instead of in a simple beam, where the shear force is zero at the ends of the beam, the results in the models showed shear forces not equaling zero at the ends of the variable leg. The shear forces at the ends of the variable leg were found to be caused by the links and a tensile or compressive force in them. The links would then act on the top chord, which resulted in the shear forces at the ends of the beam. By adding a second link to represent each sheet of sheathing, the amount of shear that each link was trying to transfer was decreased, therefore decreasing the added load applied on the top chord of the diaphragm. This resulted in reduced shear forces at the end of the variable leg. The use of two links for a sheet of sheathing and the reduced axial force can be seen in Figure 3.17.

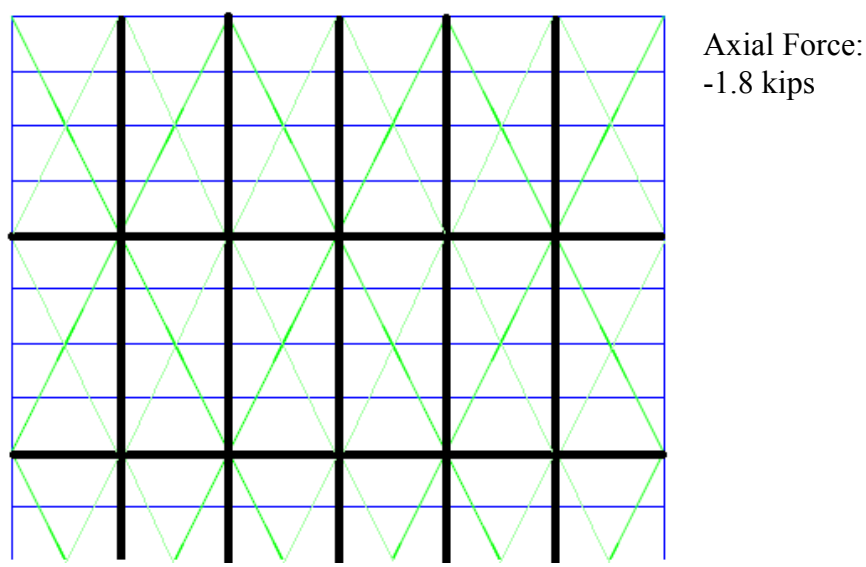

Figure 3.17 Two Links used to represent one sheet of sheathing and the reduction in the axial force of the top chord

While this significantly reduced the residual forces in the links, it did not eliminate them. Thus the results for the axial forces at the reentrant corner do contain some residual force from the non-linear links.

3.4 Discussion

Specifically, the results of this study focused on lateral load effects on the forces in the reentrant corner of single story, light-framed construction. Based on the results and knowledge of how structures behave under lateral loads, a discussion of how the results are applicable beyond the scope of this study can be made. One area of discussion is how the results would change as the height and number of stories in the structure change. Another area of discussion is how the results of the parametric study compare to how practicing engineers determine chord forces in structures.

3.4.1 How the Height of the Structure affects the Forces

Based on the scope of study, the results reflect how the length of the diaphragm and the number of interior shear walls affect the forces in the reentrant corner. What this study does not address is how the results would change as the height of the structure and number of stories change. Based on knowledge of how structures typically behave under lateral loading events one can interpolate how the results of this study might change. If one examines the shear stiffness of a column, it is in part a function of the length of the column cubed. As the length of the column increases, while other parameters such as material and section properties remain constant, the column becomes increasingly more slender and thus more flexible. This also applies to the shear stiffness of a building. As the height of the structure increases, while the plan dimensions of the structure remain constant, the structure becomes more flexible and thus deflects more. As was found in

this study, deflection has a direct correlation to the magnitude of the axial forces in the chord members at the reentrant corner. Since the top story of a multi-story building is going to deflect more than a single story building, as represented in the models, the axial forces in the chord members of the reentrant corner are also going to be greater in the top story of a multi-story building than the axial forces in the chord members in a single story building. And while the bottom story of a multi-story building won't deflect as much as the top story, again a function of height, it will have greater axial forces in the chord members since the loads are compounded as they are transferred down through the building. So while the deflection of the bottom story of a multi-story building might be more similar to the deflection of a single story building, the axial forces are going to be greater since they are compounded from above.

3.4.2 Comparison in determination of Chord Forces

In practice, most engineers idealize the diaphragm of structures to act as a simply supported beam. They then use the analog of a simply supported beam to determine the chord forces in the reentrant corner. As was found in the results of this parametric study that analog of a simply supported beam isn't always the correct analog when determining the chord forces in the reentrant corner. The results found that for most practical applications the diaphragm acts more like a propped cantilever system instead. (The simply supported beam analog worked for the 225% model and larger, however all of the models to which the simply supported beam analog was more appropriate exceeded the code maximum allowable aspect ratio of 1:3 for a diaphragm.) The axial forces for the interior and exterior chord were compared to calculated chord forces based on the simply supported beam analog and the propped cantilever analog. In comparing the calculated

chord force to the chord forces determined in SAP2000 it can be seen that the calculated chord force based on the simply supported beam analog is un-conservative. In comparing the axial forces of the interior and exterior chord to the chord forces determined by the propped cantilever analog it can be seen that in some cases the calculated chord force is un-conservative while in other cases the calculated chord force is extremely conservative. The comparison between the interior and exterior chord forces and the calculated chord forces based on the different analogs can be found in Table 3.7 and Figure 3.18.

Table 3.7 Comparison between Interior and Exterior Chord Force and Calculated Chord Forces based on different analogs.

Comparison of Chord Forces							
	Aspect Ratio						
	15%	25%	50%	75%	100%	125%	150%
Analog	Chord Force (Kips)						
Simply Supported Beam	-0.025	-0.048	-0.105	-0.163	-0.220	-0.228	-0.335
Propped Cantilever	0.002	-0.024	-0.211	-0.570	-1.102	-1.806	-2.683
Exterior Chord	-0.067	-0.152	-0.375	-0.511	-0.705	-0.727	-0.808
Interior Chord	-0.107	-0.121	-0.243	-0.247	-0.325	-0.218	-0.190
Combined	-0.074	-0.150	-0.369	-0.468	-0.716	-0.680	-1.006
Aspect Ratio	1:0.3	1:0.5	1:1	1:1.5	1:2	1:2.5	1:3

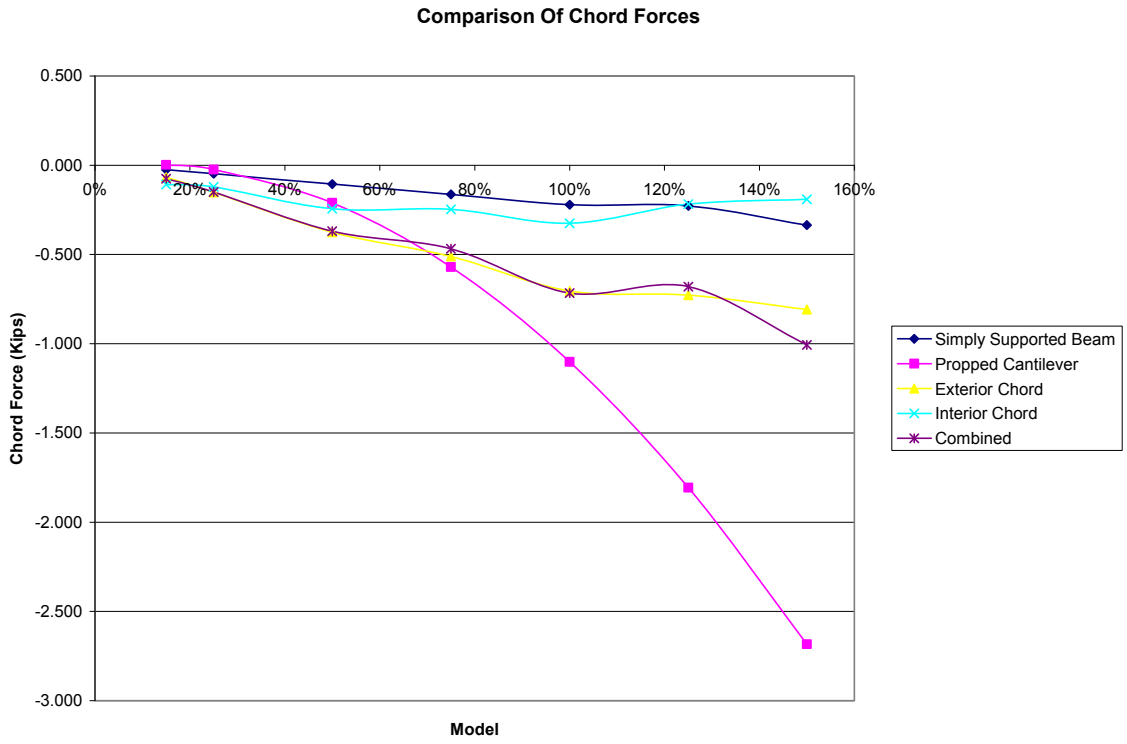

Figure 3.18 Comparison between Interior and Exterior Chord Force and Calculated Chord Forces based on different analogs

Since practicing engineers often do not have the time to perform a detail analysis to determine the chord forces, as was done in this study, a different analog is needed to better estimate what the chord forces are at the reentrant corner. A better estimation of the chord forces in the reentrant corner can be determined by combining the simply supported beam analog with the propped cantilever analog. While not exact, using a combination of the simply supported beam analog with the propped cantilever analog gives a better estimate of what the chord forces are than just using one analog alone. For a given diaphragm aspect ratio the following equations can be used to approximate the chord force at the reentrant corner:

Aspect Ratio <1:1 $$ChordForce = 3(\frac{Mss,x}{d}) + 1/4(\frac{Mpc,x}{d})$$

1:1 < Aspect Ratio < 1:2 $$ChordForce = 2(\frac{Mss,x}{d}) + 1/4(\frac{Mpc,x}{d})$$

1:2 < Aspect Ratio < 1:3 $$ChordForce = (\frac{Mss,x}{d}) + 1/4(\frac{Mpc,x}{d})$$

Where Mss,x is the bending moment at a given point x determined using the simply supported beam analog, Mpc,x is the bending moment at a given point x determined using the propped cantilever analog, and d is the depth of the diaphragm. These equations are for single story application and would need to be modified to determine the chord forces in a multi-story structure.

3.4.3 Trend in the Results for the Interior and Exterior Chord

Unlike the trend in the data for the interior and exterior struts were the results were intuitive and made logical sense, the results for the interior and exterior chord were not necessarily intuitive and did not make logical sense based off of a primary examination. Intuitively, based on the configuration of the models the system should act as a cantilever beam with the end of the variable leg being the free end and the connection at the reentrant corner assumed to be fixed. If this was the true case, the chord members at the reentrant corner should be in tension instead of in compression as was found in the results. Because of the residual forces found in the non-linear links, the models were examined again to determine if the residual force was causing the chord members to go into compression instead of tension. To examine if this was the cause of the results, the non-linear links were removed at the reentrant corner. This included the 2 non-linear links that converge at the reentrant corner from the adjacent walls and the 3 non-linear links from the roof diaphragm that also converge at the reentrant corner. In

examining the results of the axial forces in the exterior chord between the models that do contain non-linear links at the reentrant corner to the models that do not contain non-linear links at the reentrant corner it was found that with the addition of non-linear links (or sheathing) that the forces are reduced in the reentrant corner since the diaphragm is stiffer. This was consistent with results found in previous examinations. Other than stiffening the diaphragm and thus reducing the axial forces in the exterior chord the results were inconclusive as to where the non-linear links forced the exterior chord into compression instead of tension. The comparison of the axial forces in the exterior chord between the two different groups of models can be found in Table 3.8 and Figure 3.19.

Table 3.8 Comparison of Axial Forces in Exterior Chord with and with out non-linear links at the reentrant corner

Exterior Chord Axial Force		
Model	**Links at Corner**	**No Links**
15	-0.067	-0.113
25	-0.152	-0.148
50	-0.375	-0.321
75	-0.511	-0.372
100	-0.705	-0.505
125	-0.727	-0.439
150	-0.808	-0.451
175	-0.7	-0.253
200	-0.653	-0.131
225	-0.441	0.17
250	-0.292	0.394
275	-0.009607	0.767
300	0.298	1.176

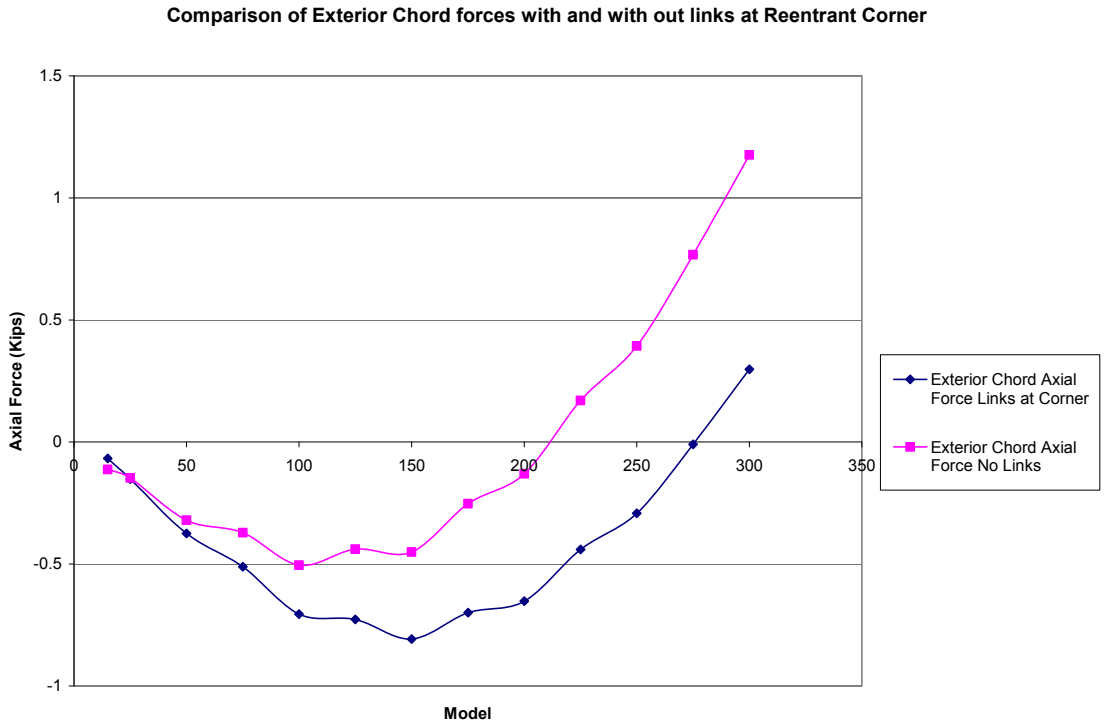

Figure 3.19 Comparison of Axial Forces in Exterior Chord with and with out non-linear links at the reentrant corner

Since the non-linear links did not contribute to the axial forces in the exterior chord being in compression, the models were looked at more globally to understand what was going on. It was found in model that the top chord of the loaded face of the variable leg was in compression. Since this was the case, it can be determined that the diaphragm of the variable leg does not act solely as a simply supported beam system or solely as a propped cantilever system. Instead it acts as a combination of the two systems. This is consistent with the equations that were developed in the previous section for determining the chord forces. Since the diaphragm acts as combination of the two systems it explains while the results for the axial forces in the chord members do not necessarily fit into all of the ideologies of either the propped cantilever system or the simply supported beam system.

CHAPTER 4: SUMMARY AND CONCLUSIONS

4.1 Summary

The objective of this study was to examine how lateral loads affect forces in the reentrant corner of structures so as to gain better understanding on the issue. For this study 30 models were analyzed using finite element analysis with varying dimensions and wall locations. Specifically, these varying parameters of length and number of interior walls were used to see how the axial forces in the reentrant corner changed accordingly. In order to obtain realistic results, the models were set up to mimic how light-framed timber construction is set up in reality. This included developing different member and material properties in SAP2000.

For analysis, each model was loaded under the same loading conditions, thus making the only variable parameter either the length of the variable leg of the building with a reentrant corner or the number of interior shear walls. Chapter 3 summarizes the results of the 30 models used and the maximum axial forces found the in the reentrant corner. Based on the results of the study, conclusions can be drawn on the affect of lateral loads on reentrant corners.

4.2 Conclusion

Based on numerical analysis of the results from the finite element study, conclusions can be made on the effect of lateral loads on reentrant corner of single story, light-framed timber structures:

- The length of the legs of a structure has a direct correlation to the magnitude of the axial forces in the struts in the reentrant corner. The longer the leg is

perpendicular to the strut, the higher the axial force will be in the strut. This is due to the diaphragm being idealized as a simple beam.

- As the length of the variable leg increases, it becomes increasingly more flexible than the constant leg. This results in the connection between the variable leg and the constant leg acting more like a fixed connection instead of a pinned connection. The analog for the diaphragm also changes then from a propped cantilever to a simply supported beam. This transition between these two analogs occurs between the 75% model and the 225% model.
- The axial forces in the interior and exterior chords follow the trend of the bending moment diagram as the length of the variable leg increases. Since it was found that the variable leg acts more similarly to a propped cantilever than a simply supported beam, the axial forces in the interior and exterior chords follow the trend of the bending moment diagram for a propped cantilever instead of a simply supported beam as initially assumed.
- There is a correlation between how the diaphragm deforms and the axial forces in the chord members in the reentrant corner. By limiting the diaphragm deflection, the axial forces in the chord members are also limited and reduced.
- The addition of interior lines of shear greatly reduces the magnitude of the axial forces in the interior and exterior strut as well as the interior and exterior chord. The decrease in the magnitude of the axial force in the struts and chords is attributed to the aspect ratio of the diaphragm. As the aspect ratio of the diaphragm decreases so do the axial forces in the struts and chords in the reentrant corner.

- The addition of an interior shear wall at the reentrant corner reduces the axial forces in the interior and exterior strut and the interior and exterior chord. The most significant change occurred after the addition of one interior shear wall. After the addition of four interior shear walls there was no significant change in the axial forces in the interior and exterior strut and the interior and exterior chord. The interior shear wall provides a line of support at the reentrant corner that transfers the load directly to the foundation. This reduces the axial forces in the struts and chords since the applied load does not need to be transferred to the exterior shear walls.
- A significant reduction of the axial force in the interior chord was found when stud walls and sheathing was added to the diaphragm. The sheathed exterior walls stiffen the roof diaphragm causing less deflection. The decrease in deflection leads to the decreased axial forces in the interior chord.
- The height and number of stories in a structure will affect the magnitude of the axial forces in the interior and exterior strut and the interior and exterior chord. The top story of a multi-story building is going to deflect more and therefore going to have higher axial forces in the interior and exterior strut and the interior and exterior chord than a single story structure. While the deflect will decrease in lower stories of a multi-story building the axial forces in the interior and exterior strut and the interior and exterior chord will increase since they are being compounded from the stories above.
- The diaphragm of the variable leg acts as a combination of the simply supported beam analog and the propped cantilever analog. Since the diaphragm behaves as

a combination of these two analogs and not simply as one or another it explains why the results for the axial forces in the exterior chord are not intuitive. This combination of systems also led to the development of equations that better estimate what the chord forces are in the reentrant corner.

References

American Society of Civil Engineers. (2010) *Minimum design loads for buildings and other structures* (ASCE 7-10). Reston, VA. American Society of Civil Engineers.

American Wood Council. (2005) *National Design Specifications for Wood Construction* (NDS 2005). Washington D.C. American Forest & Paper Association, Inc. February 2010

American Wood Council. (2005) *Special Desing Provisions for Wind and Seismic* (SDPWS 2005). Washington D.C. American Forest & Paper Association, Inc. February 2010

Amin, J.A.,& Ahuja, A.K. (2011) Experimental study of wind-induced pressures on buildings of various geometries. *International Journal of Engineering, Science, and Technology,* Vol 3, No. 5. 1-19.

APA. (1997) *Plywood Design Specification* The Engineered Wood Association. January 1997

Computers and Structures, Inc. (2011) SAP2000 (Version 15) [Computer software]. Berkeley, CA.

FEMA. (2006) *Risk Management Series Design for Earthquakes* (FEMA 454)

Krishnan, Swaminathan. (2007) Case studies of damage to 19-story irregular steel moment-frame buildings under near-source ground motion. *Earthquake Engineering and Structural Dynamics* 36. 861-885.

Malone, R. Terry., & Rice, Robert W. (2012) *The Analysis of Irregular Shaped Structures*. New York: McGraw Hill

Naeim, Farzad. (1989) *The Seismic Design Handbook.* New York: Chapman & Hall

Pang, WeiChiang., Rosowsky, David., van de Lindt, John., Pei, Shiling. (2010) Simplified Direct Displacement Design of Six-story NEESwood Capstone Building and Pre-test Seismic Performance Assessment. *World Conference on Timber Engineering* 2010

Prion, H., and Lam, F. (2000). "Finite element analysis of diaphragms with openings and offsets." *Rep. Prepared for to the Canadian Wood Council,* Dept. of Wood Science, UBC, Vancouver, B.C.

Pryor, Steve. (2009) Equivalent Rod Area

Songlai, Chen., Chengmou, Fan., & Jinglong, Pan. (2010) Experimental Study on Full-Scale Light-Frame Wood House under Lateral Load. *Journal of Structural Engineering.* July 2010. 805-812

USGS. (1985) ID. Celebi, M. 7ct. Retrieved from http://libraryphoto.cr.usgs.gov/cgi-bin/search.cgi?search_mode=exact&selection=Mexico+City+Earthquake+1985|Mexico+City|Earthquake|1985

Appendix A TJI Joist Specifications

Introduction:

Present in the tables below are the design properties and roof span values for Weyerhaeuser's True Joist TJI Joists. The values are obtained from the True Joist TJI Joist Specifier's Guide. (True Joist, 2013)

DESIGN PROPERTIES

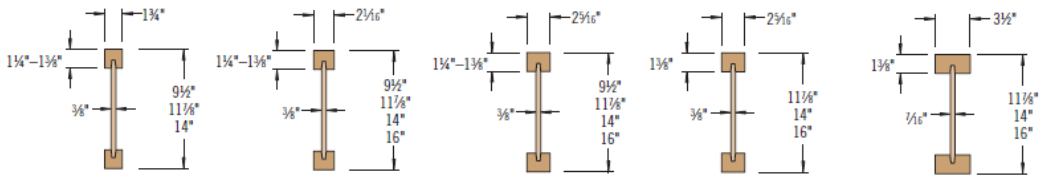

TJI® 110 Joists TJI® 210 Joists TJI® 230 Joists TJI® 360 Joists TJI® 560 Joists

Design Properties (100% Load Duration)

Depth	TJI®	Basic Properties				Reaction Properties					
		Joist Weight (lbs/ft)	Maximum Resistive Moment(1) (ft-lbs)	Joist Only EI x 10⁶ (in.²-lbs)	Maximum Vertical Shear (lbs)	1¾" End Reaction (lbs)	3½" End Reaction (lbs)	3½" Intermediate Reaction (lbs)		5¼" Intermediate Reaction (lbs)	
								No Web Stiffeners	With Web Stiffeners(2)	No Web Stiffeners	With Web Stiffeners(2)
9½"	110	2.3	2,500	157	1,220	910	1,220	1,935	N.A.	2,350	N.A.
	210	2.6	3,000	186	1,330	1,005	1,330	2,145	N.A.	2,565	N.A.
	230	2.7	3,330	206	1,330	1,060	1,330	2,410	N.A.	2,790	N.A.
11⅞"	110	2.5	3,160	267	1,560	910	1,375	1,935	2,295	2,350	2,705
	210	2.8	3,795	315	1,655	1,005	1,460	2,145	2,505	2,565	2,925
	230	3.0	4,215	347	1,655	1,060	1,485	2,410	2,765	2,790	3,150
	360	3.0	6,180	419	1,705	1,080	1,505	2,460	2,815	3,000	3,360
	560	4.0	9,500	636	2,050	1,265	1,725	3,000	3,475	3,455	3,930
14"	110	2.8	3,740	392	1,860	910	1,375	1,935	2,295	2,350	2,705
	210	3.1	4,490	462	1,945	1,005	1,460	2,145	2,505	2,565	2,925
	230	3.3	4,990	509	1,945	1,060	1,485	2,410	2,765	2,790	3,150
	360	3.3	7,335	612	1,955	1,080	1,505	2,460	2,815	3,000	3,360
	560	4.2	11,275	926	2,390	1,265	1,725	3,000	3,475	3,455	3,930
16"	210	3.3	5,140	629	2,190	1,005	1,460	2,145	2,505	2,565	2,925
	230	3.5	5,710	691	2,190	1,060	1,485	2,410	2,765	2,790	3,150
	360	3.5	8,405	830	2,190	1,080	1,505	2,460	2,815	3,000	3,360
	560	4.5	12,925	1,252	2,710	1,265	1,725	3,000	3,475	3,455	3,930

(1) **Caution: Do not** increase joist moment design properties by a repetitive member use factor.
(2) See detail W on page 6 for web stiffener requirements and nailing information.

General Notes

- Design reaction includes all loads on the joist. Design shear is computed at the inside face of supports and includes all loads on the span(s). Allowable shear may sometimes be increased at interior supports in accordance with ICC ES ESR-1153, and these increases are reflected in span tables.
- The following formulas approximate the uniform load deflection of Δ (inches):

For TJI® 110, 210, 230, and 360 Joists

$$\Delta = \frac{22.5\ wL^4}{EI} + \frac{2.67\ wL^2}{d \times 10^5}$$

For TJI® 560 Joists

$$\Delta = \frac{22.5\ wL^4}{EI} + \frac{2.29\ wL^2}{d \times 10^5}$$

w = uniform load in pounds per linear foot
L = span in feet
d = out-to-out depth of the joist in inches
EI = value from table above

ROOF SPAN TABLE

Maximum Horizontal Clear Spans—Roof

O.C. Spacing	Depth	TJI®	Design Live Load (LL) and Dead Load (DL) in PSF											
			Non-Snow (125%)				Snow Load Area (115%)							
			20LL + 15DL		20LL + 20DL		25LL + 15DL		30LL + 15DL		40LL + 15DL		50LL + 15DL	
			Low	High	Low	High	Low	High	Low	High	Low	High	Low	High
16"	9½"	110	20'-0"	17'-10"	19'-1"	16'-11"	19'-2"	17'-2"	18'-5"	16'-7"	17'-2"	15'-7"	15'-11"	14'-9"
		210	21'-2"	18'-10"	20'-2"	17'-10"	20'-3"	18'-2"	19'-6"	17'-6"	18'-2"	16'-6"	17'-2"	15'-7"
		230	21'-11"	19'-6"	20'-10"	18'-6"	20'-11"	18'-9"	20'-2"	18'-1"	18'-10"	17'-0"	17'-9"	16'-2"
	11⅞"	110	23'-11"	21'-4"	22'-9"	20'-2"	22'-8"	20'-6"	21'-5"	19'-10"	19'-5"	18'-7"	17'-11"	17'-4"
		210	25'-3"	22'-6"	24'-1"	21'-4"	24'-2"	21'-8"	23'-3"	20'-11"	21'-4"	19'-8"	19'-8"	18'-8"
		230	26'-1"	23'-3"	24'-10"	22'-0"	24'-11"	22'-4"	24'-0"	21'-7"	22'-5"	20'-4"	20'-9"	19'-3"
		360	27'-9"	24'-9"	26'-5"	23'-5"	26'-7"	23'-10"	25'-6"	23'- 0"	23'-11"	21'-7"	22'-7"	20'-6"
		560	31'-11"	28'-6"	30'-5"	27'- 0"	30'-7"	27'-5"	29'-5"	26'-5"	27'-6"	24'-10"	26'- 0"	23'-7"
	14"	110	27'-2"	24'-3"	25'-7"	23'-0"	24'-9"	23'-4"	23'-4"	22'-4"	21'-2"	20'-5"	19'-6"	18'-11"
		210	28'-9"	25'-7"	27'-4"	24'-3"	27'-1"	24'-8"	25'-7"	23'-9"	23'-3"	22'-4"	21'-5"	20'-9"
		230	29'-8"	26'-6"	28'-3"	25'-1"	28'-5"	25'-5"	27'-0"	24'-7"	24'-6"	23'-1"	22'-7"	21'-10"
		360	31'-6"	28'-2"	30'-0"	26'-8"	30'-2"	27'-1"	29'-0"	26'-1"	27'-2"	24'-7"	25'-8"	23'-4"
		560	36'-3"	32'-4"	34'-6"	30'-7"	34'-8"	31'-1"	33'-4"	30'-0"	31'-2"	28'-3"	29'-6"	26'-9"
	16"	210	31'-10"	28'-5"	30'-0"	26'-11"	29'-0"	27'-4"	27'-5"	26'-2"	24'-10"	23'-11"	22'-8"	22'-2"
		230	32'-10"	29'-4"	31'-4"	27'-9"	30'-7"	28'-2"	28'-11"	27'-3"	26'-2"	25'-3"	24'-2"	23'-5"
		360	34'-11"	31'-2"	33'-3"	29'-6"	33'-5"	30'- 0"	32'-2"	28'-11"	30'-1"	27'-2"	26'- 0"	25'-10"
		560	40'-1"	35'-9"	38'-2"	33'-11"	38'-4"	34'-5"	36'-11"	33'-2"	34'-6"	31'-3"	31'-8"	29'-8"
19.2"	9½"	110	18'-9"	16'-9"	17'-11"	15'-10"	18'-0"	16'-1"	17'-3"	15'-7"	15'-9"	14'-7"	14'-6"	13'-10"
		210	19'-10"	17'-9"	18'-11"	16'-9"	19'-0"	17'-0"	18'-3"	16'-5"	17'-1"	15'-5"	15'-11"	14'-8"
		230	20'-7"	18'-4"	19'-7"	17'-4"	19'-8"	17'-7"	18'-11"	17'-0"	17'-8"	16'-0"	16'-8"	15'-2"
	11⅞"	110	22'-5"	20'-0"	21'-5"	19'-0"	20'-9"	19'-3"	19'-7"	18'-7"	17'-9"	17'-1"	16'-4"	15'-10"
		210	23'-9"	21'-2"	22'-7"	20'-0"	22'-8"	20'-4"	21'-5"	19'-8"	19'-6"	18'-6"	17'-11"	17'-4"
		230	24'-6"	21'-10"	23'-4"	20'-8"	23'-5"	21'-0"	22'-6"	20'-3"	20'-6"	19'-1"	18'-11"	18'-1"
		360	26'-1"	23'-3"	24'-10"	22'-0"	24'-11"	22'-4"	24'- 0"	21'-7"	22'-5"	20'-3"	21'-2"	19'-3"
		560	30'- 0"	26'-9"	28'-7"	25'-4"	28'-8"	25'-9"	27'-7"	24'-10"	25'-9"	23'-4"	24'-4"	22'-2"
	14"	110	25'-1"	22'-10"	23'-4"	21'-7"	22'-7"	21'-5"	21'-4"	20'-4"	19'-4"	18'-7"	17'-0"	17'-3"
		210	27'-0"	24'-1"	25'-7"	22'-10"	24'-9"	23'-2"	23'-4"	22'-4"	21'-2"	20'-5"	18'-10"	18'-11"
		230	27'-10"	24'-10"	26'-6"	23'-7"	26'-1"	23'-11"	24'-7"	23'-1"	22'-4"	21'-6"	20'-7"	19'-11"
		360	29'-7"	26'-5"	28'-2"	25'-0"	28'-4"	25'-5"	27'-3"	24'-6"	25'-6"	23'-1"	21'-7"	21'-8"
		560	34'-0"	30'-4"	32'-5"	28'-9"	32'-7"	29'-2"	31'-4"	28'-2"	29'-3"	26'-6"	26'-5"	25'-2"
	16"	210	29'-5"	26'-8"	27'-5"	25'-4"	26'-5"	25'-2"	25'-0"	23'-11"	22'-3"	21'-10"	18'-10"	20'-2"
		230	30'-11"	27'-7"	28'-11"	26'-1"	27'-11"	26'-6"	26'-4"	25'-2"	23'-11"	23'-0"	21'-2"	21'-3"
		360	32'-10"	29'-3"	31'-3"	27'-9"	31'-5"	28'-2"	30'-2"	27'-2"	25'-7"	25'-3"	21'-7"	21'-8"
		560	37'-8"	33'-7"	35'-10"	31'-10"	36'-0"	32'-4"	34'-8"	31'-2"	31'-3"	29'-4"	26'-5"	25'-5"
24"	9½"	110	17'-5"	15'-6"	16'-7"	14'-8"	16'-5"	14'-11"	15'-6"	14'-5"	14'-1"	13'-6"	13'-0"	12'-7"
		210	18'-5"	16'-5"	17'-6"	15'-6"	17'-7"	15'-9"	16'-11"	15'-3"	15'-5"	14'-4"	14'-3"	13'-7"
		230	19'-0"	17'-0"	18'-1"	16'-1"	18'-2"	16'-4"	17'-6"	15'-9"	16'-3"	14'-10"	15'-0"	14'-0"
	11⅞"	110	20'-7"	18'-7"	19'-2"	17'-7"	18'-6"	17'-7"	17'-6"	16'-8"	15'-10"	15'-3"	13'-7"	14'-2"
		210	21'-11"	19'-7"	20'-11"	18'-7"	20'-4"	18'-10"	19'-2"	18'-2"	17'-5"	16'-9"	15'-0"	15'-6"
		230	22'-8"	20'-3"	21'-7"	19'-2"	21'-5"	19'-5"	20'-3"	18'-9"	18'-4"	17'-8"	16'-11"	16'-4"
		360	24'-1"	21'-6"	23'- 0"	20'-5"	23'-1"	20'-8"	22'-2"	20'-0"	20'-5"	18'-9"	17'-3"	17'-4"
		560	27'-9"	24'-9"	26'-5"	23'-6"	26'-7"	23'-10"	25'-6"	23'-0"	23'-10"	21'-7"	21'-1"	20'-3"
	14"	110	22'-5"	21'-1"	20'-10"	19'-6"	20'-2"	19'-2"	19'-0"	18'-2"	16'-0"	16'-7"	13'-7"	14'-7"
		210	24'-7"	22'-4"	22'-11"	21'-1"	22'-1"	21'-0"	20'-10"	19'-11"	17'-10"	18'-3"	15'-0"	16'-1"
		230	25'-9"	23'-0"	24'-1"	21'-10"	23'-4"	22'-2"	22'-0"	21'-0"	20'-0"	19'-3"	16'-11"	17'-0"
		360	27'-5"	24'-6"	26'-1"	23'-2"	26'-3"	23'-6"	25'-0"	22'-8"	20'-5"	20'-2"	17'-3"	17'-4"
		560	31'-6"	28'-1"	30'-0"	26'-8"	30'-2"	27'-0"	29'-0"	26'-1"	24'-11"	23'-7"	21'-1"	20'-3"
	16"	210	26'-3"	24'-9"	24'-6"	22'-11"	23'-8"	22'-6"	21'-9"	21'-4"	17'-10"	18'-9"	15'-0"	16'-1"
		230	27'-9"	25'-6"	25'-10"	24'-2"	24'-11"	23'-8"	23'-7"	22'-6"	20'-0"	19'-9"	16'-11"	17'-0"
		360	30'-4"	27'-1"	28'-11"	25'-8"	28'-2"	26'-1"	25'-0"	24'-1"	20'-5"	20'-2"	17'-3"	17'-4"
		560	34'-10"	31'-2"	33'-2"	29'-6"	33'-4"	29'-11"	30'-6"	28'-3"	24'-11"	23'-7"	21'-1"	20'-3"

How to Use This Table

1. Determine appropriate live and dead load, and the load duration factor.
2. If your slope is 6:12 or less, use the **Low** slope column. If it is between 6:12 and 12:12, use the **High** column.
3. Scan down the column until you find a span that meets or exceeds the span of your application.
4. Select TJI® joist and on-center spacing.

General Notes

- Table is based on:
  - Minimum bearing length of 1¾" end and 3½" intermediate, without web stiffeners.
  - Uniform loads.
  - More restrictive of simple or continuous span.
  - Minimum roof slope of ¼:12.
- Total load values are limited to deflection of L/180 and live load is based on joist deflection of L/240.
- A support beam or wall at the high end is required. Ridge board applications do not provide adequate support.
- For flat roofs or other loading conditions not shown, refer to Weyerhaeuser software.

Appendix B Diaphragm Deflection Calculations

Introduction:

Presented below are the calculations and SAP2000 results for the diaphragm deflection. The deflection for the diaphragm was calculated and analyzed for both a uniform distributed load and a point load.

Uniform Distributed Load

Maximum Diaphragm Shear

$$v = \frac{wl}{2B} = \frac{230.4\,plf\,(144\,ft)}{2(24\,ft)} = 691.2\,plf$$

Diaphragm Deflection

$$\delta_{dia} = \frac{5vL^3}{8EAW} + \frac{0.25vL}{1000G_a} + \frac{\Sigma(x\Delta_c)}{2w} \quad \text{[SDPWS Eq. 4.2-1]}$$

Where:

v = 691.2plf	[Above]
L = 144ft	[Model]
E = 263436 psi	[Manufacturer Specs]
A = 1601.3733 in^2	[Manufacturer Specs]
W = 24ft	[Model]
G_a = 20kip/in	[SDPWS T. A. 4.2A]

$$\delta_{dia} = \frac{5(691.2\,plf)(144\,ft)^3}{8(263436\,psi)(1601.3733in^2)(24\,ft)} + \frac{0.25(691.2\,plf)(144\,ft)}{1000(20kip/in)} = 1.37in$$

Point Load

Maximum Diaphragm Shear

$$v = \frac{P}{2B} = \frac{20000lb}{2(24\,ft)} = 416.6\,plf$$

Diaphragm Deflection

$$\delta_{dia} = \frac{5vL^3}{8EAW} + \frac{0.25vL}{1000G_a} + \frac{\Sigma(x\Delta_c)}{2w}$$

Where:
v = 416.6plf
L = 144ft
E = 263436 psi
A = 1601.3733 in^2
W = 24ft
G_a = 20kip/in

$$\delta_{dia} = \frac{5(416.6\,plf)(144\,ft)^3}{8(263436\,psi)(1601.3733in^2)(24\,ft)} + \frac{0.25(416.6\,plf)(144\,ft)}{1000(20kip/in)} = 0.825in$$

SAP2000 Results

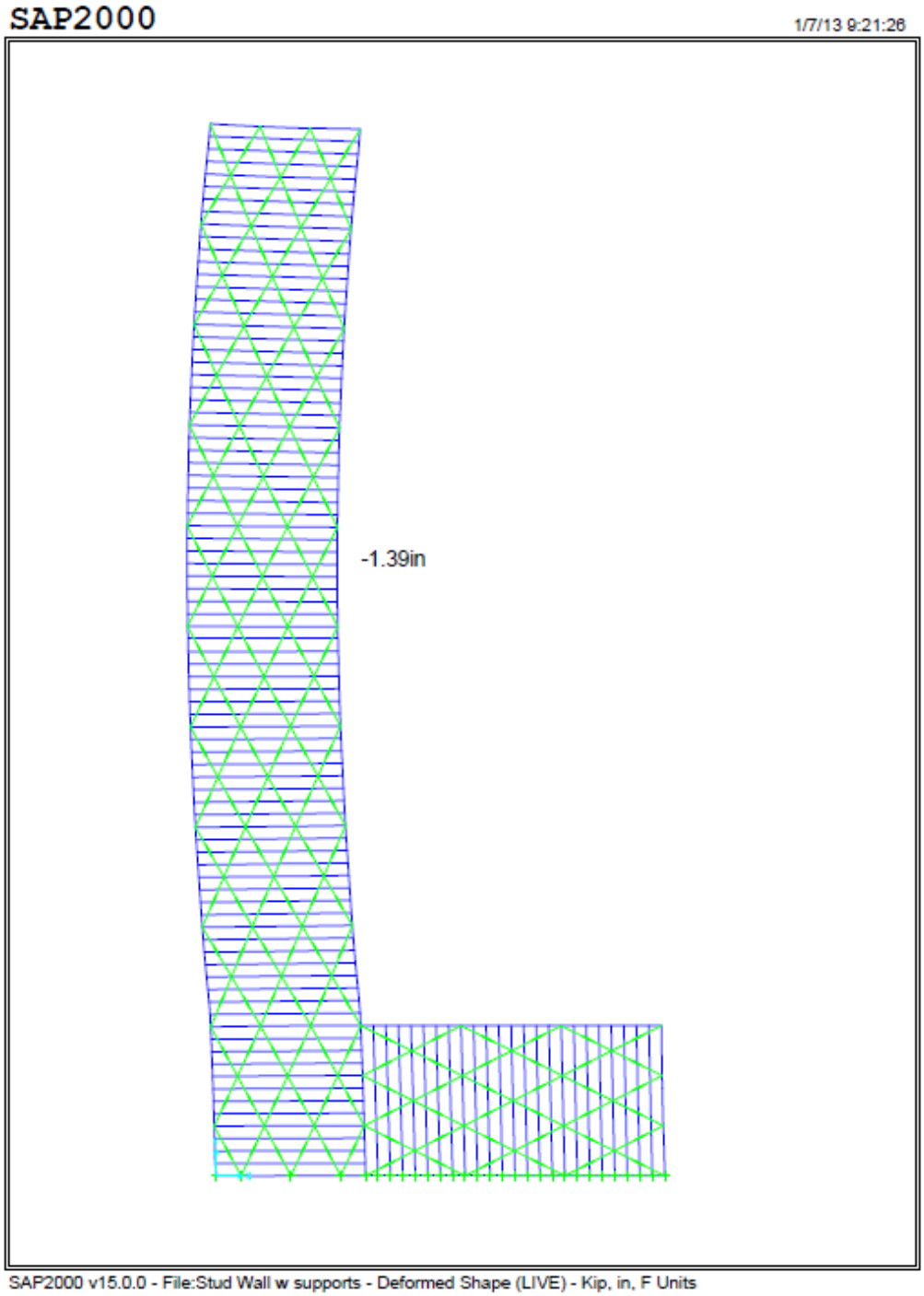

DIAPHRAGM DEFLECTION: POINT LOAD

Diaphragm is loaded with a point load at the end of the diaphragm.
~For calculations, the diaphragm is treated as a shear wall and SDPWS Eq. 4.3-1 is used

Diaphragm length of 144ft

Maximum Diaphragm Shear

$$v = \frac{P}{L} = \frac{2000lb}{24\,ft} = 83.3\,plf$$

Diaphragm Deflection

$$\delta_{sw} = \frac{8vh^3}{EAb} + \frac{vh}{1000G_a} + \frac{h\Delta_a}{b}$$ [SDPWS Eq. 4.3-1]

Where:

ν = 83.3plf	[Above]
h = 144ft	[Model]
E = 1800000psi	[NDS Supplement T4]
A = 35.0in^2	[Model]
B = 24ft	[Model]
G_a = 11 kip/ft	[SDPWS T 4.3A]

$$\delta_{sw} = \frac{8(83.3\,plf)(144\,ft)^3}{1800000\,psi(35.0in^2)(24\,ft)} + \frac{83.3\,plf\,(144\,ft)}{1000(11kip/\,ft)} = 1.09in$$

SAP2000 Result: 1.48in

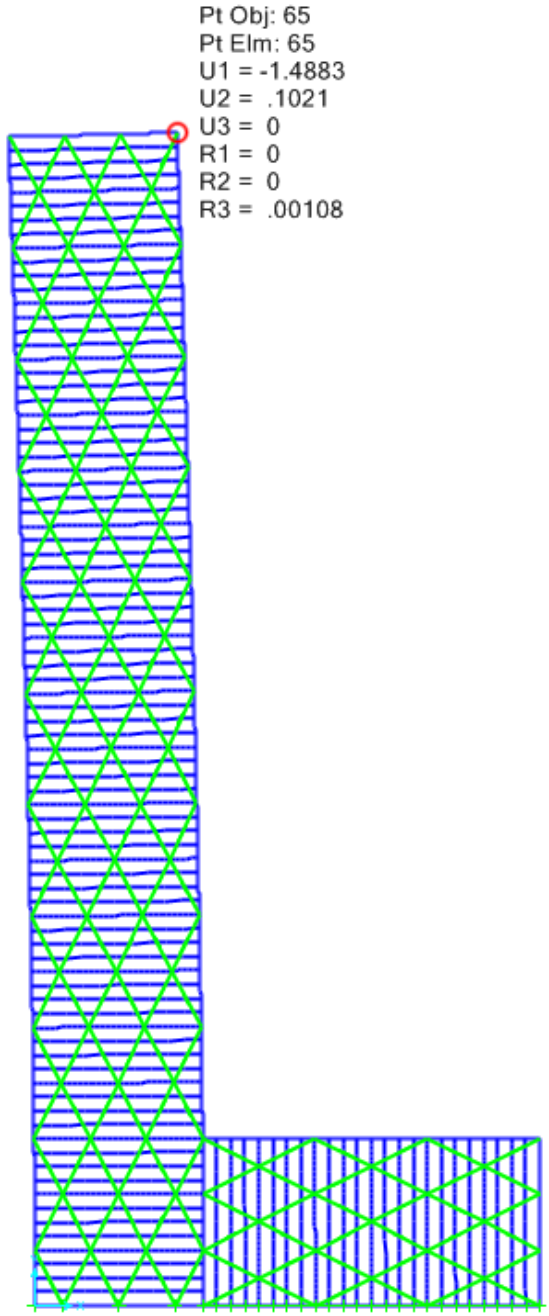

Appendix C Wind load Calculations

Introduction:

Presented below is the development of the wind load applied to the models for the parametric study. The development of the wind loads comes from ASCE 7-10 Chapter 28. (ASCE, 2010)

MWFRS Pressures (psf) (Per ASCE 7-10 Chapter 28)
V = 110 mph **Case A**

	Zones									
	Horizontal Pressures					Vertical Pressures			Overhangs	
	A	B	C	D	E	F	G	H	EOH	GOH
Ps30	19.2	-10	12.7	-5.9	-23.1	-13.1	-16	-10.1	-32.3	-25.3
λ (h-15 ft)	1	1.21	1.21	1.21	1.21	1.21	1.21	1.21	1.21	1.21
λ (h-20 ft)	1	1.29	1.29	1.29	1.29	1.29	1.29	1.29	1.29	1.29
λ (h-25 ft)	1	1.35	1.35	1.35	1.35	1.35	1.35	1.35	1.35	1.35
λ (h-30 ft)	1	1.4	1.4	1.4	1.4	1.4	1.4	1.4	1.4	1.4
λ (h-35 ft)	1.05	1.45	1.45	1.45	1.45	1.45	1.45	1.45	1.45	1.45
λ (h-40 ft)	1.09	1.49	1.49	1.49	1.49	1.49	1.49	1.49	1.49	1.49
λ (h-45 ft)	1.12	1.53	1.53	1.53	1.53	1.53	1.53	1.53	1.53	1.53
λ (h-50 ft)	1.16	1.56	1.56	1.56	1.56	1.56	1.56	1.56	1.56	1.56
λ (h-55 ft)	1.19	1.59	1.59	1.59	1.59	1.59	1.59	1.59	1.59	1.59
Kzt	1	1	1	1	1	1	1	1	1	1

ps15=λ15Kztps30	19.2	-12.1	15.367	-7.139						
ps20=λ20Kztps30	19.2	-12.9	16.383	-7.611						
ps25=λ25Kztps30	19.2	-13.5	17.145	-7.965						
ps30=λ30Kztps30	19.2	-14	17.78	-8.26						
ps35=λ35Kztps30	20.16	-14.5	18.415	-8.555						
ps40=λ40Kztps30	20.928	-14.9	18.923	-8.791						
ps45=λ45Kztps30	21.504	-15.3	19.431	-9.027						
ps50=λ50Kztps30	22.272	-15.6	19.812	-9.204						
ps55=λ55Kztps30	22.848	-15.9	20.193	-9.381	-36.729	-20.829	-25.44	-16.059	-51.357	-40.227

MWFRS Pressure: 19.2psf

$W = pressure(height) = 19.2\,psf\,(6\,ft) = 115.2\,plf$

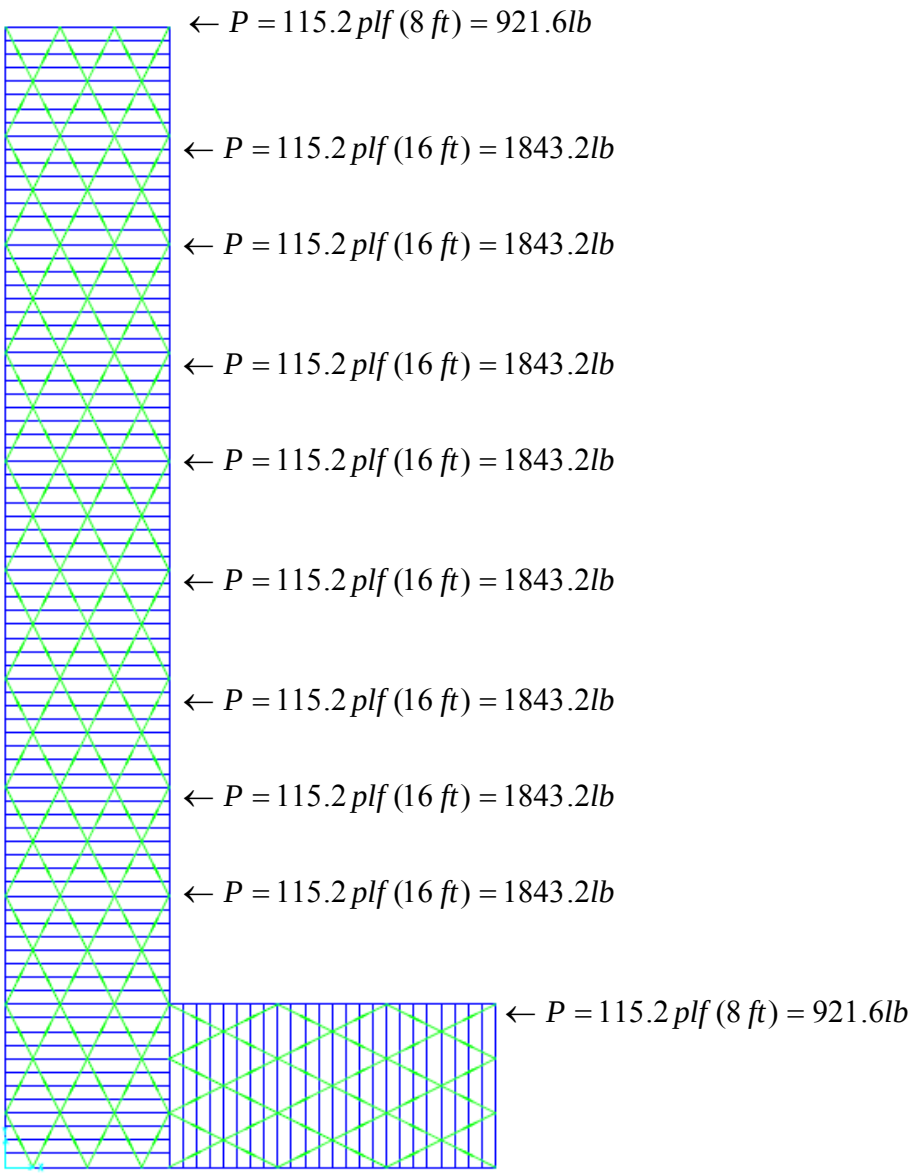

Appendix D Non-linear Link Development

Introduction:

Presented in the tables below is the development of the values for the non-linear links that were used to represent sheathing in the models.

		Secant Stiffness, K_s, 9' Walls (kip/in per ft)					Secant Stiffness, Ks, 8' Walls (kip/in per ft)				
	Elastic	Wall Drift					Wall Drift				
	Ga	0.5%	1.0%	2.0%	3.0%	4.0%	0.5%	1.0%	2.0%	3.0%	4.0%
6/12 Sing	22	0.772	0.482	0.262	0.150	0.094	1.191	0.735	0.402	0.230	0.143
3/12 D	74	2.744	1.785	1.010	0.573	0.354	4.225	2.736	1.561	0.890	0.554
Gyp	2.223333	0.185	0.088	0.033	0.014	0.005	0.291	0.134	0.047	0.017	0.003
6/12 Dbl	44	1.545	0.964	0.524	0.299	0.187	2.383	1.470	0.805	0.459	0.287

	Applied Force, 12' Walls (kip per ft)					Applied Force, 8' Walls (kip per ft)				
	Wall Drift, inches					Wall Drift, inches				
	0.54	1.08	2.16	3.24	4.32	0.48	0.96	1.92	2.88	3.84
6/12 Sing	0.417	0.521	0.566	0.485	0.404	0.572	0.706	0.772	0.661	0.550
3/12 D	1.482	1.928	2.181	1.855	1.529	2.028	2.627	2.997	2.562	2.127
Gyp	0.100	0.095	0.070	0.045	0.020	0.140	0.129	0.089	0.050	0.011
6/12 Dbl	0.834	1.041	1.132	0.970	0.809	1.144	1.411	1.545	1.323	1.101

	Ga effective, 9' Walls (kips/in)					Ga effective, 8' Walls (kips/in) (except at 0.5% nonGyp)				
	Wall Drift, % of height					Wall Drift, % of height				
	0.5%	1.0%	2.0%	3.0%	4.0%	0.5%	1.0%	2.0%	3.0%	4.0%
6/12 Sing	9.268	5.783	3.145	1.797	1.123	9.530	5.881	3.218	1.837	1.146
3/12 D	32.923	21.418	12.115	6.871	4.248	33.800	21.892	12.488	7.117	4.432
Gyp	2.223	1.058	0.390	0.167	0.056	2.325	1.073	0.373	0.139	0.022
6/12 Dbl	18.537	11.567	6.289	3.594	2.247	19.060	11.762	6.437	3.674	2.293

Equivalent Steel Rod Area
Calculator
Note: All wood sheathing was 15/32 'Rated Sheathing' (not Struct 1) with 10d common nails

6		6/12	6/12	6/12	6/12	6/12	6/12	6/12	6/12	6/12	6/12	6/12	6/12	6/12
5		6/12-D	6/12-D	6/12-D	3/12-D	6/12-D	6/12-D	6/12-D	6/12-D	6/12-D	3/12-D	6/12-D	6/12-D	3/12-D
4		6/12-D	6/12-D	6/12-D	3/12-D	6/12-D	6/12-D	6/12-D	6/12-D	6/12-D	3/12-D	6/12-D	6/12-D	3/12-D
3		6/12-D	6/12-D	6/12-D	3/12-D	6/12-D	6/12-D	6/12-D	6/12-D	6/12-D	3/12-D	6/12-D	6/12-D	3/12-D
2		6/12-D	6/12-D	6/12-D	3/12-D	6/12-D	6/12-D	6/12-D	6/12-D	6/12-D	3/12-D	6/12-D	6/12-D	3/12-D
1		6/12-D	6/12-D	6/12-D	3/12-D	6/12-D	6/12-D	6/12-D	6/12-D	6/12-D	3/12-D	6/12-D	6/12-D	3/12-D

		East-West								Hor. Force for Shear Only, at Disp. Indicated, kips				
FLOOR	WALL	h, ft	b, ft	b', ft	Nailing	Cosine	Elast. G_a, k/in	Elast. K_{hor}, k/in	Elast. K_{slope}, k/in	0.50%	1%	2%	3%	4%
1	S1	12	4		6/12 Sing	0.316228	11	3.67	36.67	4.98	6.06	6.41	5.42	4.42
1	S1	12	4		6/12 Sing	0.316228	11	3.67	36.67	4.98	6.06	6.41	5.42	4.42
1	Dia1	8	4		6/12 Sing	0.447214	11	5.50	27.50	5.13	6.16	6.54	5.49	4.45
1	Dia1	8	4		6/12 Sing	0.447214	11	5.50	27.50	5.13	6.16	6.54	5.49	4.45

FLOOR	WALL	East-West h, ft	b, ft	b', ft	Nailing	Cosine	Elast. G_a, k/in	Elast. K_{hor}, k/in	Elast. K_{slope}, k/in	Slope Force for Shear Only, at Disp. Indicated, kips 0.01	0.01	0.02	0.03	0.04	k eff
1	S1	12	4		6/12 Sing	0.316228	11	3.67	36.67	15.76	19.16	20.28	17.13	13.98	11.60
1	S1	12	4		6/12 Sing	0.316228	11	3.67	36.67	15.76	19.16	20.28	17.13	13.98	11.60
1	Dia1	8	4		6/12 Sing	0.447214	11	5.50	27.50	11.48	13.78	14.62	12.28	9.94	12.30
1	Dia1	8	4		6/12 Sing	0.447214	11	5.50	27.50	11.48	13.78	14.62	12.28	9.94	12.30

Force and Deformation Pairs for Inclined Multilinear Plastic Wall Springs

		S1-Tension		S1-Comp		Dia1-Comp		Dia1-Tens	
		Disp., in.	Force, kips	Disp., in.	Force, kips	Disp., in.	Force, kips	Disp., in.	Force, kips
0.04		1.82	13.98	1.00	0.00	1.00	0.00	1.72	9.94
0.03		1.37	17.13	0.00	0.00	0.00	0.00	1.29	12.28
0.02	-0.005	0.91	20.28	-0.23	-15.76	-0.21	-11.48	0.86	14.62
0.01	-0.01	0.46	19.16	-0.46	-19.16	-0.43	-13.78	0.43	13.78
0.005	-0.02	0.23	15.76	-0.91	-20.28	-0.86	-14.62	0.21	11.48
	-0.03	0.00	0.00	-1.37	-17.13	-1.29	-12.28	0.00	0.00
	-0.04	-1.00	0.00	-1.82	-13.98	-1.72	-9.94	-1.00	0.00

Appendix E Model Results

Introduction:

Presented below are the tables of the analysis results for the interior and exterior struts and the interior and exterior chords for each of the models. The table includes values for axial forces, shear in both the strong axis and week axis, torsion, bending moment in the strong and week axis and stresses in the members. The following abbreviations are used to describe the results:

P = Axial Force

V2 = Shear in Strong Axis

V3 = Shear in Weak Axis

T = Torsion

M2 = Bending Moment in Strong Axis

M3 = Bending Moment in Week Axis

S11Max = Maximum In Plane Direct Stress

S11Min = Minimum In Plan Direct Stress

TABLE: Element Forces - Frames Member 2 Exterior Strut												
Model	Frame	Station	StepType	P	V2	V3	T	M2	M3	S11Max	S11Min	FrameElem
Text	Text	in	Text	Kip	Kip	Kip	Kip-in	Kip-in	Kip-in	Kip/in2	Kip/in2	Text
15%	551	0	Max	0.00803	0.061	-0.0024	-0.021	-0.042	1.555	0.0168	-0.0199	551-1
15%	551	4.8	Max	0.00803	0.061	-0.0024	-0.021	-0.03	1.263	0.0133	-0.0157	551-1
15%	551	4.8	Max	0.00803	0.061	-0.0024	-0.021	-0.03	1.263	0.0133	-0.0157	551-2
15%	551	9.6	Max	0.00803	0.061	-0.0024	-0.021	-0.018	0.972	0.0098	-0.0116	551-2
15%	551	9.6	Max	0.00803	0.061	-0.0024	-0.021	-0.018	0.972	0.0098	-0.0116	551-3
15%	551	14.4	Max	0.00803	0.061	-0.0024	-0.021	-0.007	0.681	0.0063	-0.0074	551-3
15%	551	14.4	Max	0.00803	0.061	-0.0024	-0.021	-0.007	0.681	0.0063	-0.0074	551-4
15%	551	19.2	Max	0.00803	0.061	-0.0024	-0.021	0.00457	0.389	0.0038	-0.0042	551-4
15%	551	19.2	Max	0.00803	0.061	-0.0024	-0.021	0.00457	0.389	0.0038	-0.0042	551-5
15%	551	24	Max	0.00803	0.061	-0.0024	-0.021	0.016	0.098	0.0027	-0.0024	551-5
15%	551	0	Min	0.00803	0.061	-0.0024	-0.021	-0.042	1.555	0.0168	-0.0199	551-1
15%	551	4.8	Min	0.00803	0.061	-0.0024	-0.021	-0.03	1.263	0.0133	-0.0157	551-1
15%	551	4.8	Min	0.00803	0.061	-0.0024	-0.021	-0.03	1.263	0.0133	-0.0157	551-2
15%	551	9.6	Min	0.00803	0.061	-0.0024	-0.021	-0.018	0.972	0.0098	-0.0116	551-2
15%	551	9.6	Min	0.00803	0.061	-0.0024	-0.021	-0.018	0.972	0.0098	-0.0116	551-3
15%	551	14.4	Min	0.00803	0.061	-0.0024	-0.021	-0.007	0.681	0.0063	-0.0074	551-3
15%	551	14.4	Min	0.00803	0.061	-0.0024	-0.021	-0.007	0.681	0.0063	-0.0074	551-4
15%	551	19.2	Min	0.00803	0.061	-0.0024	-0.021	0.00457	0.389	0.0038	-0.0042	551-4
15%	551	19.2	Min	0.00803	0.061	-0.0024	-0.021	0.00457	0.389	0.0038	-0.0042	551-5
15%	551	24	Min	0.00803	0.061	-0.0024	-0.021	0.016	0.098	0.0027	-0.0024	551-5
25%	551	0	Max	0.321	0.062	-0.0014	-0.026	-0.016	1.35	0.0216	-0.0062	551-1
25%	551	4.8	Max	0.321	0.062	-0.0014	-0.026	-0.0098	1.053	0.0186	-0.0025	551-1
25%	551	4.8	Max	0.321	0.062	-0.0014	-0.026	-0.0098	1.053	0.0186	-0.0025	551-2
25%	551	9.6	Max	0.321	0.062	-0.0014	-0.026	-0.0032	0.757	0.0155	0.0012	551-2
25%	551	9.6	Max	0.321	0.062	-0.0014	-0.026	-0.0032	0.757	0.0155	0.0012	551-3
25%	551	14.4	Max	0.321	0.062	-0.0014	-0.026	0.00343	0.46	0.0132	0.0041	551-3
25%	551	14.4	Max	0.321	0.062	-0.0014	-0.026	0.00343	0.46	0.0132	0.0041	551-4
25%	551	19.2	Max	0.321	0.062	-0.0014	-0.026	0.01	0.164	0.0115	0.0065	551-4
25%	551	19.2	Max	0.321	0.062	-0.0014	-0.026	0.01	0.164	0.0115	0.0065	551-5
25%	551	24	Max	0.321	0.062	-0.0014	-0.026	0.017	-0.133	0.0123	0.0064	551-5

25%	551	0	Min	0.321	0.062	-0.0014	-0.026	-0.016	1.35	0.0216	-0.0062	551-1
25%	551	4.8	Min	0.321	0.062	-0.0014	-0.026	-0.0098	1.053	0.0186	-0.0025	551-1
25%	551	4.8	Min	0.321	0.062	-0.0014	-0.026	-0.0098	1.053	0.0186	-0.0025	551-2
25%	551	9.6	Min	0.321	0.062	-0.0014	-0.026	-0.0032	0.757	0.0155	0.0012	551-2
25%	551	9.6	Min	0.321	0.062	-0.0014	-0.026	-0.0032	0.757	0.0155	0.0012	551-3
25%	551	14.4	Min	0.321	0.062	-0.0014	-0.026	0.00343	0.46	0.0132	0.0041	551-3
25%	551	14.4	Min	0.321	0.062	-0.0014	-0.026	0.00343	0.46	0.0132	0.0041	551-4
25%	551	19.2	Min	0.321	0.062	-0.0014	-0.026	0.01	0.164	0.0115	0.0065	551-4
25%	551	19.2	Min	0.321	0.062	-0.0014	-0.026	0.01	0.164	0.0115	0.0065	551-5
25%	551	24	Min	0.321	0.062	-0.0014	-0.026	0.017	-0.133	0.0123	0.0064	551-5
50%	551	0	Max	0.741	0.068	-0.0011	-0.034	-0.0075	1.203	0.0315	0.0082	551-1
50%	551	4.8	Max	0.741	0.068	-0.0011	-0.034	-0.002	0.878	0.0283	0.012	551-1
50%	551	4.8	Max	0.741	0.068	-0.0011	-0.034	-0.002	0.878	0.0283	0.012	551-2
50%	551	9.6	Max	0.741	0.068	-0.0011	-0.034	0.00338	0.554	0.0259	0.0152	551-2
50%	551	9.6	Max	0.741	0.068	-0.0011	-0.034	0.00338	0.554	0.0259	0.0152	551-3
50%	551	14.4	Max	0.741	0.068	-0.0011	-0.034	0.00881	0.23	0.0239	0.0179	551-3
50%	551	14.4	Max	0.741	0.068	-0.0011	-0.034	0.00881	0.23	0.0239	0.0179	551-4
50%	551	19.2	Max	0.741	0.068	-0.0011	-0.034	0.014	-0.094	0.0236	0.019	551-4
50%	551	19.2	Max	0.741	0.068	-0.0011	-0.034	0.014	-0.094	0.0236	0.019	551-5
50%	551	24	Max	0.741	0.068	-0.0011	-0.034	0.02	-0.418	0.0275	0.0158	551-5
50%	551	0	Min	0.741	0.068	-0.0011	-0.034	-0.0075	1.203	0.0315	0.0082	551-1
50%	551	4.8	Min	0.741	0.068	-0.0011	-0.034	-0.002	0.878	0.0283	0.012	551-1
50%	551	4.8	Min	0.741	0.068	-0.0011	-0.034	-0.002	0.878	0.0283	0.012	551-2
50%	551	9.6	Min	0.741	0.068	-0.0011	-0.034	0.00338	0.554	0.0259	0.0152	551-2
50%	551	9.6	Min	0.741	0.068	-0.0011	-0.034	0.00338	0.554	0.0259	0.0152	551-3
50%	551	14.4	Min	0.741	0.068	-0.0011	-0.034	0.00881	0.23	0.0239	0.0179	551-3
50%	551	14.4	Min	0.741	0.068	-0.0011	-0.034	0.00881	0.23	0.0239	0.0179	551-4
50%	551	19.2	Min	0.741	0.068	-0.0011	-0.034	0.014	-0.094	0.0236	0.019	551-4
50%	551	19.2	Min	0.741	0.068	-0.0011	-0.034	0.014	-0.094	0.0236	0.019	551-5
50%	551	24	Min	0.741	0.068	-0.0011	-0.034	0.02	-0.418	0.0275	0.0158	551-5
75%	551	0	Max	1.351	0.073	0.00024	-0.052	0.027	1.164	0.0507	0.0239	551-1
75%	551	4.8	Max	1.351	0.073	0.00024	-0.052	0.026	0.813	0.0478	0.0276	551-1
75%	551	4.8	Max	1.351	0.073	0.00024	-0.052	0.026	0.813	0.0478	0.0276	551-2

75%	551	9.6	Max	1.351	0.073	0.00024	-0.052	0.025	0.461	0.0448	0.0313	551-2
75%	551	9.6	Max	1.351	0.073	0.00024	-0.052	0.025	0.461	0.0448	0.0313	551-3
75%	551	14.4	Max	1.351	0.073	0.00024	-0.052	0.024	0.109	0.0419	0.035	551-3
75%	551	14.4	Max	1.351	0.073	0.00024	-0.052	0.024	0.109	0.0419	0.035	551-4
75%	551	19.2	Max	1.351	0.073	0.00024	-0.052	0.023	-0.243	0.0434	0.0343	551-4
75%	551	19.2	Max	1.351	0.073	0.00024	-0.052	0.023	-0.243	0.0434	0.0343	551-5
75%	551	24	Max	1.351	0.073	0.00024	-0.052	0.022	-0.595	0.0469	0.0316	551-5
75%	551	0	Min	1.351	0.073	0.00024	-0.052	0.027	1.164	0.0507	0.0239	551-1
75%	551	4.8	Min	1.351	0.073	0.00024	-0.052	0.026	0.813	0.0478	0.0276	551-1
75%	551	4.8	Min	1.351	0.073	0.00024	-0.052	0.026	0.813	0.0478	0.0276	551-2
75%	551	9.6	Min	1.351	0.073	0.00024	-0.052	0.025	0.461	0.0448	0.0313	551-2
75%	551	9.6	Min	1.351	0.073	0.00024	-0.052	0.025	0.461	0.0448	0.0313	551-3
75%	551	14.4	Min	1.351	0.073	0.00024	-0.052	0.024	0.109	0.0419	0.035	551-3
75%	551	14.4	Min	1.351	0.073	0.00024	-0.052	0.024	0.109	0.0419	0.035	551-4
75%	551	19.2	Min	1.351	0.073	0.00024	-0.052	0.023	-0.243	0.0434	0.0343	551-4
75%	551	19.2	Min	1.351	0.073	0.00024	-0.052	0.023	-0.243	0.0434	0.0343	551-5
75%	551	24	Min	1.351	0.073	0.00024	-0.052	0.022	-0.595	0.0469	0.0316	551-5
100%	551	0	Max	1.768	0.083	0.00082	-0.063	0.044	1.289	0.0653	0.0329	551-1
100%	551	4.8	Max	1.768	0.083	0.00082	-0.063	0.04	0.89	0.0617	0.0373	551-1
100%	551	4.8	Max	1.768	0.083	0.00082	-0.063	0.04	0.89	0.0617	0.0373	551-2
100%	551	9.6	Max	1.768	0.083	0.00082	-0.063	0.036	0.491	0.0581	0.0418	551-2
100%	551	9.6	Max	1.768	0.083	0.00082	-0.063	0.036	0.491	0.0581	0.0418	551-3
100%	551	14.4	Max	1.768	0.083	0.00082	-0.063	0.032	0.091	0.0546	0.0463	551-3
100%	551	14.4	Max	1.768	0.083	0.00082	-0.063	0.032	0.091	0.0546	0.0463	551-4
100%	551	19.2	Max	1.768	0.083	0.00082	-0.063	0.028	-0.308	0.0566	0.0452	551-4
100%	551	19.2	Max	1.768	0.083	0.00082	-0.063	0.028	-0.308	0.0566	0.0452	551-5
100%	551	24	Max	1.768	0.083	0.00082	-0.063	0.024	-0.707	0.0602	0.0424	551-5
100%	551	0	Min	1.768	0.083	0.00082	-0.063	0.044	1.289	0.0653	0.0329	551-1
100%	551	4.8	Min	1.768	0.083	0.00082	-0.063	0.04	0.89	0.0617	0.0373	551-1
100%	551	4.8	Min	1.768	0.083	0.00082	-0.063	0.04	0.89	0.0617	0.0373	551-2
100%	551	9.6	Min	1.768	0.083	0.00082	-0.063	0.036	0.491	0.0581	0.0418	551-2
100%	551	9.6	Min	1.768	0.083	0.00082	-0.063	0.036	0.491	0.0581	0.0418	551-3
100%	551	14.4	Min	1.768	0.083	0.00082	-0.063	0.032	0.091	0.0546	0.0463	551-3

100%	551	14.4	Min	1.768	0.083	0.00082	-0.063	0.032	0.091	0.0546	0.0463	551-4
100%	551	19.2	Min	1.768	0.083	0.00082	-0.063	0.028	-0.308	0.0566	0.0452	551-4
100%	551	19.2	Min	1.768	0.083	0.00082	-0.063	0.028	-0.308	0.0566	0.0452	551-5
100%	551	24	Min	1.768	0.083	0.00082	-0.063	0.024	-0.707	0.0602	0.0424	551-5
125%	551	0	Max	2.436	0.093	0.00275	-0.088	0.091	1.448	0.0905	0.0454	551-1
125%	551	4.8	Max	2.436	0.093	0.00275	-0.088	0.078	1.001	0.0856	0.0514	551-1
125%	551	4.8	Max	2.436	0.093	0.00275	-0.088	0.078	1.001	0.0856	0.0514	551-2
125%	551	9.6	Max	2.436	0.093	0.00275	-0.088	0.065	0.554	0.0807	0.0573	551-2
125%	551	9.6	Max	2.436	0.093	0.00275	-0.088	0.065	0.554	0.0807	0.0573	551-3
125%	551	14.4	Max	2.436	0.093	0.00275	-0.088	0.052	0.107	0.0758	0.0632	551-3
125%	551	14.4	Max	2.436	0.093	0.00275	-0.088	0.052	0.107	0.0758	0.0632	551-4
125%	551	19.2	Max	2.436	0.093	0.00275	-0.088	0.039	-0.34	0.0771	0.0629	551-4
125%	551	19.2	Max	2.436	0.093	0.00275	-0.088	0.039	-0.34	0.0771	0.0629	551-5
125%	551	24	Max	2.436	0.093	0.00275	-0.088	0.026	-0.787	0.0802	0.0607	551-5
125%	551	0	Min	2.436	0.093	0.00275	-0.088	0.091	1.448	0.0905	0.0454	551-1
125%	551	4.8	Min	2.436	0.093	0.00275	-0.088	0.078	1.001	0.0856	0.0514	551-1
125%	551	4.8	Min	2.436	0.093	0.00275	-0.088	0.078	1.001	0.0856	0.0514	551-2
125%	551	9.6	Min	2.436	0.093	0.00275	-0.088	0.065	0.554	0.0807	0.0573	551-2
125%	551	9.6	Min	2.436	0.093	0.00275	-0.088	0.065	0.554	0.0807	0.0573	551-3
125%	551	14.4	Min	2.436	0.093	0.00275	-0.088	0.052	0.107	0.0758	0.0632	551-3
125%	551	14.4	Min	2.436	0.093	0.00275	-0.088	0.052	0.107	0.0758	0.0632	551-4
125%	551	19.2	Min	2.436	0.093	0.00275	-0.088	0.039	-0.34	0.0771	0.0629	551-4
125%	551	19.2	Min	2.436	0.093	0.00275	-0.088	0.039	-0.34	0.0771	0.0629	551-5
125%	551	24	Min	2.436	0.093	0.00275	-0.088	0.026	-0.787	0.0802	0.0607	551-5
150%	551	0	Max	2.925	0.101	0.00396	-0.104	0.122	1.561	0.1086	0.0551	551-1
150%	551	4.8	Max	2.925	0.101	0.00396	-0.104	0.103	1.077	0.1028	0.062	551-1
150%	551	4.8	Max	2.925	0.101	0.00396	-0.104	0.103	1.077	0.1028	0.062	551-2
150%	551	9.6	Max	2.925	0.101	0.00396	-0.104	0.084	0.592	0.097	0.0689	551-2
150%	551	9.6	Max	2.925	0.101	0.00396	-0.104	0.084	0.592	0.097	0.0689	551-3
150%	551	14.4	Max	2.925	0.101	0.00396	-0.104	0.065	0.108	0.0912	0.0758	551-3
150%	551	14.4	Max	2.925	0.101	0.00396	-0.104	0.065	0.108	0.0912	0.0758	551-4
150%	551	19.2	Max	2.925	0.101	0.00396	-0.104	0.046	-0.376	0.0922	0.0758	551-4
150%	551	19.2	Max	2.925	0.101	0.00396	-0.104	0.046	-0.376	0.0922	0.0758	551-5

150%	551	24	Max	2.925	0.101	0.00396	-0.104	0.027	-0.861	0.0951	0.0739	551-5
150%	551	0	Min	2.925	0.101	0.00396	-0.104	0.122	1.561	0.1086	0.0551	551-1
150%	551	4.8	Min	2.925	0.101	0.00396	-0.104	0.103	1.077	0.1028	0.062	551-1
150%	551	4.8	Min	2.925	0.101	0.00396	-0.104	0.103	1.077	0.1028	0.062	551-2
150%	551	9.6	Min	2.925	0.101	0.00396	-0.104	0.084	0.592	0.097	0.0689	551-2
150%	551	9.6	Min	2.925	0.101	0.00396	-0.104	0.084	0.592	0.097	0.0689	551-3
150%	551	14.4	Min	2.925	0.101	0.00396	-0.104	0.065	0.108	0.0912	0.0758	551-3
150%	551	14.4	Min	2.925	0.101	0.00396	-0.104	0.065	0.108	0.0912	0.0758	551-4
150%	551	19.2	Min	2.925	0.101	0.00396	-0.104	0.046	-0.376	0.0922	0.0758	551-4
150%	551	19.2	Min	2.925	0.101	0.00396	-0.104	0.046	-0.376	0.0922	0.0758	551-5
150%	551	24	Min	2.925	0.101	0.00396	-0.104	0.027	-0.861	0.0951	0.0739	551-5
175%	551	0	Max	3.657	0.099	0.00662	-0.134	0.186	1.511	0.1357	0.0699	551-1
175%	551	4.8	Max	3.657	0.099	0.00662	-0.134	0.154	1.034	0.1286	0.0781	551-1
175%	551	4.8	Max	3.657	0.099	0.00662	-0.134	0.154	1.034	0.1286	0.0781	551-2
175%	551	9.6	Max	3.657	0.099	0.00662	-0.134	0.123	0.556	0.1215	0.0862	551-2
175%	551	9.6	Max	3.657	0.099	0.00662	-0.134	0.123	0.556	0.1215	0.0862	551-3
175%	551	14.4	Max	3.657	0.099	0.00662	-0.134	0.091	0.079	0.1145	0.0943	551-3
175%	551	14.4	Max	3.657	0.099	0.00662	-0.134	0.091	0.079	0.1145	0.0943	551-4
175%	551	19.2	Max	3.657	0.099	0.00662	-0.134	0.059	-0.398	0.1146	0.0952	551-4
175%	551	19.2	Max	3.657	0.099	0.00662	-0.134	0.059	-0.398	0.1146	0.0952	551-5
175%	551	24	Max	3.657	0.099	0.00662	-0.134	0.027	-0.876	0.1162	0.0947	551-5
175%	551	0	Min	3.657	0.099	0.00662	-0.134	0.186	1.511	0.1357	0.0699	551-1
175%	551	4.8	Min	3.657	0.099	0.00662	-0.134	0.154	1.034	0.1286	0.0781	551-1
175%	551	4.8	Min	3.657	0.099	0.00662	-0.134	0.154	1.034	0.1286	0.0781	551-2
175%	551	9.6	Min	3.657	0.099	0.00662	-0.134	0.123	0.556	0.1215	0.0862	551-2
175%	551	9.6	Min	3.657	0.099	0.00662	-0.134	0.123	0.556	0.1215	0.0862	551-3
175%	551	14.4	Min	3.657	0.099	0.00662	-0.134	0.091	0.079	0.1145	0.0943	551-3
175%	551	14.4	Min	3.657	0.099	0.00662	-0.134	0.091	0.079	0.1145	0.0943	551-4
175%	551	19.2	Min	3.657	0.099	0.00662	-0.134	0.059	-0.398	0.1146	0.0952	551-4
175%	551	19.2	Min	3.657	0.099	0.00662	-0.134	0.059	-0.398	0.1146	0.0952	551-5
175%	551	24	Min	3.657	0.099	0.00662	-0.134	0.027	-0.876	0.1162	0.0947	551-5
200%	551	0	Max	4.234	0.101	0.00856	-0.156	0.233	1.514	0.157	0.0815	551-1
200%	551	4.8	Max	4.234	0.101	0.00856	-0.156	0.192	1.03	0.1489	0.0907	551-1

200%	551	4.8	Max	4.234	0.101	0.00856	-0.156	0.192	1.03	0.1489	0.0907	551-2
200%	551	9.6	Max	4.234	0.101	0.00856	-0.156	0.151	0.546	0.1409	0.0998	551-2
200%	551	9.6	Max	4.234	0.101	0.00856	-0.156	0.151	0.546	0.1409	0.0998	551-3
200%	551	14.4	Max	4.234	0.101	0.00856	-0.156	0.11	0.062	0.1328	0.109	551-3
200%	551	14.4	Max	4.234	0.101	0.00856	-0.156	0.11	0.062	0.1328	0.109	551-4
200%	551	19.2	Max	4.234	0.101	0.00856	-0.156	0.069	-0.422	0.1324	0.1105	551-4
200%	551	19.2	Max	4.234	0.101	0.00856	-0.156	0.069	-0.422	0.1324	0.1105	551-5
200%	551	24	Max	4.234	0.101	0.00856	-0.156	0.028	-0.906	0.1331	0.1109	551-5
200%	551	0	Min	4.234	0.101	0.00856	-0.156	0.233	1.514	0.157	0.0815	551-1
200%	551	4.8	Min	4.234	0.101	0.00856	-0.156	0.192	1.03	0.1489	0.0907	551-1
200%	551	4.8	Min	4.234	0.101	0.00856	-0.156	0.192	1.03	0.1489	0.0907	551-2
200%	551	9.6	Min	4.234	0.101	0.00856	-0.156	0.151	0.546	0.1409	0.0998	551-2
200%	551	9.6	Min	4.234	0.101	0.00856	-0.156	0.151	0.546	0.1409	0.0998	551-3
200%	551	14.4	Min	4.234	0.101	0.00856	-0.156	0.11	0.062	0.1328	0.109	551-3
200%	551	14.4	Min	4.234	0.101	0.00856	-0.156	0.11	0.062	0.1328	0.109	551-4
200%	551	19.2	Min	4.234	0.101	0.00856	-0.156	0.069	-0.422	0.1324	0.1105	551-4
200%	551	19.2	Min	4.234	0.101	0.00856	-0.156	0.069	-0.422	0.1324	0.1105	551-5
200%	551	24	Min	4.234	0.101	0.00856	-0.156	0.028	-0.906	0.1331	0.1109	551-5
225%	551	0	Max	5.007	0.095	0.012	-0.19	0.308	1.393	0.1859	0.0971	551-1
225%	551	4.8	Max	5.007	0.095	0.012	-0.19	0.252	0.936	0.1765	0.1076	551-1
225%	551	4.8	Max	5.007	0.095	0.012	-0.19	0.252	0.936	0.1765	0.1076	551-2
225%	551	9.6	Max	5.007	0.095	0.012	-0.19	0.196	0.478	0.167	0.118	551-2
225%	551	9.6	Max	5.007	0.095	0.012	-0.19	0.196	0.478	0.167	0.118	551-3
225%	551	14.4	Max	5.007	0.095	0.012	-0.19	0.14	0.02	0.1576	0.1285	551-3
225%	551	14.4	Max	5.007	0.095	0.012	-0.19	0.14	0.02	0.1576	0.1285	551-4
225%	551	19.2	Max	5.007	0.095	0.012	-0.19	0.083	-0.438	0.1561	0.131	551-4
225%	551	19.2	Max	5.007	0.095	0.012	-0.19	0.083	-0.438	0.1561	0.131	551-5
225%	551	24	Max	5.007	0.095	0.012	-0.19	0.027	-0.895	0.155	0.1332	551-5
225%	551	0	Min	5.007	0.095	0.012	-0.19	0.308	1.393	0.1859	0.0971	551-1
225%	551	4.8	Min	5.007	0.095	0.012	-0.19	0.252	0.936	0.1765	0.1076	551-1
225%	551	4.8	Min	5.007	0.095	0.012	-0.19	0.252	0.936	0.1765	0.1076	551-2
225%	551	9.6	Min	5.007	0.095	0.012	-0.19	0.196	0.478	0.167	0.118	551-2
225%	551	9.6	Min	5.007	0.095	0.012	-0.19	0.196	0.478	0.167	0.118	551-3

225%	551	14.4	Min	5.007	0.095	0.012	-0.19	0.14	0.02	0.1576	0.1285	551-3
225%	551	14.4	Min	5.007	0.095	0.012	-0.19	0.14	0.02	0.1576	0.1285	551-4
225%	551	19.2	Min	5.007	0.095	0.012	-0.19	0.083	-0.438	0.1561	0.131	551-4
225%	551	19.2	Min	5.007	0.095	0.012	-0.19	0.083	-0.438	0.1561	0.131	551-5
225%	551	24	Min	5.007	0.095	0.012	-0.19	0.027	-0.895	0.155	0.1332	551-5
250%	551	0	Max	5.621	0.091	0.014	-0.216	0.368	1.298	0.2089	0.1094	551-1
250%	551	4.8	Max	5.621	0.091	0.014	-0.216	0.3	0.861	0.1984	0.1209	551-1
250%	551	4.8	Max	5.621	0.091	0.014	-0.216	0.3	0.861	0.1984	0.1209	551-2
250%	551	9.6	Max	5.621	0.091	0.014	-0.216	0.231	0.424	0.1878	0.1324	551-2
250%	551	9.6	Max	5.621	0.091	0.014	-0.216	0.231	0.424	0.1878	0.1324	551-3
250%	551	14.4	Max	5.621	0.091	0.014	-0.216	0.163	-0.013	0.1775	0.1437	551-3
250%	551	14.4	Max	5.621	0.091	0.014	-0.216	0.163	-0.013	0.1775	0.1437	551-4
250%	551	19.2	Max	5.621	0.091	0.014	-0.216	0.095	-0.451	0.1749	0.1473	551-4
250%	551	19.2	Max	5.621	0.091	0.014	-0.216	0.095	-0.451	0.1749	0.1473	551-5
250%	551	24	Max	5.621	0.091	0.014	-0.216	0.026	-0.888	0.1723	0.1509	551-5
250%	551	0	Min	5.621	0.091	0.014	-0.216	0.368	1.298	0.2089	0.1094	551-1
250%	551	4.8	Min	5.621	0.091	0.014	-0.216	0.3	0.861	0.1984	0.1209	551-1
250%	551	4.8	Min	5.621	0.091	0.014	-0.216	0.3	0.861	0.1984	0.1209	551-2
250%	551	9.6	Min	5.621	0.091	0.014	-0.216	0.231	0.424	0.1878	0.1324	551-2
250%	551	9.6	Min	5.621	0.091	0.014	-0.216	0.231	0.424	0.1878	0.1324	551-3
250%	551	14.4	Min	5.621	0.091	0.014	-0.216	0.163	-0.013	0.1775	0.1437	551-3
250%	551	14.4	Min	5.621	0.091	0.014	-0.216	0.163	-0.013	0.1775	0.1437	551-4
250%	551	19.2	Min	5.621	0.091	0.014	-0.216	0.095	-0.451	0.1749	0.1473	551-4
250%	551	19.2	Min	5.621	0.091	0.014	-0.216	0.095	-0.451	0.1749	0.1473	551-5
250%	551	24	Min	5.621	0.091	0.014	-0.216	0.026	-0.888	0.1723	0.1509	551-5
275%	551	0	Max	6.427	0.082	0.018	-0.252	0.457	1.127	0.2397	0.1251	551-1
275%	551	4.8	Max	6.427	0.082	0.018	-0.252	0.37	0.732	0.2276	0.138	551-1
275%	551	4.8	Max	6.427	0.082	0.018	-0.252	0.37	0.732	0.2276	0.138	551-2
275%	551	9.6	Max	6.427	0.082	0.018	-0.252	0.284	0.337	0.2156	0.151	551-2
275%	551	9.6	Max	6.427	0.082	0.018	-0.252	0.284	0.337	0.2156	0.151	551-3
275%	551	14.4	Max	6.427	0.082	0.018	-0.252	0.197	-0.058	0.2045	0.1629	551-3
275%	551	14.4	Max	6.427	0.082	0.018	-0.252	0.197	-0.058	0.2045	0.1629	551-4
275%	551	19.2	Max	6.427	0.082	0.018	-0.252	0.11	-0.453	0.1996	0.1686	551-4

275%	551	19.2	Max	6.427	0.082	0.018	-0.252	0.11	-0.453	0.1996	0.1686	551-5
275%	551	24	Max	6.427	0.082	0.018	-0.252	0.024	-0.848	0.1947	0.1744	551-5
275%	551	0	Min	6.427	0.082	0.018	-0.252	0.457	1.127	0.2397	0.1251	551-1
275%	551	4.8	Min	6.427	0.082	0.018	-0.252	0.37	0.732	0.2276	0.138	551-1
275%	551	4.8	Min	6.427	0.082	0.018	-0.252	0.37	0.732	0.2276	0.138	551-2
275%	551	9.6	Min	6.427	0.082	0.018	-0.252	0.284	0.337	0.2156	0.151	551-2
275%	551	9.6	Min	6.427	0.082	0.018	-0.252	0.284	0.337	0.2156	0.151	551-3
275%	551	14.4	Min	6.427	0.082	0.018	-0.252	0.197	-0.058	0.2045	0.1629	551-3
275%	551	14.4	Min	6.427	0.082	0.018	-0.252	0.197	-0.058	0.2045	0.1629	551-4
275%	551	19.2	Min	6.427	0.082	0.018	-0.252	0.11	-0.453	0.1996	0.1686	551-4
275%	551	19.2	Min	6.427	0.082	0.018	-0.252	0.11	-0.453	0.1996	0.1686	551-5
275%	551	24	Min	6.427	0.082	0.018	-0.252	0.024	-0.848	0.1947	0.1744	551-5
300%	551	0	Max	7.319	0.074	0.022	-0.291	0.555	0.974	0.274	0.142	551-1
300%	551	4.8	Max	7.319	0.074	0.022	-0.291	0.448	0.616	0.2602	0.1566	551-1
300%	551	4.8	Max	7.319	0.074	0.022	-0.291	0.448	0.616	0.2602	0.1566	551-2
300%	551	9.6	Max	7.319	0.074	0.022	-0.291	0.342	0.259	0.2464	0.1713	551-2
300%	551	9.6	Max	7.319	0.074	0.022	-0.291	0.342	0.259	0.2464	0.1713	551-3
300%	551	14.4	Max	7.319	0.074	0.022	-0.291	0.235	-0.099	0.2343	0.1841	551-3
300%	551	14.4	Max	7.319	0.074	0.022	-0.291	0.235	-0.099	0.2343	0.1841	551-4
300%	551	19.2	Max	7.319	0.074	0.022	-0.291	0.128	-0.457	0.227	0.1922	551-4
300%	551	19.2	Max	7.319	0.074	0.022	-0.291	0.128	-0.457	0.227	0.1922	551-5
300%	551	24	Max	7.319	0.074	0.022	-0.291	0.022	-0.814	0.2196	0.2004	551-5
300%	551	0	Min	7.319	0.074	0.022	-0.291	0.555	0.974	0.274	0.142	551-1
300%	551	4.8	Min	7.319	0.074	0.022	-0.291	0.448	0.616	0.2602	0.1566	551-1
300%	551	4.8	Min	7.319	0.074	0.022	-0.291	0.448	0.616	0.2602	0.1566	551-2
300%	551	9.6	Min	7.319	0.074	0.022	-0.291	0.342	0.259	0.2464	0.1713	551-2
300%	551	9.6	Min	7.319	0.074	0.022	-0.291	0.342	0.259	0.2464	0.1713	551-3
300%	551	14.4	Min	7.319	0.074	0.022	-0.291	0.235	-0.099	0.2343	0.1841	551-3
300%	551	14.4	Min	7.319	0.074	0.022	-0.291	0.235	-0.099	0.2343	0.1841	551-4
300%	551	19.2	Min	7.319	0.074	0.022	-0.291	0.128	-0.457	0.227	0.1922	551-4
300%	551	19.2	Min	7.319	0.074	0.022	-0.291	0.128	-0.457	0.227	0.1922	551-5
300%	551	24	Min	7.319	0.074	0.022	-0.291	0.022	-0.814	0.2196	0.2004	551-5

TABLE: Element Forces - Frames Member 4 Interior Strut												
Model	Frame	Station	StepType	P	V2	V3	T	M2	M3	S11Max	S11Min	FrameElem
Text	Text	in	Text	Kip	Kip	Kip	Kip-in	Kip-in	Kip-in	Kip/in2	Kip/in2	Text
15%	1129	0	Max	-0.324	-0.043	0.000194	0.003929	-0.00627	-3.007	0.000246	-0.00065	1129-1
15%	1129	24	Max	-0.324	-0.043	0.000194	0.003929	-0.011	-1.97	0.000102	-0.00051	1129-1
15%	1129	24	Max	-0.324	-0.043	0.000214	0.001802	-0.011	-1.97	0.000102	-0.00051	1129-2
15%	1129	48	Max	-0.324	-0.043	0.000214	0.001802	-0.016	-0.934	-4E-05	-0.00036	1129-2
15%	1129	0	Min	-0.324	-0.043	0.000194	0.003929	-0.00627	-3.007	0.000246	-0.00065	1129-1
15%	1129	24	Min	-0.324	-0.043	0.000194	0.003929	-0.011	-1.97	0.000102	-0.00051	1129-1
15%	1129	24	Min	-0.324	-0.043	0.000214	0.001802	-0.011	-1.97	0.000102	-0.00051	1129-2
15%	1129	48	Min	-0.324	-0.043	0.000214	0.001802	-0.016	-0.934	-4E-05	-0.00036	1129-2
25%	1129	0	Max	-0.032	-0.00264	0.001791	0.00023	0.095	-1.184	0.000306	-0.00035	1129-1
25%	1129	24	Max	-0.032	-0.00264	0.001791	0.00023	0.052	-1.121	0.000228	-0.00027	1129-1
25%	1129	24	Max	-0.032	-0.00264	0.001816	-0.002	0.051	-1.121	0.000226	-0.00027	1129-2
25%	1129	48	Max	-0.032	-0.00264	0.001816	-0.002	0.007878	-1.058	0.000147	-0.00019	1129-2
25%	1129	0	Min	-0.032	-0.00264	0.001791	0.00023	0.095	-1.184	0.000306	-0.00035	1129-1
25%	1129	24	Min	-0.032	-0.00264	0.001791	0.00023	0.052	-1.121	0.000228	-0.00027	1129-1
25%	1129	24	Min	-0.032	-0.00264	0.001816	-0.002	0.051	-1.121	0.000226	-0.00027	1129-2
25%	1129	48	Min	-0.032	-0.00264	0.001816	-0.002	0.007878	-1.058	0.000147	-0.00019	1129-2
50%	1129	0	Max	0.444	-0.018	0.007359	0.000674	0.3	-0.73	0.000864	-0.00031	1129-1
50%	1129	24	Max	0.444	-0.018	0.007359	0.000674	0.123	-0.299	0.000518	3.6E-05	1129-1
50%	1129	24	Max	0.444	-0.018	0.00738	-0.00081	0.122	-0.299	0.000516	3.77E-05	1129-2
50%	1129	48	Max	0.444	-0.018	0.00738	-0.00081	-0.055	0.132	0.000385	0.000169	1129-2
50%	1129	0	Min	0.444	-0.018	0.007359	0.000674	0.3	-0.73	0.000864	-0.00031	1129-1
50%	1129	24	Min	0.444	-0.018	0.007359	0.000674	0.123	-0.299	0.000518	3.6E-05	1129-1
50%	1129	24	Min	0.444	-0.018	0.00738	-0.00081	0.122	-0.299	0.000516	3.77E-05	1129-2
50%	1129	48	Min	0.444	-0.018	0.00738	-0.00081	-0.055	0.132	0.000385	0.000169	1129-2
75%	1129	0	Max	1.118	-0.0023	0.015	0.003377	0.585	-0.106	0.0017	-0.00026	1129-1
75%	1129	24	Max	1.118	-0.0023	0.015	0.003377	0.225	-0.051	0.0011	0.00033	1129-1
75%	1129	24	Max	1.118	-0.0023	0.015	-0.00571	0.222	-0.051	0.0011	0.000335	1129-2
75%	1129	48	Max	1.118	-0.0023	0.015	-0.00571	-0.142	0.004737	0.000926	0.00047	1129-2

75%	1129	0	Min	1.118	-0.0023	0.015	0.003377	0.585	-0.106	0.0017	-0.00026	1129-1
75%	1129	24	Min	1.118	-0.0023	0.015	0.003377	0.225	-0.051	0.0011	0.00033	1129-1
75%	1129	24	Min	1.118	-0.0023	0.015	-0.00571	0.222	-0.051	0.0011	0.000335	1129-2
75%	1129	48	Min	1.118	-0.0023	0.015	-0.00571	-0.142	0.004737	0.000926	0.00047	1129-2
100%	1129	0	Max	1.581	0.005045	0.021	0.004463	0.824	0.045	0.0023	-0.00034	1129-1
100%	1129	24	Max	1.581	0.005045	0.021	0.004463	0.313	-0.077	0.0015	0.000474	1129-1
100%	1129	24	Max	1.581	0.005045	0.021	-0.00764	0.309	-0.077	0.0015	0.00048	1129-2
100%	1129	48	Max	1.581	0.005045	0.021	-0.00764	-0.206	-0.198	0.0013	0.000628	1129-2
100%	1129	0	Min	1.581	0.005045	0.021	0.004463	0.824	0.045	0.0023	-0.00034	1129-1
100%	1129	24	Min	1.581	0.005045	0.021	0.004463	0.313	-0.077	0.0015	0.000474	1129-1
100%	1129	24	Min	1.581	0.005045	0.021	-0.00764	0.309	-0.077	0.0015	0.00048	1129-2
100%	1129	48	Min	1.581	0.005045	0.021	-0.00764	-0.206	-0.198	0.0013	0.000628	1129-2
125%	1129	0	Max	2.316	0.012	0.03	0.01	1.13	0.077	0.0033	-0.00038	1129-1
125%	1129	24	Max	2.316	0.012	0.03	0.01	0.404	-0.216	0.0021	0.000767	1129-1
125%	1129	24	Max	2.316	0.012	0.031	-0.015	0.397	-0.216	0.0021	0.000777	1129-2
125%	1129	48	Max	2.316	0.012	0.031	-0.015	-0.336	-0.509	0.0021	0.000833	1129-2
125%	1129	0	Min	2.316	0.012	0.03	0.01	1.13	0.077	0.0033	-0.00038	1129-1
125%	1129	24	Min	2.316	0.012	0.03	0.01	0.404	-0.216	0.0021	0.000767	1129-1
125%	1129	24	Min	2.316	0.012	0.031	-0.015	0.397	-0.216	0.0021	0.000777	1129-2
125%	1129	48	Min	2.316	0.012	0.031	-0.015	-0.336	-0.509	0.0021	0.000833	1129-2
150%	1129	0	Max	2.856	0.016	0.037	0.014	1.379	0.089	0.004	-0.00044	1129-1
150%	1129	24	Max	2.856	0.016	0.037	0.014	0.483	-0.286	0.0026	0.000966	1129-1
150%	1129	24	Max	2.856	0.016	0.038	-0.019	0.475	-0.286	0.0026	0.000979	1129-2
150%	1129	48	Max	2.856	0.016	0.038	-0.019	-0.43	-0.66	0.0026	0.000998	1129-2
150%	1129	0	Min	2.856	0.016	0.037	0.014	1.379	0.089	0.004	-0.00044	1129-1
150%	1129	24	Min	2.856	0.016	0.037	0.014	0.483	-0.286	0.0026	0.000966	1129-1
150%	1129	24	Min	2.856	0.016	0.038	-0.019	0.475	-0.286	0.0026	0.000979	1129-2
150%	1129	48	Min	2.856	0.016	0.038	-0.019	-0.43	-0.66	0.0026	0.000998	1129-2
175%	1129	0	Max	3.661	0.02	0.047	0.022	1.693	0.021	0.005	-0.00043	1129-1
175%	1129	24	Max	3.661	0.02	0.047	0.022	0.564	-0.459	0.0033	0.0013	1129-1
175%	1129	24	Max	3.661	0.02	0.048	-0.028	0.552	-0.459	0.0032	0.0013	1129-2
175%	1129	48	Max	3.661	0.02	0.048	-0.028	-0.592	-0.939	0.0034	0.0012	1129-2

175%	1129	0	Min	3.661	0.02	0.047	0.022	1.693	0.021	0.005	-0.00043	1129-1
175%	1129	24	Min	3.661	0.02	0.047	0.022	0.564	-0.459	0.0033	0.0013	1129-1
175%	1129	24	Min	3.661	0.02	0.048	-0.028	0.552	-0.459	0.0032	0.0013	1129-2
175%	1129	48	Min	3.661	0.02	0.048	-0.028	-0.592	-0.939	0.0034	0.0012	1129-2
200%	1129	0	Max	4.295	0.023	0.055	0.028	1.949	-0.016	0.0058	-0.00045	1129-1
200%	1129	24	Max	4.295	0.023	0.055	0.028	0.634	-0.576	0.0038	0.0016	1129-1
200%	1129	24	Max	4.295	0.023	0.056	-0.035	0.619	-0.576	0.0038	0.0016	1129-2
200%	1129	48	Max	4.295	0.023	0.056	-0.035	-0.713	-1.136	0.004	0.0014	1129-2
200%	1129	0	Min	4.295	0.023	0.055	0.028	1.949	-0.016	0.0058	-0.00045	1129-1
200%	1129	24	Min	4.295	0.023	0.055	0.028	0.634	-0.576	0.0038	0.0016	1129-1
200%	1129	24	Min	4.295	0.023	0.056	-0.035	0.619	-0.576	0.0038	0.0016	1129-2
200%	1129	48	Min	4.295	0.023	0.056	-0.035	-0.713	-1.136	0.004	0.0014	1129-2
225%	1129	0	Max	5.147	0.028	0.064	0.038	2.249	-0.103	0.0068	-0.00041	1129-1
225%	1129	24	Max	5.147	0.028	0.064	0.038	0.704	-0.776	0.0045	0.002	1129-1
225%	1129	24	Max	5.147	0.028	0.065	-0.045	0.684	-0.776	0.0044	0.002	1129-2
225%	1129	48	Max	5.147	0.028	0.065	-0.045	-0.884	-1.448	0.0048	0.0016	1129-2
225%	1129	0	Min	5.147	0.028	0.064	0.038	2.249	-0.103	0.0068	-0.00041	1129-1
225%	1129	24	Min	5.147	0.028	0.064	0.038	0.704	-0.776	0.0045	0.002	1129-1
225%	1129	24	Min	5.147	0.028	0.065	-0.045	0.684	-0.776	0.0044	0.002	1129-2
225%	1129	48	Min	5.147	0.028	0.065	-0.045	-0.884	-1.448	0.0048	0.0016	1129-2
250%	1129	0	Max	5.825	0.032	0.072	0.046	2.487	-0.173	0.0077	-0.00038	1129-1
250%	1129	24	Max	5.825	0.032	0.072	0.046	0.754	-0.933	0.005	0.0023	1129-1
250%	1129	24	Max	5.825	0.032	0.073	-0.053	0.731	-0.933	0.0049	0.0023	1129-2
250%	1129	48	Max	5.825	0.032	0.073	-0.053	-1.03	-1.693	0.0055	0.0017	1129-2
250%	1129	0	Min	5.825	0.032	0.072	0.046	2.487	-0.173	0.0077	-0.00038	1129-1
250%	1129	24	Min	5.825	0.032	0.072	0.046	0.754	-0.933	0.005	0.0023	1129-1
250%	1129	24	Min	5.825	0.032	0.073	-0.053	0.731	-0.933	0.0049	0.0023	1129-2
250%	1129	48	Min	5.825	0.032	0.073	-0.053	-1.03	-1.693	0.0055	0.0017	1129-2
275%	1129	0	Max	6.716	0.035	0.081	0.058	2.741	-0.353	0.0086	-0.00026	1129-1
275%	1129	24	Max	6.716	0.035	0.081	0.058	0.809	-1.198	0.0057	0.0027	1129-1
275%	1129	24	Max	6.716	0.035	0.082	-0.065	0.78	-1.198	0.0056	0.0028	1129-2
275%	1129	48	Max	6.716	0.035	0.082	-0.065	-1.187	-2.043	0.0064	0.002	1129-2

275%	1129	0	Min	6.716	0.035	0.081	0.058	2.741	-0.353	0.0086	-0.00026	1129-1
275%	1129	24	Min	6.716	0.035	0.081	0.058	0.809	-1.198	0.0057	0.0027	1129-1
275%	1129	24	Min	6.716	0.035	0.082	-0.065	0.78	-1.198	0.0056	0.0028	1129-2
275%	1129	48	Min	6.716	0.035	0.082	-0.065	-1.187	-2.043	0.0064	0.002	1129-2
300%	1129	0	Max	7.699	0.039	0.089	0.07	3.009	-0.549	0.0097	-0.0001	1129-1
300%	1129	24	Max	7.699	0.039	0.089	0.07	0.867	-1.482	0.0064	0.0032	1129-1
300%	1129	24	Max	7.699	0.039	0.091	-0.077	0.832	-1.482	0.0064	0.0033	1129-2
300%	1129	48	Max	7.699	0.039	0.091	-0.077	-1.351	-2.414	0.0073	0.0023	1129-2
300%	1129	0	Min	7.699	0.039	0.089	0.07	3.009	-0.549	0.0097	-0.0001	1129-1
300%	1129	24	Min	7.699	0.039	0.089	0.07	0.867	-1.482	0.0064	0.0032	1129-1
300%	1129	24	Min	7.699	0.039	0.091	-0.077	0.832	-1.482	0.0064	0.0033	1129-2
300%	1129	48	Min	7.699	0.039	0.091	-0.077	-1.351	-2.414	0.0073	0.0023	1129-2

TABLE: Element Forces - Frames Member 1 Exterior Chord												
Model	Frame	Station	StepType	P	V2	V3	T	M2	M3	S11Max	S11Min	FrameElem
Text	Text	in	Text	Kip	Kip	Kip	Kip-in	Kip-in	Kip-in	Kip/in2	Kip/in2	Text
15%	305	0	Max	-0.067	0.016	0.001858	-0.00285	0.046	0.916	0.0101	-0.016	305-1
15%	305	4.8	Max	-0.067	0.016	0.001858	-0.00285	0.037	0.838	0.0086	-0.0143	305-1
15%	305	4.8	Max	-0.067	0.016	0.001858	-0.00285	0.037	0.838	0.0086	-0.0143	305-2
15%	305	9.6	Max	-0.067	0.016	0.001858	-0.00285	0.028	0.759	0.007	-0.0126	305-2
15%	305	9.6	Max	-0.067	0.016	0.001858	-0.00285	0.028	0.759	0.007	-0.0126	305-3
15%	305	14.4	Max	-0.067	0.016	0.001858	-0.00285	0.019	0.681	0.0055	-0.0108	305-3
15%	305	14.4	Max	-0.067	0.016	0.001858	-0.00285	0.019	0.681	0.0055	-0.0108	305-4
15%	305	19.2	Max	-0.067	0.016	0.001858	-0.00285	0.011	0.602	0.004	-0.0091	305-4
15%	305	19.2	Max	-0.067	0.016	0.001858	-0.00285	0.011	0.602	0.004	-0.0091	305-5
15%	305	24	Max	-0.067	0.016	0.001858	-0.00285	0.001657	0.523	0.0024	-0.0074	305-5
15%	305	0	Min	-0.067	0.016	0.001858	-0.00285	0.046	0.916	0.0101	-0.016	305-1
15%	305	4.8	Min	-0.067	0.016	0.001858	-0.00285	0.037	0.838	0.0086	-0.0143	305-1
15%	305	4.8	Min	-0.067	0.016	0.001858	-0.00285	0.037	0.838	0.0086	-0.0143	305-2
15%	305	9.6	Min	-0.067	0.016	0.001858	-0.00285	0.028	0.759	0.007	-0.0126	305-2
15%	305	9.6	Min	-0.067	0.016	0.001858	-0.00285	0.028	0.759	0.007	-0.0126	305-3
15%	305	14.4	Min	-0.067	0.016	0.001858	-0.00285	0.019	0.681	0.0055	-0.0108	305-3
15%	305	14.4	Min	-0.067	0.016	0.001858	-0.00285	0.019	0.681	0.0055	-0.0108	305-4
15%	305	19.2	Min	-0.067	0.016	0.001858	-0.00285	0.011	0.602	0.004	-0.0091	305-4
15%	305	19.2	Min	-0.067	0.016	0.001858	-0.00285	0.011	0.602	0.004	-0.0091	305-5
15%	305	24	Min	-0.067	0.016	0.001858	-0.00285	0.001657	0.523	0.0024	-0.0074	305-5
25%	305	0	Max	-0.152	0.007378	-0.00119	0.024	-0.044	0.349	0.003	-0.0125	305-1
25%	305	4.8	Max	-0.152	0.007378	-0.00119	0.024	-0.039	0.314	0.0021	-0.0115	305-1
25%	305	4.8	Max	-0.152	0.007378	-0.00119	0.024	-0.039	0.314	0.0021	-0.0115	305-2
25%	305	9.6	Max	-0.152	0.007378	-0.00119	0.024	-0.033	0.278	0.0013	-0.0106	305-2
25%	305	9.6	Max	-0.152	0.007378	-0.00119	0.024	-0.033	0.278	0.0013	-0.0106	305-3
25%	305	14.4	Max	-0.152	0.007378	-0.00119	0.024	-0.027	0.243	0.000383	-0.0096	305-3
25%	305	14.4	Max	-0.152	0.007378	-0.00119	0.024	-0.027	0.243	0.000383	-0.0096	305-4
25%	305	19.2	Max	-0.152	0.007378	-0.00119	0.024	-0.022	0.208	-0.00049	-0.0087	305-4
25%	305	19.2	Max	-0.152	0.007378	-0.00119	0.024	-0.022	0.208	-0.00049	-0.0087	305-5

25%	305	24	Max	-0.152	0.007378	-0.00119	0.024	-0.016	0.172	-0.0014	-0.0077	305-5
25%	305	0	Min	-0.152	0.007378	-0.00119	0.024	-0.044	0.349	0.003	-0.0125	305-1
25%	305	4.8	Min	-0.152	0.007378	-0.00119	0.024	-0.039	0.314	0.0021	-0.0115	305-1
25%	305	4.8	Min	-0.152	0.007378	-0.00119	0.024	-0.039	0.314	0.0021	-0.0115	305-2
25%	305	9.6	Min	-0.152	0.007378	-0.00119	0.024	-0.033	0.278	0.0013	-0.0106	305-2
25%	305	9.6	Min	-0.152	0.007378	-0.00119	0.024	-0.033	0.278	0.0013	-0.0106	305-3
25%	305	14.4	Min	-0.152	0.007378	-0.00119	0.024	-0.027	0.243	0.000383	-0.0096	305-3
25%	305	14.4	Min	-0.152	0.007378	-0.00119	0.024	-0.027	0.243	0.000383	-0.0096	305-4
25%	305	19.2	Min	-0.152	0.007378	-0.00119	0.024	-0.022	0.208	-0.00049	-0.0087	305-4
25%	305	19.2	Min	-0.152	0.007378	-0.00119	0.024	-0.022	0.208	-0.00049	-0.0087	305-5
25%	305	24	Min	-0.152	0.007378	-0.00119	0.024	-0.016	0.172	-0.0014	-0.0077	305-5
50%	305	0	Max	-0.375	0.037	-0.00204	0.008029	-0.061	0.664	0.000844	-0.0238	305-1
50%	305	4.8	Max	-0.375	0.037	-0.00204	0.008029	-0.051	0.486	-0.0016	-0.0209	305-1
50%	305	4.8	Max	-0.375	0.037	-0.00204	0.008029	-0.051	0.486	-0.0016	-0.0209	305-2
50%	305	9.6	Max	-0.375	0.037	-0.00204	0.008029	-0.041	0.308	-0.004	-0.0181	305-2
50%	305	9.6	Max	-0.375	0.037	-0.00204	0.008029	-0.041	0.308	-0.004	-0.0181	305-3
50%	305	14.4	Max	-0.375	0.037	-0.00204	0.008029	-0.032	0.129	-0.0064	-0.0153	305-3
50%	305	14.4	Max	-0.375	0.037	-0.00204	0.008029	-0.032	0.129	-0.0064	-0.0153	305-4
50%	305	19.2	Max	-0.375	0.037	-0.00204	0.008029	-0.022	-0.049	-0.008	-0.0134	305-4
50%	305	19.2	Max	-0.375	0.037	-0.00204	0.008029	-0.022	-0.049	-0.008	-0.0134	305-5
50%	305	24	Max	-0.375	0.037	-0.00204	0.008029	-0.012	-0.227	-0.0072	-0.0138	305-5
50%	305	0	Min	-0.375	0.037	-0.00204	0.008029	-0.061	0.664	0.000844	-0.0238	305-1
50%	305	4.8	Min	-0.375	0.037	-0.00204	0.008029	-0.051	0.486	-0.0016	-0.0209	305-1
50%	305	4.8	Min	-0.375	0.037	-0.00204	0.008029	-0.051	0.486	-0.0016	-0.0209	305-2
50%	305	9.6	Min	-0.375	0.037	-0.00204	0.008029	-0.041	0.308	-0.004	-0.0181	305-2
50%	305	9.6	Min	-0.375	0.037	-0.00204	0.008029	-0.041	0.308	-0.004	-0.0181	305-3
50%	305	14.4	Min	-0.375	0.037	-0.00204	0.008029	-0.032	0.129	-0.0064	-0.0153	305-3
50%	305	14.4	Min	-0.375	0.037	-0.00204	0.008029	-0.032	0.129	-0.0064	-0.0153	305-4
50%	305	19.2	Min	-0.375	0.037	-0.00204	0.008029	-0.022	-0.049	-0.008	-0.0134	305-4
50%	305	19.2	Min	-0.375	0.037	-0.00204	0.008029	-0.022	-0.049	-0.008	-0.0134	305-5
50%	305	24	Min	-0.375	0.037	-0.00204	0.008029	-0.012	-0.227	-0.0072	-0.0138	305-5
75%	305	0	Max	-0.511	0.054	-0.00582	0.009263	-0.153	1.179	0.0106	-0.0424	305-1
75%	305	4.8	Max	-0.511	0.054	-0.00582	0.009263	-0.125	0.922	0.0056	-0.0369	305-1

75%	305	4.8	Max	-0.511	0.054	-0.00582	0.009263	-0.125	0.922	0.0056	-0.0369	305-2
75%	305	9.6	Max	-0.511	0.054	-0.00582	0.009263	-0.097	0.665	0.00071	-0.0314	305-2
75%	305	9.6	Max	-0.511	0.054	-0.00582	0.009263	-0.097	0.665	0.00071	-0.0314	305-3
75%	305	14.4	Max	-0.511	0.054	-0.00582	0.009263	-0.069	0.408	-0.0042	-0.0259	305-3
75%	305	14.4	Max	-0.511	0.054	-0.00582	0.009263	-0.069	0.408	-0.0042	-0.0259	305-4
75%	305	19.2	Max	-0.511	0.054	-0.00582	0.009263	-0.042	0.15	-0.0091	-0.0204	305-4
75%	305	19.2	Max	-0.511	0.054	-0.00582	0.009263	-0.042	0.15	-0.0091	-0.0204	305-5
75%	305	24	Max	-0.511	0.054	-0.00582	0.009263	-0.014	-0.107	-0.0121	-0.0169	305-5
75%	305	0	Min	-0.511	0.054	-0.00582	0.009263	-0.153	1.179	0.0106	-0.0424	305-1
75%	305	4.8	Min	-0.511	0.054	-0.00582	0.009263	-0.125	0.922	0.0056	-0.0369	305-1
75%	305	4.8	Min	-0.511	0.054	-0.00582	0.009263	-0.125	0.922	0.0056	-0.0369	305-2
75%	305	9.6	Min	-0.511	0.054	-0.00582	0.009263	-0.097	0.665	0.00071	-0.0314	305-2
75%	305	9.6	Min	-0.511	0.054	-0.00582	0.009263	-0.097	0.665	0.00071	-0.0314	305-3
75%	305	14.4	Min	-0.511	0.054	-0.00582	0.009263	-0.069	0.408	-0.0042	-0.0259	305-3
75%	305	14.4	Min	-0.511	0.054	-0.00582	0.009263	-0.069	0.408	-0.0042	-0.0259	305-4
75%	305	19.2	Min	-0.511	0.054	-0.00582	0.009263	-0.042	0.15	-0.0091	-0.0204	305-4
75%	305	19.2	Min	-0.511	0.054	-0.00582	0.009263	-0.042	0.15	-0.0091	-0.0204	305-5
75%	305	24	Min	-0.511	0.054	-0.00582	0.009263	-0.014	-0.107	-0.0121	-0.0169	305-5
100%	305	0	Max	-0.705	0.062	-0.00839	0.009947	-0.217	1.427	0.0135	-0.057	305-1
100%	305	4.8	Max	-0.705	0.062	-0.00839	0.009947	-0.177	1.128	0.007	-0.0498	305-1
100%	305	4.8	Max	-0.705	0.062	-0.00839	0.009947	-0.177	1.128	0.007	-0.0498	305-2
100%	305	9.6	Max	-0.705	0.062	-0.00839	0.009947	-0.136	0.828	0.000476	-0.0426	305-2
100%	305	9.6	Max	-0.705	0.062	-0.00839	0.009947	-0.136	0.828	0.000476	-0.0426	305-3
100%	305	14.4	Max	-0.705	0.062	-0.00839	0.009947	-0.096	0.528	-0.0061	-0.0354	305-3
100%	305	14.4	Max	-0.705	0.062	-0.00839	0.009947	-0.096	0.528	-0.0061	-0.0354	305-4
100%	305	19.2	Max	-0.705	0.062	-0.00839	0.009947	-0.056	0.228	-0.0126	-0.0282	305-4
100%	305	19.2	Max	-0.705	0.062	-0.00839	0.009947	-0.056	0.228	-0.0126	-0.0282	305-5
100%	305	24	Max	-0.705	0.062	-0.00839	0.009947	-0.016	-0.071	-0.0178	-0.0223	305-5
100%	305	0	Min	-0.705	0.062	-0.00839	0.009947	-0.217	1.427	0.0135	-0.057	305-1
100%	305	4.8	Min	-0.705	0.062	-0.00839	0.009947	-0.177	1.128	0.007	-0.0498	305-1
100%	305	4.8	Min	-0.705	0.062	-0.00839	0.009947	-0.177	1.128	0.007	-0.0498	305-2
100%	305	9.6	Min	-0.705	0.062	-0.00839	0.009947	-0.136	0.828	0.000476	-0.0426	305-2
100%	305	9.6	Min	-0.705	0.062	-0.00839	0.009947	-0.136	0.828	0.000476	-0.0426	305-3

100%	305	14.4	Min	-0.705	0.062	-0.00839	0.009947	-0.096	0.528	-0.0061	-0.0354	305-3
100%	305	14.4	Min	-0.705	0.062	-0.00839	0.009947	-0.096	0.528	-0.0061	-0.0354	305-4
100%	305	19.2	Min	-0.705	0.062	-0.00839	0.009947	-0.056	0.228	-0.0126	-0.0282	305-4
100%	305	19.2	Min	-0.705	0.062	-0.00839	0.009947	-0.056	0.228	-0.0126	-0.0282	305-5
100%	305	24	Min	-0.705	0.062	-0.00839	0.009947	-0.016	-0.071	-0.0178	-0.0223	305-5
125%	305	0	Max	-0.727	0.059	-0.013	0.024	-0.32	1.786	0.0264	-0.072	305-1
125%	305	4.8	Max	-0.727	0.059	-0.013	0.024	-0.259	1.503	0.0179	-0.0628	305-1
125%	305	4.8	Max	-0.727	0.059	-0.013	0.024	-0.259	1.503	0.0179	-0.0628	305-2
125%	305	9.6	Max	-0.727	0.059	-0.013	0.024	-0.198	1.221	0.0093	-0.0536	305-2
125%	305	9.6	Max	-0.727	0.059	-0.013	0.024	-0.198	1.221	0.0093	-0.0536	305-3
125%	305	14.4	Max	-0.727	0.059	-0.013	0.024	-0.137	0.939	0.000757	-0.0444	305-3
125%	305	14.4	Max	-0.727	0.059	-0.013	0.024	-0.137	0.939	0.000757	-0.0444	305-4
125%	305	19.2	Max	-0.727	0.059	-0.013	0.024	-0.075	0.656	-0.0078	-0.0352	305-4
125%	305	19.2	Max	-0.727	0.059	-0.013	0.024	-0.075	0.656	-0.0078	-0.0352	305-5
125%	305	24	Max	-0.727	0.059	-0.013	0.024	-0.014	0.374	-0.0164	-0.026	305-5
125%	305	0	Min	-0.727	0.059	-0.013	0.024	-0.32	1.786	0.0264	-0.072	305-1
125%	305	4.8	Min	-0.727	0.059	-0.013	0.024	-0.259	1.503	0.0179	-0.0628	305-1
125%	305	4.8	Min	-0.727	0.059	-0.013	0.024	-0.259	1.503	0.0179	-0.0628	305-2
125%	305	9.6	Min	-0.727	0.059	-0.013	0.024	-0.198	1.221	0.0093	-0.0536	305-2
125%	305	9.6	Min	-0.727	0.059	-0.013	0.024	-0.198	1.221	0.0093	-0.0536	305-3
125%	305	14.4	Min	-0.727	0.059	-0.013	0.024	-0.137	0.939	0.000757	-0.0444	305-3
125%	305	14.4	Min	-0.727	0.059	-0.013	0.024	-0.137	0.939	0.000757	-0.0444	305-4
125%	305	19.2	Min	-0.727	0.059	-0.013	0.024	-0.075	0.656	-0.0078	-0.0352	305-4
125%	305	19.2	Min	-0.727	0.059	-0.013	0.024	-0.075	0.656	-0.0078	-0.0352	305-5
125%	305	24	Min	-0.727	0.059	-0.013	0.024	-0.014	0.374	-0.0164	-0.026	305-5
150%	305	0	Max	-0.808	0.067	-0.016	0.031	-0.394	2.145	0.0346	-0.0856	305-1
150%	305	4.8	Max	-0.808	0.067	-0.016	0.031	-0.318	1.825	0.0242	-0.0745	305-1
150%	305	4.8	Max	-0.808	0.067	-0.016	0.031	-0.318	1.825	0.0242	-0.0745	305-2
150%	305	9.6	Max	-0.808	0.067	-0.016	0.031	-0.242	1.505	0.0138	-0.0634	305-2
150%	305	9.6	Max	-0.808	0.067	-0.016	0.031	-0.242	1.505	0.0138	-0.0634	305-3
150%	305	14.4	Max	-0.808	0.067	-0.016	0.031	-0.166	1.185	0.0034	-0.0523	305-3
150%	305	14.4	Max	-0.808	0.067	-0.016	0.031	-0.166	1.185	0.0034	-0.0523	305-4
150%	305	19.2	Max	-0.808	0.067	-0.016	0.031	-0.09	0.866	-0.0069	-0.0412	305-4

150%	305	19.2	Max	-0.808	0.067	-0.016	0.031	-0.09	0.866	-0.0069	-0.0412	305-5
150%	305	24	Max	-0.808	0.067	-0.016	0.031	-0.014	0.546	-0.0173	-0.0301	305-5
150%	305	0	Min	-0.808	0.067	-0.016	0.031	-0.394	2.145	0.0346	-0.0856	305-1
150%	305	4.8	Min	-0.808	0.067	-0.016	0.031	-0.318	1.825	0.0242	-0.0745	305-1
150%	305	4.8	Min	-0.808	0.067	-0.016	0.031	-0.318	1.825	0.0242	-0.0745	305-2
150%	305	9.6	Min	-0.808	0.067	-0.016	0.031	-0.242	1.505	0.0138	-0.0634	305-2
150%	305	9.6	Min	-0.808	0.067	-0.016	0.031	-0.242	1.505	0.0138	-0.0634	305-3
150%	305	14.4	Min	-0.808	0.067	-0.016	0.031	-0.166	1.185	0.0034	-0.0523	305-3
150%	305	14.4	Min	-0.808	0.067	-0.016	0.031	-0.166	1.185	0.0034	-0.0523	305-4
150%	305	19.2	Min	-0.808	0.067	-0.016	0.031	-0.09	0.866	-0.0069	-0.0412	305-4
150%	305	19.2	Min	-0.808	0.067	-0.016	0.031	-0.09	0.866	-0.0069	-0.0412	305-5
150%	305	24	Min	-0.808	0.067	-0.016	0.031	-0.014	0.546	-0.0173	-0.0301	305-5
175%	305	0	Max	-0.7	0.103	-0.021	0.051	-0.507	3.232	0.0579	-0.1052	305-1
175%	305	4.8	Max	-0.7	0.103	-0.021	0.051	-0.408	2.74	0.0438	-0.0899	305-1
175%	305	4.8	Max	-0.7	0.103	-0.021	0.051	-0.408	2.74	0.0438	-0.0899	305-2
175%	305	9.6	Max	-0.7	0.103	-0.021	0.051	-0.308	2.247	0.0296	-0.0747	305-2
175%	305	9.6	Max	-0.7	0.103	-0.021	0.051	-0.308	2.247	0.0296	-0.0747	305-3
175%	305	14.4	Max	-0.7	0.103	-0.021	0.051	-0.209	1.755	0.0155	-0.0594	305-3
175%	305	14.4	Max	-0.7	0.103	-0.021	0.051	-0.209	1.755	0.0155	-0.0594	305-4
175%	305	19.2	Max	-0.7	0.103	-0.021	0.051	-0.11	1.263	0.0013	-0.0442	305-4
175%	305	19.2	Max	-0.7	0.103	-0.021	0.051	-0.11	1.263	0.0013	-0.0442	305-5
175%	305	24	Max	-0.7	0.103	-0.021	0.051	-0.01	0.77	-0.0128	-0.0289	305-5
175%	305	0	Min	-0.7	0.103	-0.021	0.051	-0.507	3.232	0.0579	-0.1052	305-1
175%	305	4.8	Min	-0.7	0.103	-0.021	0.051	-0.408	2.74	0.0438	-0.0899	305-1
175%	305	4.8	Min	-0.7	0.103	-0.021	0.051	-0.408	2.74	0.0438	-0.0899	305-2
175%	305	9.6	Min	-0.7	0.103	-0.021	0.051	-0.308	2.247	0.0296	-0.0747	305-2
175%	305	9.6	Min	-0.7	0.103	-0.021	0.051	-0.308	2.247	0.0296	-0.0747	305-3
175%	305	14.4	Min	-0.7	0.103	-0.021	0.051	-0.209	1.755	0.0155	-0.0594	305-3
175%	305	14.4	Min	-0.7	0.103	-0.021	0.051	-0.209	1.755	0.0155	-0.0594	305-4
175%	305	19.2	Min	-0.7	0.103	-0.021	0.051	-0.11	1.263	0.0013	-0.0442	305-4
175%	305	19.2	Min	-0.7	0.103	-0.021	0.051	-0.11	1.263	0.0013	-0.0442	305-5
175%	305	24	Min	-0.7	0.103	-0.021	0.051	-0.01	0.77	-0.0128	-0.0289	305-5
200%	305	0	Max	-0.653	0.128	-0.024	0.064	-0.595	4	0.0745	-0.1207	305-1

200%	305	4.8	Max	-0.653	0.128	-0.024	0.064	-0.478	3.386	0.0575	-0.1024	305-1
200%	305	4.8	Max	-0.653	0.128	-0.024	0.064	-0.478	3.386	0.0575	-0.1024	305-2
200%	305	9.6	Max	-0.653	0.128	-0.024	0.064	-0.361	2.773	0.0405	-0.084	305-2
200%	305	9.6	Max	-0.653	0.128	-0.024	0.064	-0.361	2.773	0.0405	-0.084	305-3
200%	305	14.4	Max	-0.653	0.128	-0.024	0.064	-0.243	2.159	0.0235	-0.0657	305-3
200%	305	14.4	Max	-0.653	0.128	-0.024	0.064	-0.243	2.159	0.0235	-0.0657	305-4
200%	305	19.2	Max	-0.653	0.128	-0.024	0.064	-0.126	1.545	0.0066	-0.0473	305-4
200%	305	19.2	Max	-0.653	0.128	-0.024	0.064	-0.126	1.545	0.0066	-0.0473	305-5
200%	305	24	Max	-0.653	0.128	-0.024	0.064	-0.00824	0.931	-0.0104	-0.029	305-5
200%	305	0	Min	-0.653	0.128	-0.024	0.064	-0.595	4	0.0745	-0.1207	305-1
200%	305	4.8	Min	-0.653	0.128	-0.024	0.064	-0.478	3.386	0.0575	-0.1024	305-1
200%	305	4.8	Min	-0.653	0.128	-0.024	0.064	-0.478	3.386	0.0575	-0.1024	305-2
200%	305	9.6	Min	-0.653	0.128	-0.024	0.064	-0.361	2.773	0.0405	-0.084	305-2
200%	305	9.6	Min	-0.653	0.128	-0.024	0.064	-0.361	2.773	0.0405	-0.084	305-3
200%	305	14.4	Min	-0.653	0.128	-0.024	0.064	-0.243	2.159	0.0235	-0.0657	305-3
200%	305	14.4	Min	-0.653	0.128	-0.024	0.064	-0.243	2.159	0.0235	-0.0657	305-4
200%	305	19.2	Min	-0.653	0.128	-0.024	0.064	-0.126	1.545	0.0066	-0.0473	305-4
200%	305	19.2	Min	-0.653	0.128	-0.024	0.064	-0.126	1.545	0.0066	-0.0473	305-5
200%	305	24	Min	-0.653	0.128	-0.024	0.064	-0.00824	0.931	-0.0104	-0.029	305-5
225%	305	0	Max	-0.441	0.17	-0.03	0.087	-0.713	5.277	0.1028	-0.1398	305-1
225%	305	4.8	Max	-0.441	0.17	-0.03	0.087	-0.571	4.46	0.0817	-0.1168	305-1
225%	305	4.8	Max	-0.441	0.17	-0.03	0.087	-0.571	4.46	0.0817	-0.1168	305-2
225%	305	9.6	Max	-0.441	0.17	-0.03	0.087	-0.429	3.643	0.0606	-0.0939	305-2
225%	305	9.6	Max	-0.441	0.17	-0.03	0.087	-0.429	3.643	0.0606	-0.0939	305-3
225%	305	14.4	Max	-0.441	0.17	-0.03	0.087	-0.287	2.825	0.0394	-0.0709	305-3
225%	305	14.4	Max	-0.441	0.17	-0.03	0.087	-0.287	2.825	0.0394	-0.0709	305-4
225%	305	19.2	Max	-0.441	0.17	-0.03	0.087	-0.145	2.008	0.0183	-0.048	305-4
225%	305	19.2	Max	-0.441	0.17	-0.03	0.087	-0.145	2.008	0.0183	-0.048	305-5
225%	305	24	Max	-0.441	0.17	-0.03	0.087	-0.00293	1.191	-0.0028	-0.025	305-5
225%	305	0	Min	-0.441	0.17	-0.03	0.087	-0.713	5.277	0.1028	-0.1398	305-1
225%	305	4.8	Min	-0.441	0.17	-0.03	0.087	-0.571	4.46	0.0817	-0.1168	305-1
225%	305	4.8	Min	-0.441	0.17	-0.03	0.087	-0.571	4.46	0.0817	-0.1168	305-2
225%	305	9.6	Min	-0.441	0.17	-0.03	0.087	-0.429	3.643	0.0606	-0.0939	305-2

225%	305	9.6	Min	-0.441	0.17	-0.03	0.087	-0.429	3.643	0.0606	-0.0939	305-3
225%	305	14.4	Min	-0.441	0.17	-0.03	0.087	-0.287	2.825	0.0394	-0.0709	305-3
225%	305	14.4	Min	-0.441	0.17	-0.03	0.087	-0.287	2.825	0.0394	-0.0709	305-4
225%	305	19.2	Min	-0.441	0.17	-0.03	0.087	-0.145	2.008	0.0183	-0.048	305-4
225%	305	19.2	Min	-0.441	0.17	-0.03	0.087	-0.145	2.008	0.0183	-0.048	305-5
225%	305	24	Min	-0.441	0.17	-0.03	0.087	-0.00293	1.191	-0.0028	-0.025	305-5
250%	305	0	Max	-0.292	0.203	-0.034	0.105	-0.806	6.279	0.1246	-0.1553	305-1
250%	305	4.8	Max	-0.292	0.203	-0.034	0.105	-0.645	5.303	0.1002	-0.1287	305-1
250%	305	4.8	Max	-0.292	0.203	-0.034	0.105	-0.645	5.303	0.1002	-0.1287	305-2
250%	305	9.6	Max	-0.292	0.203	-0.034	0.105	-0.483	4.326	0.0758	-0.1022	305-2
250%	305	9.6	Max	-0.292	0.203	-0.034	0.105	-0.483	4.326	0.0758	-0.1022	305-3
250%	305	14.4	Max	-0.292	0.203	-0.034	0.105	-0.322	3.349	0.0514	-0.0756	305-3
250%	305	14.4	Max	-0.292	0.203	-0.034	0.105	-0.322	3.349	0.0514	-0.0756	305-4
250%	305	19.2	Max	-0.292	0.203	-0.034	0.105	-0.16	2.373	0.027	-0.049	305-4
250%	305	19.2	Max	-0.292	0.203	-0.034	0.105	-0.16	2.373	0.027	-0.049	305-5
250%	305	24	Max	-0.292	0.203	-0.034	0.105	0.001049	1.396	0.0028	-0.0227	305-5
250%	305	0	Min	-0.292	0.203	-0.034	0.105	-0.806	6.279	0.1246	-0.1553	305-1
250%	305	4.8	Min	-0.292	0.203	-0.034	0.105	-0.645	5.303	0.1002	-0.1287	305-1
250%	305	4.8	Min	-0.292	0.203	-0.034	0.105	-0.645	5.303	0.1002	-0.1287	305-2
250%	305	9.6	Min	-0.292	0.203	-0.034	0.105	-0.483	4.326	0.0758	-0.1022	305-2
250%	305	9.6	Min	-0.292	0.203	-0.034	0.105	-0.483	4.326	0.0758	-0.1022	305-3
250%	305	14.4	Min	-0.292	0.203	-0.034	0.105	-0.322	3.349	0.0514	-0.0756	305-3
250%	305	14.4	Min	-0.292	0.203	-0.034	0.105	-0.322	3.349	0.0514	-0.0756	305-4
250%	305	19.2	Min	-0.292	0.203	-0.034	0.105	-0.16	2.373	0.027	-0.049	305-4
250%	305	19.2	Min	-0.292	0.203	-0.034	0.105	-0.16	2.373	0.027	-0.049	305-5
250%	305	24	Min	-0.292	0.203	-0.034	0.105	0.001049	1.396	0.0028	-0.0227	305-5
275%	305	0	Max	-0.00961	0.251	-0.039	0.132	-0.921	7.704	0.1558	-0.1736	305-1
275%	305	4.8	Max	-0.00961	0.251	-0.039	0.132	-0.736	6.499	0.1272	-0.1423	305-1
275%	305	4.8	Max	-0.00961	0.251	-0.039	0.132	-0.736	6.499	0.1272	-0.1423	305-2
275%	305	9.6	Max	-0.00961	0.251	-0.039	0.132	-0.551	5.294	0.0985	-0.1109	305-2
275%	305	9.6	Max	-0.00961	0.251	-0.039	0.132	-0.551	5.294	0.0985	-0.1109	305-3
275%	305	14.4	Max	-0.00961	0.251	-0.039	0.132	-0.365	4.089	0.0698	-0.0795	305-3
275%	305	14.4	Max	-0.00961	0.251	-0.039	0.132	-0.365	4.089	0.0698	-0.0795	305-4

275%	305	19.2	Max	-0.00961	0.251	-0.039	0.132	-0.18	2.884	0.0412	-0.0482	305-4
275%	305	19.2	Max	-0.00961	0.251	-0.039	0.132	-0.18	2.884	0.0412	-0.0482	305-5
275%	305	24	Max	-0.00961	0.251	-0.039	0.132	0.005186	1.678	0.0136	-0.0179	305-5
275%	305	0	Min	-0.00961	0.251	-0.039	0.132	-0.921	7.704	0.1558	-0.1736	305-1
275%	305	4.8	Min	-0.00961	0.251	-0.039	0.132	-0.736	6.499	0.1272	-0.1423	305-1
275%	305	4.8	Min	-0.00961	0.251	-0.039	0.132	-0.736	6.499	0.1272	-0.1423	305-2
275%	305	9.6	Min	-0.00961	0.251	-0.039	0.132	-0.551	5.294	0.0985	-0.1109	305-2
275%	305	9.6	Min	-0.00961	0.251	-0.039	0.132	-0.551	5.294	0.0985	-0.1109	305-3
275%	305	14.4	Min	-0.00961	0.251	-0.039	0.132	-0.365	4.089	0.0698	-0.0795	305-3
275%	305	14.4	Min	-0.00961	0.251	-0.039	0.132	-0.365	4.089	0.0698	-0.0795	305-4
275%	305	19.2	Min	-0.00961	0.251	-0.039	0.132	-0.18	2.884	0.0412	-0.0482	305-4
275%	305	19.2	Min	-0.00961	0.251	-0.039	0.132	-0.18	2.884	0.0412	-0.0482	305-5
275%	305	24	Min	-0.00961	0.251	-0.039	0.132	0.005186	1.678	0.0136	-0.0179	305-5
300%	305	0	Max	0.298	0.302	-0.044	0.159	-1.048	9.22	0.1897	-0.1934	305-1
300%	305	4.8	Max	0.298	0.302	-0.044	0.159	-0.837	7.772	0.1564	-0.1568	305-1
300%	305	4.8	Max	0.298	0.302	-0.044	0.159	-0.837	7.772	0.1564	-0.1568	305-2
300%	305	9.6	Max	0.298	0.302	-0.044	0.159	-0.625	6.323	0.1231	-0.1203	305-2
300%	305	9.6	Max	0.298	0.302	-0.044	0.159	-0.625	6.323	0.1231	-0.1203	305-3
300%	305	14.4	Max	0.298	0.302	-0.044	0.159	-0.414	4.875	0.0898	-0.0837	305-3
300%	305	14.4	Max	0.298	0.302	-0.044	0.159	-0.414	4.875	0.0898	-0.0837	305-4
300%	305	19.2	Max	0.298	0.302	-0.044	0.159	-0.202	3.427	0.0565	-0.0472	305-4
300%	305	19.2	Max	0.298	0.302	-0.044	0.159	-0.202	3.427	0.0565	-0.0472	305-5
300%	305	24	Max	0.298	0.302	-0.044	0.159	0.009276	1.979	0.0252	-0.0126	305-5
300%	305	0	Min	0.298	0.302	-0.044	0.159	-1.048	9.22	0.1897	-0.1934	305-1
300%	305	4.8	Min	0.298	0.302	-0.044	0.159	-0.837	7.772	0.1564	-0.1568	305-1
300%	305	4.8	Min	0.298	0.302	-0.044	0.159	-0.837	7.772	0.1564	-0.1568	305-2
300%	305	9.6	Min	0.298	0.302	-0.044	0.159	-0.625	6.323	0.1231	-0.1203	305-2
300%	305	9.6	Min	0.298	0.302	-0.044	0.159	-0.625	6.323	0.1231	-0.1203	305-3
300%	305	14.4	Min	0.298	0.302	-0.044	0.159	-0.414	4.875	0.0898	-0.0837	305-3
300%	305	14.4	Min	0.298	0.302	-0.044	0.159	-0.414	4.875	0.0898	-0.0837	305-4
300%	305	19.2	Min	0.298	0.302	-0.044	0.159	-0.202	3.427	0.0565	-0.0472	305-4
300%	305	19.2	Min	0.298	0.302	-0.044	0.159	-0.202	3.427	0.0565	-0.0472	305-5
300%	305	24	Min	0.298	0.302	-0.044	0.159	0.009276	1.979	0.0252	-0.0126	305-5

TABLE: Element Forces - Frames Member 4 Interior Chord												
Model	Frame	Station	StepType	P	V2	V3	T	M2	M3	S11Max	S11Min	FrameElem
Text	Text	in	Text	Kip	Kip	Kip	Kip-in	Kip-in	Kip-in	Kip/in2	Kip/in2	Text
15%	4	0	Max	-0.107	0.058	0.001412	0.02	0.001634	3.567	0.000455	-0.00059	4-1
15%	4	4.8	Max	-0.107	0.058	0.001412	0.02	-0.00515	3.287	0.00042	-0.00055	4-1
15%	4	4.8	Max	-0.107	0.058	0.001412	0.02	-0.00515	3.287	0.00042	-0.00055	4-2
15%	4	9.6	Max	-0.107	0.058	0.001412	0.02	-0.012	3.006	0.00039	-0.00052	4-2
15%	4	9.6	Max	-0.107	0.058	0.001412	0.02	-0.012	3.006	0.00039	-0.00052	4-3
15%	4	14.4	Max	-0.107	0.058	0.001412	0.02	-0.019	2.725	0.00036	-0.00049	4-3
15%	4	14.4	Max	-0.107	0.058	0.001412	0.02	-0.019	2.725	0.00036	-0.00049	4-4
15%	4	19.2	Max	-0.107	0.058	0.001412	0.02	-0.025	2.444	0.00033	-0.00046	4-4
15%	4	19.2	Max	-0.107	0.058	0.001412	0.02	-0.025	2.444	0.00033	-0.00046	4-5
15%	4	24	Max	-0.107	0.058	0.001412	0.02	-0.032	2.163	0.0003	-0.00043	4-5
15%	4	0	Min	-0.107	0.058	0.001412	0.02	0.001634	3.567	0.000455	-0.00059	4-1
15%	4	4.8	Min	-0.107	0.058	0.001412	0.02	-0.00515	3.287	0.00042	-0.00055	4-1
15%	4	4.8	Min	-0.107	0.058	0.001412	0.02	-0.00515	3.287	0.00042	-0.00055	4-2
15%	4	9.6	Min	-0.107	0.058	0.001412	0.02	-0.012	3.006	0.00039	-0.00052	4-2
15%	4	9.6	Min	-0.107	0.058	0.001412	0.02	-0.012	3.006	0.00039	-0.00052	4-3
15%	4	14.4	Min	-0.107	0.058	0.001412	0.02	-0.019	2.725	0.00036	-0.00049	4-3
15%	4	14.4	Min	-0.107	0.058	0.001412	0.02	-0.019	2.725	0.00036	-0.00049	4-4
15%	4	19.2	Min	-0.107	0.058	0.001412	0.02	-0.025	2.444	0.00033	-0.00046	4-4
15%	4	19.2	Min	-0.107	0.058	0.001412	0.02	-0.025	2.444	0.00033	-0.00046	4-5
15%	4	24	Min	-0.107	0.058	0.001412	0.02	-0.032	2.163	0.0003	-0.00043	4-5
25%	4	0	Max	-0.121	0.04	-0.00085	0.014	-0.036	2.268	0.000313	-0.00046	4-1
25%	4	4.8	Max	-0.121	0.04	-0.00085	0.014	-0.032	2.074	0.000278	-0.00043	4-1
25%	4	4.8	Max	-0.121	0.04	-0.00085	0.014	-0.032	2.074	0.000278	-0.00043	4-2
25%	4	9.6	Max	-0.121	0.04	-0.00085	0.014	-0.028	1.881	0.000244	-0.00039	4-2
25%	4	9.6	Max	-0.121	0.04	-0.00085	0.014	-0.028	1.881	0.000244	-0.00039	4-3
25%	4	14.4	Max	-0.121	0.04	-0.00085	0.014	-0.024	1.687	0.000209	-0.00036	4-3
25%	4	14.4	Max	-0.121	0.04	-0.00085	0.014	-0.024	1.687	0.000209	-0.00036	4-4
25%	4	19.2	Max	-0.121	0.04	-0.00085	0.014	-0.02	1.493	0.000174	-0.00033	4-4

25%	4	19.2	Max	-0.121	0.04	-0.00085	0.014	-0.02	1.493	0.000174	-0.00033	4-5
25%	4	24	Max	-0.121	0.04	-0.00085	0.014	-0.016	1.299	0.000139	-0.00029	4-5
25%	4	0	Min	-0.121	0.04	-0.00085	0.014	-0.036	2.268	0.000313	-0.00046	4-1
25%	4	4.8	Min	-0.121	0.04	-0.00085	0.014	-0.032	2.074	0.000278	-0.00043	4-1
25%	4	4.8	Min	-0.121	0.04	-0.00085	0.014	-0.032	2.074	0.000278	-0.00043	4-2
25%	4	9.6	Min	-0.121	0.04	-0.00085	0.014	-0.028	1.881	0.000244	-0.00039	4-2
25%	4	9.6	Min	-0.121	0.04	-0.00085	0.014	-0.028	1.881	0.000244	-0.00039	4-3
25%	4	14.4	Min	-0.121	0.04	-0.00085	0.014	-0.024	1.687	0.000209	-0.00036	4-3
25%	4	14.4	Min	-0.121	0.04	-0.00085	0.014	-0.024	1.687	0.000209	-0.00036	4-4
25%	4	19.2	Min	-0.121	0.04	-0.00085	0.014	-0.02	1.493	0.000174	-0.00033	4-4
25%	4	19.2	Min	-0.121	0.04	-0.00085	0.014	-0.02	1.493	0.000174	-0.00033	4-5
25%	4	24	Min	-0.121	0.04	-0.00085	0.014	-0.016	1.299	0.000139	-0.00029	4-5
50%	4	0	Max	-0.243	0.027	-0.00826	0.00885	-0.235	1.452	0.000436	-0.00074	4-1
50%	4	4.8	Max	-0.243	0.027	-0.00826	0.00885	-0.195	1.322	0.000354	-0.00066	4-1
50%	4	4.8	Max	-0.243	0.027	-0.00826	0.00885	-0.195	1.322	0.000354	-0.00066	4-2
50%	4	9.6	Max	-0.243	0.027	-0.00826	0.00885	-0.155	1.192	0.000271	-0.00057	4-2
50%	4	9.6	Max	-0.243	0.027	-0.00826	0.00885	-0.155	1.192	0.000271	-0.00057	4-3
50%	4	14.4	Max	-0.243	0.027	-0.00826	0.00885	-0.116	1.063	0.000189	-0.00049	4-3
50%	4	14.4	Max	-0.243	0.027	-0.00826	0.00885	-0.116	1.063	0.000189	-0.00049	4-4
50%	4	19.2	Max	-0.243	0.027	-0.00826	0.00885	-0.076	0.933	0.000106	-0.00041	4-4
50%	4	19.2	Max	-0.243	0.027	-0.00826	0.00885	-0.076	0.933	0.000106	-0.00041	4-5
50%	4	24	Max	-0.243	0.027	-0.00826	0.00885	-0.037	0.803	2.36E-05	-0.00033	4-5
50%	4	0	Min	-0.243	0.027	-0.00826	0.00885	-0.235	1.452	0.000436	-0.00074	4-1
50%	4	4.8	Min	-0.243	0.027	-0.00826	0.00885	-0.195	1.322	0.000354	-0.00066	4-1
50%	4	4.8	Min	-0.243	0.027	-0.00826	0.00885	-0.195	1.322	0.000354	-0.00066	4-2
50%	4	9.6	Min	-0.243	0.027	-0.00826	0.00885	-0.155	1.192	0.000271	-0.00057	4-2
50%	4	9.6	Min	-0.243	0.027	-0.00826	0.00885	-0.155	1.192	0.000271	-0.00057	4-3
50%	4	14.4	Min	-0.243	0.027	-0.00826	0.00885	-0.116	1.063	0.000189	-0.00049	4-3
50%	4	14.4	Min	-0.243	0.027	-0.00826	0.00885	-0.116	1.063	0.000189	-0.00049	4-4
50%	4	19.2	Min	-0.243	0.027	-0.00826	0.00885	-0.076	0.933	0.000106	-0.00041	4-4
50%	4	19.2	Min	-0.243	0.027	-0.00826	0.00885	-0.076	0.933	0.000106	-0.00041	4-5
50%	4	24	Min	-0.243	0.027	-0.00826	0.00885	-0.037	0.803	2.36E-05	-0.00033	4-5

75%	4	0	Max	-0.247	0.024	-0.018	0.00735	-0.466	1.209	0.000771	-0.0011	4-1
75%	4	4.8	Max	-0.247	0.024	-0.018	0.00735	-0.378	1.094	0.000612	-0.00092	4-1
75%	4	4.8	Max	-0.247	0.024	-0.018	0.00735	-0.378	1.094	0.000612	-0.00092	4-2
75%	4	9.6	Max	-0.247	0.024	-0.018	0.00735	-0.29	0.979	0.000454	-0.00076	4-2
75%	4	9.6	Max	-0.247	0.024	-0.018	0.00735	-0.29	0.979	0.000454	-0.00076	4-3
75%	4	14.4	Max	-0.247	0.024	-0.018	0.00735	-0.202	0.864	0.000295	-0.0006	4-3
75%	4	14.4	Max	-0.247	0.024	-0.018	0.00735	-0.202	0.864	0.000295	-0.0006	4-4
75%	4	19.2	Max	-0.247	0.024	-0.018	0.00735	-0.113	0.749	0.000137	-0.00045	4-4
75%	4	19.2	Max	-0.247	0.024	-0.018	0.00735	-0.113	0.749	0.000137	-0.00045	4-5
75%	4	24	Max	-0.247	0.024	-0.018	0.00735	-0.025	0.634	-2.1E-05	-0.00029	4-5
75%	4	0	Min	-0.247	0.024	-0.018	0.00735	-0.466	1.209	0.000771	-0.0011	4-1
75%	4	4.8	Min	-0.247	0.024	-0.018	0.00735	-0.378	1.094	0.000612	-0.00092	4-1
75%	4	4.8	Min	-0.247	0.024	-0.018	0.00735	-0.378	1.094	0.000612	-0.00092	4-2
75%	4	9.6	Min	-0.247	0.024	-0.018	0.00735	-0.29	0.979	0.000454	-0.00076	4-2
75%	4	9.6	Min	-0.247	0.024	-0.018	0.00735	-0.29	0.979	0.000454	-0.00076	4-3
75%	4	14.4	Min	-0.247	0.024	-0.018	0.00735	-0.202	0.864	0.000295	-0.0006	4-3
75%	4	14.4	Min	-0.247	0.024	-0.018	0.00735	-0.202	0.864	0.000295	-0.0006	4-4
75%	4	19.2	Min	-0.247	0.024	-0.018	0.00735	-0.113	0.749	0.000137	-0.00045	4-4
75%	4	19.2	Min	-0.247	0.024	-0.018	0.00735	-0.113	0.749	0.000137	-0.00045	4-5
75%	4	24	Min	-0.247	0.024	-0.018	0.00735	-0.025	0.634	-2.1E-05	-0.00029	4-5
100%	4	0	Max	-0.325	0.026	-0.026	0.007826	-0.66	1.308	0.001	-0.0015	4-1
100%	4	4.8	Max	-0.325	0.026	-0.026	0.007826	-0.533	1.182	0.000825	-0.0012	4-1
100%	4	4.8	Max	-0.325	0.026	-0.026	0.007826	-0.533	1.182	0.000825	-0.0012	4-2
100%	4	9.6	Max	-0.325	0.026	-0.026	0.007826	-0.407	1.057	0.000603	-0.001	4-2
100%	4	9.6	Max	-0.325	0.026	-0.026	0.007826	-0.407	1.057	0.000603	-0.001	4-3
100%	4	14.4	Max	-0.325	0.026	-0.026	0.007826	-0.28	0.931	0.000382	-0.00079	4-3
100%	4	14.4	Max	-0.325	0.026	-0.026	0.007826	-0.28	0.931	0.000382	-0.00079	4-4
100%	4	19.2	Max	-0.325	0.026	-0.026	0.007826	-0.153	0.806	0.00016	-0.00057	4-4
100%	4	19.2	Max	-0.325	0.026	-0.026	0.007826	-0.153	0.806	0.00016	-0.00057	4-5
100%	4	24	Max	-0.325	0.026	-0.026	0.007826	-0.026	0.68	-6.2E-05	-0.00034	4-5
100%	4	0	Min	-0.325	0.026	-0.026	0.007826	-0.66	1.308	0.001	-0.0015	4-1
100%	4	4.8	Min	-0.325	0.026	-0.026	0.007826	-0.533	1.182	0.000825	-0.0012	4-1

100%	4	4.8	Min	-0.325	0.026	-0.026	0.007826	-0.533	1.182	0.000825	-0.0012	4-2
100%	4	9.6	Min	-0.325	0.026	-0.026	0.007826	-0.407	1.057	0.000603	-0.001	4-2
100%	4	9.6	Min	-0.325	0.026	-0.026	0.007826	-0.407	1.057	0.000603	-0.001	4-3
100%	4	14.4	Min	-0.325	0.026	-0.026	0.007826	-0.28	0.931	0.000382	-0.00079	4-3
100%	4	14.4	Min	-0.325	0.026	-0.026	0.007826	-0.28	0.931	0.000382	-0.00079	4-4
100%	4	19.2	Min	-0.325	0.026	-0.026	0.007826	-0.153	0.806	0.00016	-0.00057	4-4
100%	4	19.2	Min	-0.325	0.026	-0.026	0.007826	-0.153	0.806	0.00016	-0.00057	4-5
100%	4	24	Min	-0.325	0.026	-0.026	0.007826	-0.026	0.68	-6.2E-05	-0.00034	4-5
125%	4	0	Max	-0.218	0.033	-0.038	0.009812	-0.914	1.64	0.0016	-0.0018	4-1
125%	4	4.8	Max	-0.218	0.033	-0.038	0.009812	-0.731	1.483	0.0013	-0.0015	4-1
125%	4	4.8	Max	-0.218	0.033	-0.038	0.009812	-0.731	1.483	0.0013	-0.0015	4-2
125%	4	9.6	Max	-0.218	0.033	-0.038	0.009812	-0.549	1.327	0.000938	-0.0012	4-2
125%	4	9.6	Max	-0.218	0.033	-0.038	0.009812	-0.549	1.327	0.000938	-0.0012	4-3
125%	4	14.4	Max	-0.218	0.033	-0.038	0.009812	-0.367	1.17	0.000623	-0.0009	4-3
125%	4	14.4	Max	-0.218	0.033	-0.038	0.009812	-0.367	1.17	0.000623	-0.0009	4-4
125%	4	19.2	Max	-0.218	0.033	-0.038	0.009812	-0.184	1.014	0.000307	-0.00058	4-4
125%	4	19.2	Max	-0.218	0.033	-0.038	0.009812	-0.184	1.014	0.000307	-0.00058	4-5
125%	4	24	Max	-0.218	0.033	-0.038	0.009812	-0.00218	0.858	-8.1E-06	-0.00026	4-5
125%	4	0	Min	-0.218	0.033	-0.038	0.009812	-0.914	1.64	0.0016	-0.0018	4-1
125%	4	4.8	Min	-0.218	0.033	-0.038	0.009812	-0.731	1.483	0.0013	-0.0015	4-1
125%	4	4.8	Min	-0.218	0.033	-0.038	0.009812	-0.731	1.483	0.0013	-0.0015	4-2
125%	4	9.6	Min	-0.218	0.033	-0.038	0.009812	-0.549	1.327	0.000938	-0.0012	4-2
125%	4	9.6	Min	-0.218	0.033	-0.038	0.009812	-0.549	1.327	0.000938	-0.0012	4-3
125%	4	14.4	Min	-0.218	0.033	-0.038	0.009812	-0.367	1.17	0.000623	-0.0009	4-3
125%	4	14.4	Min	-0.218	0.033	-0.038	0.009812	-0.367	1.17	0.000623	-0.0009	4-4
125%	4	19.2	Min	-0.218	0.033	-0.038	0.009812	-0.184	1.014	0.000307	-0.00058	4-4
125%	4	19.2	Min	-0.218	0.033	-0.038	0.009812	-0.184	1.014	0.000307	-0.00058	4-5
125%	4	24	Min	-0.218	0.033	-0.038	0.009812	-0.00218	0.858	-8.1E-06	-0.00026	4-5
150%	4	0	Max	-0.19	0.037	-0.047	0.011	-1.123	1.861	0.002	-0.0022	4-1
150%	4	4.8	Max	-0.19	0.037	-0.047	0.011	-0.896	1.684	0.0016	-0.0018	4-1
150%	4	4.8	Max	-0.19	0.037	-0.047	0.011	-0.896	1.684	0.0016	-0.0018	4-2
150%	4	9.6	Max	-0.19	0.037	-0.047	0.011	-0.67	1.508	0.0012	-0.0014	4-2

150%	4	9.6	Max	-0.19	0.037	-0.047	0.011	-0.67	1.508	0.0012	-0.0014	4-3
150%	4	14.4	Max	-0.19	0.037	-0.047	0.011	-0.444	1.331	0.000787	-0.001	4-3
150%	4	14.4	Max	-0.19	0.037	-0.047	0.011	-0.444	1.331	0.000787	-0.001	4-4
150%	4	19.2	Max	-0.19	0.037	-0.047	0.011	-0.217	1.154	0.000398	-0.00064	4-4
150%	4	19.2	Max	-0.19	0.037	-0.047	0.011	-0.217	1.154	0.000398	-0.00064	4-5
150%	4	24	Max	-0.19	0.037	-0.047	0.011	0.008825	0.978	3.78E-05	-0.00028	4-5
150%	4	0	Min	-0.19	0.037	-0.047	0.011	-1.123	1.861	0.002	-0.0022	4-1
150%	4	4.8	Min	-0.19	0.037	-0.047	0.011	-0.896	1.684	0.0016	-0.0018	4-1
150%	4	4.8	Min	-0.19	0.037	-0.047	0.011	-0.896	1.684	0.0016	-0.0018	4-2
150%	4	9.6	Min	-0.19	0.037	-0.047	0.011	-0.67	1.508	0.0012	-0.0014	4-2
150%	4	9.6	Min	-0.19	0.037	-0.047	0.011	-0.67	1.508	0.0012	-0.0014	4-3
150%	4	14.4	Min	-0.19	0.037	-0.047	0.011	-0.444	1.331	0.000787	-0.001	4-3
150%	4	14.4	Min	-0.19	0.037	-0.047	0.011	-0.444	1.331	0.000787	-0.001	4-4
150%	4	19.2	Min	-0.19	0.037	-0.047	0.011	-0.217	1.154	0.000398	-0.00064	4-4
150%	4	19.2	Min	-0.19	0.037	-0.047	0.011	-0.217	1.154	0.000398	-0.00064	4-5
150%	4	24	Min	-0.19	0.037	-0.047	0.011	0.008825	0.978	3.78E-05	-0.00028	4-5
175%	4	0	Max	0.035	0.043	-0.06	0.013	-1.392	2.251	0.0026	-0.0025	4-1
175%	4	4.8	Max	0.035	0.043	-0.06	0.013	-1.104	2.043	0.0021	-0.002	4-1
175%	4	4.8	Max	0.035	0.043	-0.06	0.013	-1.104	2.043	0.0021	-0.002	4-2
175%	4	9.6	Max	0.035	0.043	-0.06	0.013	-0.816	1.836	0.0016	-0.0016	4-2
175%	4	9.6	Max	0.035	0.043	-0.06	0.013	-0.816	1.836	0.0016	-0.0016	4-3
175%	4	14.4	Max	0.035	0.043	-0.06	0.013	-0.528	1.628	0.0011	-0.0011	4-3
175%	4	14.4	Max	0.035	0.043	-0.06	0.013	-0.528	1.628	0.0011	-0.0011	4-4
175%	4	19.2	Max	0.035	0.043	-0.06	0.013	-0.24	1.421	0.000615	-0.00057	4-4
175%	4	19.2	Max	0.035	0.043	-0.06	0.013	-0.24	1.421	0.000615	-0.00057	4-5
175%	4	24	Max	0.035	0.043	-0.06	0.013	0.048	1.213	0.000275	-0.00023	4-5
175%	4	0	Min	0.035	0.043	-0.06	0.013	-1.392	2.251	0.0026	-0.0025	4-1
175%	4	4.8	Min	0.035	0.043	-0.06	0.013	-1.104	2.043	0.0021	-0.002	4-1
175%	4	4.8	Min	0.035	0.043	-0.06	0.013	-1.104	2.043	0.0021	-0.002	4-2
175%	4	9.6	Min	0.035	0.043	-0.06	0.013	-0.816	1.836	0.0016	-0.0016	4-2
175%	4	9.6	Min	0.035	0.043	-0.06	0.013	-0.816	1.836	0.0016	-0.0016	4-3
175%	4	14.4	Min	0.035	0.043	-0.06	0.013	-0.528	1.628	0.0011	-0.0011	4-3

175%	4	14.4	Min	0.035	0.043	-0.06	0.013	-0.528	1.628	0.0011	-0.0011	4-4
175%	4	19.2	Min	0.035	0.043	-0.06	0.013	-0.24	1.421	0.000615	-0.00057	4-4
175%	4	19.2	Min	0.035	0.043	-0.06	0.013	-0.24	1.421	0.000615	-0.00057	4-5
175%	4	24	Min	0.035	0.043	-0.06	0.013	0.048	1.213	0.000275	-0.00023	4-5
200%	4	0	Max	0.184	0.048	-0.07	0.015	-1.61	2.543	0.0031	-0.0028	4-1
200%	4	4.8	Max	0.184	0.048	-0.07	0.015	-1.273	2.312	0.0025	-0.0023	4-1
200%	4	4.8	Max	0.184	0.048	-0.07	0.015	-1.273	2.312	0.0025	-0.0023	4-2
200%	4	9.6	Max	0.184	0.048	-0.07	0.015	-0.935	2.08	0.0019	-0.0017	4-2
200%	4	9.6	Max	0.184	0.048	-0.07	0.015	-0.935	2.08	0.0019	-0.0017	4-3
200%	4	14.4	Max	0.184	0.048	-0.07	0.015	-0.598	1.849	0.0013	-0.0011	4-3
200%	4	14.4	Max	0.184	0.048	-0.07	0.015	-0.598	1.849	0.0013	-0.0011	4-4
200%	4	19.2	Max	0.184	0.048	-0.07	0.015	-0.26	1.618	0.000768	-0.00054	4-4
200%	4	19.2	Max	0.184	0.048	-0.07	0.015	-0.26	1.618	0.000768	-0.00054	4-5
200%	4	24	Max	0.184	0.048	-0.07	0.015	0.077	1.386	0.000441	-0.00021	4-5
200%	4	0	Min	0.184	0.048	-0.07	0.015	-1.61	2.543	0.0031	-0.0028	4-1
200%	4	4.8	Min	0.184	0.048	-0.07	0.015	-1.273	2.312	0.0025	-0.0023	4-1
200%	4	4.8	Min	0.184	0.048	-0.07	0.015	-1.273	2.312	0.0025	-0.0023	4-2
200%	4	9.6	Min	0.184	0.048	-0.07	0.015	-0.935	2.08	0.0019	-0.0017	4-2
200%	4	9.6	Min	0.184	0.048	-0.07	0.015	-0.935	2.08	0.0019	-0.0017	4-3
200%	4	14.4	Min	0.184	0.048	-0.07	0.015	-0.598	1.849	0.0013	-0.0011	4-3
200%	4	14.4	Min	0.184	0.048	-0.07	0.015	-0.598	1.849	0.0013	-0.0011	4-4
200%	4	19.2	Min	0.184	0.048	-0.07	0.015	-0.26	1.618	0.000768	-0.00054	4-4
200%	4	19.2	Min	0.184	0.048	-0.07	0.015	-0.26	1.618	0.000768	-0.00054	4-5
200%	4	24	Min	0.184	0.048	-0.07	0.015	0.077	1.386	0.000441	-0.00021	4-5
225%	4	0	Max	0.497	0.055	-0.083	0.017	-1.872	2.957	0.0037	-0.0031	4-1
225%	4	4.8	Max	0.497	0.055	-0.083	0.017	-1.473	2.694	0.0031	-0.0024	4-1
225%	4	4.8	Max	0.497	0.055	-0.083	0.017	-1.473	2.694	0.0031	-0.0024	4-2
225%	4	9.6	Max	0.497	0.055	-0.083	0.017	-1.073	2.431	0.0024	-0.0018	4-2
225%	4	9.6	Max	0.497	0.055	-0.083	0.017	-1.073	2.431	0.0024	-0.0018	4-3
225%	4	14.4	Max	0.497	0.055	-0.083	0.017	-0.673	2.168	0.0017	-0.0011	4-3
225%	4	14.4	Max	0.497	0.055	-0.083	0.017	-0.673	2.168	0.0017	-0.0011	4-4
225%	4	19.2	Max	0.497	0.055	-0.083	0.017	-0.273	1.905	0.001	-0.00041	4-4

225%	4	19.2	Max	0.497	0.055	-0.083	0.017	-0.273	1.905	0.001	-0.00041	4-5
225%	4	24	Max	0.497	0.055	-0.083	0.017	0.126	1.642	0.000752	-0.00013	4-5
225%	4	0	Min	0.497	0.055	-0.083	0.017	-1.872	2.957	0.0037	-0.0031	4-1
225%	4	4.8	Min	0.497	0.055	-0.083	0.017	-1.473	2.694	0.0031	-0.0024	4-1
225%	4	4.8	Min	0.497	0.055	-0.083	0.017	-1.473	2.694	0.0031	-0.0024	4-2
225%	4	9.6	Min	0.497	0.055	-0.083	0.017	-1.073	2.431	0.0024	-0.0018	4-2
225%	4	9.6	Min	0.497	0.055	-0.083	0.017	-1.073	2.431	0.0024	-0.0018	4-3
225%	4	14.4	Min	0.497	0.055	-0.083	0.017	-0.673	2.168	0.0017	-0.0011	4-3
225%	4	14.4	Min	0.497	0.055	-0.083	0.017	-0.673	2.168	0.0017	-0.0011	4-4
225%	4	19.2	Min	0.497	0.055	-0.083	0.017	-0.273	1.905	0.001	-0.00041	4-4
225%	4	19.2	Min	0.497	0.055	-0.083	0.017	-0.273	1.905	0.001	-0.00041	4-5
225%	4	24	Min	0.497	0.055	-0.083	0.017	0.126	1.642	0.000752	-0.00013	4-5
250%	4	0	Max	0.725	0.06	-0.093	0.019	-2.083	3.283	0.0043	-0.0034	4-1
250%	4	4.8	Max	0.725	0.06	-0.093	0.019	-1.634	2.995	0.0035	-0.0026	4-1
250%	4	4.8	Max	0.725	0.06	-0.093	0.019	-1.634	2.995	0.0035	-0.0026	4-2
250%	4	9.6	Max	0.725	0.06	-0.093	0.019	-1.185	2.708	0.0027	-0.0018	4-2
250%	4	9.6	Max	0.725	0.06	-0.093	0.019	-1.185	2.708	0.0027	-0.0018	4-3
250%	4	14.4	Max	0.725	0.06	-0.093	0.019	-0.737	2.42	0.002	-0.0011	4-3
250%	4	14.4	Max	0.725	0.06	-0.093	0.019	-0.737	2.42	0.002	-0.0011	4-4
250%	4	19.2	Max	0.725	0.06	-0.093	0.019	-0.288	2.132	0.0012	-0.00032	4-4
250%	4	19.2	Max	0.725	0.06	-0.093	0.019	-0.288	2.132	0.0012	-0.00032	4-5
250%	4	24	Max	0.725	0.06	-0.093	0.019	0.161	1.845	0.000979	-7.3E-05	4-5
250%	4	0	Min	0.725	0.06	-0.093	0.019	-2.083	3.283	0.0043	-0.0034	4-1
250%	4	4.8	Min	0.725	0.06	-0.093	0.019	-1.634	2.995	0.0035	-0.0026	4-1
250%	4	4.8	Min	0.725	0.06	-0.093	0.019	-1.634	2.995	0.0035	-0.0026	4-2
250%	4	9.6	Min	0.725	0.06	-0.093	0.019	-1.185	2.708	0.0027	-0.0018	4-2
250%	4	9.6	Min	0.725	0.06	-0.093	0.019	-1.185	2.708	0.0027	-0.0018	4-3
250%	4	14.4	Min	0.725	0.06	-0.093	0.019	-0.737	2.42	0.002	-0.0011	4-3
250%	4	14.4	Min	0.725	0.06	-0.093	0.019	-0.737	2.42	0.002	-0.0011	4-4
250%	4	19.2	Min	0.725	0.06	-0.093	0.019	-0.288	2.132	0.0012	-0.00032	4-4
250%	4	19.2	Min	0.725	0.06	-0.093	0.019	-0.288	2.132	0.0012	-0.00032	4-5
250%	4	24	Min	0.725	0.06	-0.093	0.019	0.161	1.845	0.000979	-7.3E-05	4-5

275%	4	0	Max	1.092	0.067	-0.105	0.022	-2.315	3.761	0.0049	-0.0036	4-1
275%	4	4.8	Max	1.092	0.067	-0.105	0.022	-1.809	3.439	0.0041	-0.0027	4-1
275%	4	4.8	Max	1.092	0.067	-0.105	0.022	-1.809	3.439	0.0041	-0.0027	4-2
275%	4	9.6	Max	1.092	0.067	-0.105	0.022	-1.302	3.116	0.0032	-0.0019	4-2
275%	4	9.6	Max	1.092	0.067	-0.105	0.022	-1.302	3.116	0.0032	-0.0019	4-3
275%	4	14.4	Max	1.092	0.067	-0.105	0.022	-0.796	2.793	0.0024	-0.001	4-3
275%	4	14.4	Max	1.092	0.067	-0.105	0.022	-0.796	2.793	0.0024	-0.001	4-4
275%	4	19.2	Max	1.092	0.067	-0.105	0.022	-0.29	2.471	0.0015	-0.00014	4-4
275%	4	19.2	Max	1.092	0.067	-0.105	0.022	-0.29	2.471	0.0015	-0.00014	4-5
275%	4	24	Max	1.092	0.067	-0.105	0.022	0.216	2.148	0.0013	2.21E-05	4-5
275%	4	0	Min	1.092	0.067	-0.105	0.022	-2.315	3.761	0.0049	-0.0036	4-1
275%	4	4.8	Min	1.092	0.067	-0.105	0.022	-1.809	3.439	0.0041	-0.0027	4-1
275%	4	4.8	Min	1.092	0.067	-0.105	0.022	-1.809	3.439	0.0041	-0.0027	4-2
275%	4	9.6	Min	1.092	0.067	-0.105	0.022	-1.302	3.116	0.0032	-0.0019	4-2
275%	4	9.6	Min	1.092	0.067	-0.105	0.022	-1.302	3.116	0.0032	-0.0019	4-3
275%	4	14.4	Min	1.092	0.067	-0.105	0.022	-0.796	2.793	0.0024	-0.001	4-3
275%	4	14.4	Min	1.092	0.067	-0.105	0.022	-0.796	2.793	0.0024	-0.001	4-4
275%	4	19.2	Min	1.092	0.067	-0.105	0.022	-0.29	2.471	0.0015	-0.00014	4-4
275%	4	19.2	Min	1.092	0.067	-0.105	0.022	-0.29	2.471	0.0015	-0.00014	4-5
275%	4	24	Min	1.092	0.067	-0.105	0.022	0.216	2.148	0.0013	2.21E-05	4-5
300%	4	0	Max	1.489	0.075	-0.118	0.024	-2.56	4.291	0.0057	-0.0038	4-1
300%	4	4.8	Max	1.489	0.075	-0.118	0.024	-1.991	3.929	0.0047	-0.0028	4-1
300%	4	4.8	Max	1.489	0.075	-0.118	0.024	-1.991	3.929	0.0047	-0.0028	4-2
300%	4	9.6	Max	1.489	0.075	-0.118	0.024	-1.423	3.566	0.0037	-0.0019	4-2
300%	4	9.6	Max	1.489	0.075	-0.118	0.024	-1.423	3.566	0.0037	-0.0019	4-3
300%	4	14.4	Max	1.489	0.075	-0.118	0.024	-0.855	3.204	0.0028	-0.00091	4-3
300%	4	14.4	Max	1.489	0.075	-0.118	0.024	-0.855	3.204	0.0028	-0.00091	4-4
300%	4	19.2	Max	1.489	0.075	-0.118	0.024	-0.286	2.842	0.0018	5.68E-05	4-4
300%	4	19.2	Max	1.489	0.075	-0.118	0.024	-0.286	2.842	0.0018	5.68E-05	4-5
300%	4	24	Max	1.489	0.075	-0.118	0.024	0.282	2.48	0.0017	0.000116	4-5
300%	4	0	Min	1.489	0.075	-0.118	0.024	-2.56	4.291	0.0057	-0.0038	4-1
300%	4	4.8	Min	1.489	0.075	-0.118	0.024	-1.991	3.929	0.0047	-0.0028	4-1

300%	4	4.8	Min	1.489	0.075	-0.118	0.024	-1.991	3.929	0.0047	-0.0028	4-2
300%	4	9.6	Min	1.489	0.075	-0.118	0.024	-1.423	3.566	0.0037	-0.0019	4-2
300%	4	9.6	Min	1.489	0.075	-0.118	0.024	-1.423	3.566	0.0037	-0.0019	4-3
300%	4	14.4	Min	1.489	0.075	-0.118	0.024	-0.855	3.204	0.0028	-0.00091	4-3
300%	4	14.4	Min	1.489	0.075	-0.118	0.024	-0.855	3.204	0.0028	-0.00091	4-4
300%	4	19.2	Min	1.489	0.075	-0.118	0.024	-0.286	2.842	0.0018	5.68E-05	4-4
300%	4	19.2	Min	1.489	0.075	-0.118	0.024	-0.286	2.842	0.0018	5.68E-05	4-5
300%	4	24	Min	1.489	0.075	-0.118	0.024	0.282	2.48	0.0017	0.000116	4-5